USGS
science for a changing world

Prepared in cooperation with the Water Replenishment District of Southern California

Characterization of Potential Transport Pathways and Implications for Groundwater Management Near an Anticline in the Central Basin Area, Los Angeles County, California

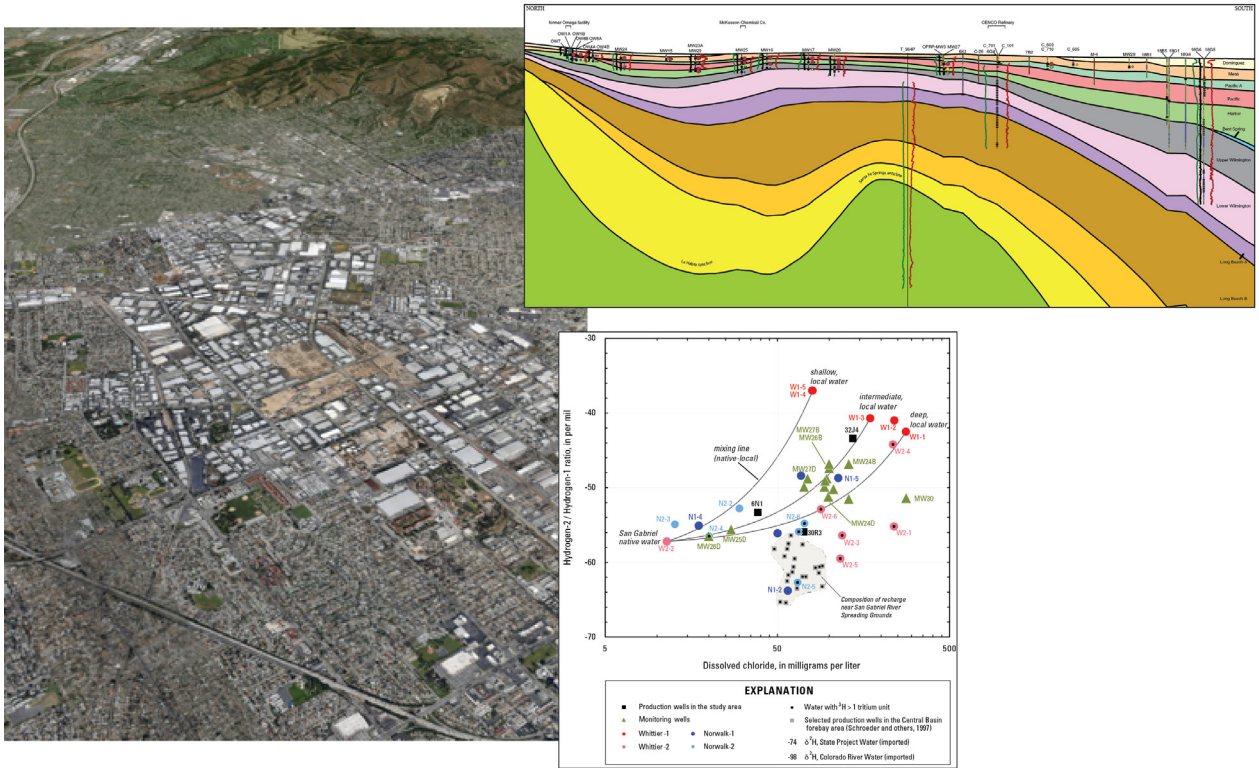

Open-File Report 2014–1087

U.S. Department of the Interior
U.S. Geological Survey

COVER

Aerial View to the northeast of the Santa Fe Springs–Whittier–Norwalk study area (Puente Hills at top of photo), along with figures showing the study cross section and groundwater chemistry data. Photo credit: Google Earth, Landsat Imagery, April 2013

Characterization of Potential Transport Pathways and Implications for Groundwater Management Near an Anticline in the Central Basin Area, Los Angeles County, California

By Daniel J. Ponti, Brian J. Wagner, Michael Land, and Matthew K. Landon

Prepared in cooperation with the Water Replenishment District of Southern California

Open-File Report 2014–1087

U.S. Department of the Interior
U.S. Geological Survey

U.S. Department of the Interior
SALLY JEWELL, Secretary

U.S. Geological Survey
Suzette M. Kimball, Acting Director

U.S. Geological Survey, Reston, Virginia: 2014

Suggested citation:
Ponti, D.J., Wagner, B.J., Land, M., and Landon, M.K., 2014, Characterization of potential transport pathways and implications for groundwater management near an anticline in the Central Basin area, Los Angeles County, California: U.S. Geological Survey Open-File Report 2014-1087, 75 p. and appendix, *http://dx.doi.org/10.3133/ofr20141087*.

ISSN 2331-1258 (online)

Contents

Abstract 1
Introduction 3
  Purpose and Scope 4
  Study Area 4
Geologic and Hydrologic Framework 7
  Objectives and Approach 7
  Geologic Setting 8
  Previous Work and Formal Stratigraphic Nomenclature 8
  Methodology 10
    Existing Sequence Stratigraphic Models 10
    Data Collection and Compilation 10
    Analysis and Model Construction 12
  Modeled Stratigraphic Units 15
    "Bedrock" Units 15
      "Miocene" 15
      "Repetto" 16
    Late Pliocene and Quaternary Chronostratigraphic Units 16
      Long Beach C 16
      Long Beach BC 18
      Long Beach B 18
      Long Beach A 18
      Lower Wilmington 19
      Upper Wilmington 20
      Bent Spring 20
      Harbor 20
      Pacific 21
      Pacific A 21
      Mesa 22
      Dominguez 22
  Geologic Structures 23
  Comparison to Current Hydrostratigraphic Framework and Aquifer Nomenclature 23
  Hydrologic Characteristics and Contaminant Occurrence Along Study Cross Section 26
    General Observations 26
    Hydrologic Conditions and Occurrence of Inter-sequence Flow 30
Groundwater Sampling and Geochemistry 35
  Methods of Analysis 35
    Selection of Wells 38
    Sample Collection and Analysis 38
  Results of Groundwater Sampling 44
    Isotopes 44
    Inorganics 47
    Volatile Organic Compounds 49
  Sources of Groundwater Recharge and Relation to Contaminant Occurrence 50
Groundwater-Flow and Particle-Tracking Model 52
  Model Description 52

Governing Equations and Model Code 52
Discretization 53
Parameterization of Subsurface Hydraulic Characteristics 54
Boundary Conditions 55
Evaluation of Alternative Model Parameters 57
Calibration Data 57
Calibration Methods 59
Model Fit 59
Calibration Results 61
Groundwater Elevations 61
Contaminant Occurrence 61
Model Limitations 64
Discussion and Conclusions 66
References Cited 70

Plates

Plate 1. Chronostratigraphy, Borehole Data and Contaminant Distribution Along a Cross Section Through the Santa Fe Springs–Whittier–Norwalk Area, Los Angeles County, California (available as a .pdf file only online at *http://pubs.usgs.gov/of/2014/1087/*).

Figures

High resolution figures are available in PDF format at *http://pubs.usgs.gov/of/2014/1087/*.

Figure 1. Map showing Los Angeles Coastal Plain and location of study area (shaded). 3
Figure 2. Map showing physiography and the generalized surficial geology and chronostratigraphy of the Santa Fe Springs–Whittier–Norwalk area 5
Figure 3. Three-dimensional stratigraphic model of the Santa Fe Springs–Whittier–Norwalk area. 14
Figure 4. Sequence boundaries interpreted from selected seismic reflection data in the Santa Fe Springs–Norwalk–Whittier area 17
Figure 5. Boundaries of chronostratigraphic units compared to classical aquifer geometry derived from lithostratigraphic correlations. 25
Figure 6. Hydrographs for selected wells along the study cross section 31
Figure 7. Hydrographs for study cross section wells, grouped by chronostratigraphic unit 32
Figure 8. Conceptual model for groundwater flow near the Santa Fe Springs Anticline crest. 34
Figure 9. Plot of δ^2H and $\delta^{18}O$ values for water in study area 45
Figure 10. Plot of δ^2H and dissolved chloride in samples. 48
Figure 11. Plot of δ^2H and reported volatile organic compounds. 51
Figure 12. Schematic of cross-sectional groundwater model. 54
Figure 13. Results of the groundwater-flow and particle-tracking analyses. *A*, parameter values that provide the best fit to groundwater elevation data; *B*, parameter values that reproduce contaminant-occurrence observations at wells MW23 and MW24. 63

Tables

Table 1. Site identification and well-construction information, Central Basin groundwater contamination study, Los Angeles County, California (available as a .xlsx file only online at *http://pubs.usgs.gov/of/2014/1087/*). 11
Table 2. Modeled chronostratigraphic units, Central Basin groundwater contamination study, Los Angeles County, California. 13
Table 3. Comparison of chronostratigraphic units and major aquifers in two parts of the study area, Central Basin groundwater contamination study, Los Angeles County, California. 27
Table 4. Compilation of selected volatile organic compounds, reported 2004–10, from wells along study cross section, Central Basin groundwater contamination study, Los Angeles County, California (available as a .xlsx file only online at http://pubs.usgs.gov/of/2014/1087/)..... 28
Table 5. Well identification and sample information for wells sampled, 2010–11, Central Basin groundwater contamination study, Los Angeles County, California. 36
Table 6. Major sources of groundwater recharge and descriptive information, Central Basin groundwater contamination study, Los Angeles County, California. 37
Table 7. Summary of selected well-construction information, as well as chemical and isotopic data (available as a .xlsx file only online at http://pubs.usgs.gov/of/2014/1087/). 38
Table 8. Results for analyses of stable isotope ratios, carbon-14 activities, and tritium in samples collected, 2010–11, Central Basin groundwater contamination study, Los Angeles County, California. 40
Table 9. Concentration of selected inorganic constituents in samples collected, 2010–11, Central Basin groundwater contamination study, Los Angeles County, California. 41
Table 10. Volatile organic compounds detected in samples collected, 2010–11, Central Basin groundwater contamination study, Los Angeles County, California. 42
Table 11. Estimates of hydraulic conductivity (reported), Central Basin groundwater contamination study, Los Angeles County, California 55
Table 12. Parameter ranges used in Monte Carlo sensitivity analysis of groundwater-flow and particle-tracking model along with calibrated parameter values, Central Basin groundwater contamination study, Los Angeles County, California. 57
Table 13. Comparison of observed and simulated groundwater elevation and contaminant occurrence, Central Basin groundwater contamination study, Los Angeles County, California. 58

Appendices

Appendix A. Interpretive Borehole Logs for Holes Located Along the Study Cross Section or Used for Stratigraphic Control, Central Basin Groundwater Contamination Study, Los Angeles County, California (available as a .pdf file only online at *http://pubs.usgs.gov/of/2014/1087/*).

Abbreviations

bls	below land surface
ft	feet
GMWL	global meteoric water line
GPS	global positioning system
ka	thousand years
km	kilometer
L	liter
Ma	million years
MCL	maximum contaminant level
NWIS	National Water Information System
µg/L	micrograms per liter
mg/L	milligrams per liter
mL	milliliter
OSC	characteristic Omega source contaminants
OSL	optically stimulated luminescence
OU	operable unit
pCi/L	picocurries per liter
pmc	percent modern carbon
per mil	parts per thousand
TL	thermoluminescence
TU	tritium units
VOC	volatile organic compounds

Acronyms

DTSC	California Department of Toxic Substances Control
EPA	United States Environmental Protection Agency
MODFLOW	a three-dimensional (3D) finite-difference groundwater model developed by USGS
MODFLOW GHB	the General-Head Boundary package for MODFLOW, used to simulate head-dependent flux boundaries.
MODFLOW-NWT	a Newton-Raphson formulation for MODFLOW-2005, intended for solving problems involving drying and rewetting nonlinearities of the unconfined groundwater-flow equation.
MODPATH	a particle-tracking postprocessor model for MODFLOW
NBS	National Bureau of Standards
NWIS	USGS National Water Information System
NWQL	USGS National Water Quality Laboratory
PEST	an open-source, public-domain software suite that allows model-independent parameter estimation and parameter/predictive-uncertainty analysis.
RWQCB	Regional Water Quality Control Board
SCEC	Southern California Earthquake Center
USGS	United States Geological Survey
WRD	Water Replenishment District of Southern California

Selected chemical names

Freon 11	trichlorofluoromethane
Freon 113	chlorotrifluoromethane
$\delta^{2}H$	ratio of hydrogen-2/hydrogen-1
$\delta^{18}O$	ratio of oxygen-18/oxygen-16
^{3}H	tritium
PCE	tetrachloroethene
TCE	trichloroethene

Conversion Factors

Inch/Pound to SI

Multiply	By	To obtain
	Length	
inch (in.)	2.54	centimeter (cm)
foot (ft)	0.3048	meter (m)
mile (mi)	1.609	kilometer (km)
	Area	
acre	4,047	square meter (m^2)
square foot (ft^2)	0.09290	square meter (m^2)
	Volume	
cubic foot (ft^3)	0.02832	cubic meter (m^3)
acre-foot (acre-ft)	1,233	cubic meter (m^3)
	Radioactivity	
picocurie per liter (pCi/L)	0.037	becquerel per liter (Bq/L)
picocurie per liter (pCi/L)	3.2	tritium unit (TU)
	Hydraulic conductivity	
foot per day (ft/d)	0.3048	meter per day (m/d)
	Hydraulic gradient	
foot per mile (ft/mi)	0.1894	meter per kilometer (m/km)
	Transmissivity*	
foot squared per day (ft^2/d)	0.09290	meter squared per day (m^2/d)

Temperature in degrees Fahrenheit (°F) may be converted to degrees Celsius (°C) as follows: °C=(°F-32)/1.8

Vertical coordinate information is referenced to the North American Vertical Datum of 1988 (NAVD 88).

Horizontal coordinate information is referenced to the North American Datum of 1983 (NAD 83).
Elevation, as used in this report, refers to distance above sea level.

*Transmissivity: The standard unit for transmissivity is cubic foot per day per square foot times foot of aquifer thickness [(ft^3/d)/ft^2]ft. In this report, the mathematically reduced form, foot squared per day (ft^2/d), is used for convenience.

Specific conductance is given in microsiemens per centimeter at 25 degrees Celsius (µS/cm at 25 °C).
Concentrations of chemical constituents in water are given either in milligrams per liter (mg/L) or micrograms per liter (µg/L).

Characterization of Potential Transport Pathways and Implications for Groundwater Management Near an Anticline in the Central Basin Area, Los Angeles County, California

By Daniel J. Ponti, Brian J. Wagner, Michael Land, and Matthew K. Landon

Abstract

The Central Groundwater Basin (Central Basin) of southern Los Angeles County includes ~280 mi^2 of the Los Angeles Coastal Plain and serves as the primary source of water for more than two million residents. In the Santa Fe Springs–Whittier–Norwalk area, located in the northeastern part of the basin, several sources of volatile organic compounds have been identified. The volatile organic compunds are thought to have contributed to a large, commingled contaminant plume in groundwater that extends south-southwest downgradient from the Omega Chemical Corporation Superfund Site across folded geologic strata, known as the Santa Fe Springs Anticline. A multifaceted study—that incorporated a three-dimensional sequence-stratigraphic geologic model, two-dimensional groundwater particle-tracking simulations, and new groundwater chemistry data—was conducted to gain insight into the geologic and hydrologic controls on contaminant migration in the study area and to assess the potential for this shallow groundwater contamination to migrate into producing aquifer zones. Conceptual flow models were developed along a flow-parallel cross section based on the modeled stratigraphic architecture, observed geochemistry, and numerical model simulations that generally agree with observed water levels and contaminant distributions. These models predict that contaminants introduced into groundwater at shallow depths near the Omega Chemical Corporation Superfund Site and along the study cross section will likely migrate downgradient to depths intercepted by public supply wells. These conclusions, however, are subject to limitations and simplifications inherent in the modeling approaches used, as well as a significant scarcity of available geologic and hydrogeochemical information at depth and in the downgradient parts of the study area.

In this study, a three-dimensional sequence-stratigraphic model of Quaternary and late Pliocene-age deposits was developed to identify unconformities (time-horizons) that define the geologic structure and bound chronostratigraphic units (containing genetically related aquifers and aquitards) that can be correlated regionally. This model suggests that syndepositional deformation of the Santa Fe Springs Anticline appears to have caused relative thinning of the stratigraphic units over the crest of the fold and, possibly, preferential erosion of capping aquitards near the anticline crest that could provide pathways for migration of contaminants downward into older units. To the south and southwest of the Santa Fe Springs Anticline crest, the units thicken as they plunge deeper into the Central Basin. Contaminated parts of these units, where they occur near the anticline crest, are likely genetically connected to the aquifers that are being pumped in the Central Basin; thus natural conduits appear to

exist for shallow groundwater to migrate downward under appropriate hydrologic conditions. Vertically oriented downward gradients are observed from multilevel monitoring wells drilled near the anticline crest, and head measurements within individual chronostratigraphic units also show that groundwater within the units flows south-southwest from the Omega Chemical Corporation Superfund Site, across the anticline, and into the Central Basin. These hydrologic observations are therefore consistent with a conceptual model for contaminant transport whereby groundwater would preferentially migrate vertically downward near the anticline crest from young stratigraphic sequences into older ones, and then continue to flow within the stratigraphic units to greater depths as the units plunge into the Central Basin.

Water chemistry data were used to evaluate the connections between shallow groundwater and production zones in the deeper parts of the groundwater system. Most groundwater in the study area, particularly along the study cross section, has chloride and oxygen isotope values consistent with being mixtures of water that enters the Central Basin through Whittier Narrows, and local water derived from precipitation falling directly onto the study area and the nearby Puente Hills. Mixing calculations based on the oxygen isotope values of water indicate that varying fractions of local water (30 to 60 percent) are present in groundwater from the youngest and shallowest stratigraphic units. In addition, volatile organic compound concentrations are greatest in zones of shallow groundwater and are associated with isotopic values indicating groundwater largely derived from local precipitation. In contrast, local water is generally not present or abundant (<10 percent) in the deeper stratigraphic units upgradient of the anticline, but local water is observed in one of these units from a well located downgradient of the anticline, where high levels of volatile organic compounds are also detected. This observation is consistent with the distribution of contaminants along the study cross section that suggests that shallow groundwater is migrating into older units near the crest of the Santa Fe Springs Anticline.

To further assess the potential for shallow groundwater contamination to migrate into deeper zones used for public supply, a two-dimensional steady-state groundwater-flow and particle-tracking simulation model was developed along the study cross section using the U.S. Geological Survey MODFLOW and MODPATH codes. The simulation model is defined to incorporate the chronostratigraphic layering developed for this study, and it was calibrated using hydraulic-head observations from 32 locations and contaminant-occurrence observations from 19 locations. An inverse method based on a Monte Carlo sensitivity analysis was used to estimate horizontal and vertical hydraulic conductivities within layers that best reproduce the hydraulic-head and contaminant-occurrence data. The model was first calibrated to find the parameters that best fit the hydraulic-head data. The resulting simulation had particle trajectories that reached a maximum depth of about 230 ft below land surface at the downstream boundary, but it was unable to reproduce the contaminant-occurrence data for three observations at the deepest observation wells. The simulation model was then calibrated to find the flow paths that best reproduced the contaminant-occurrence observations at the deepest observation wells. For this simulation, particle trajectories reached a maximum of ~600 ft below land surface at the downstream boundary, a depth that intersects the perforated sections of many public supply wells.

These analyses are limited by the two-dimensional modeling framework that was used to characterize the three-dimensional geologic and hydrologic controls that influence contaminant migration. They were also limited by data that are typically too shallow to provide the information needed to best characterize the potential for transport pathways to deeper zones of the groundwater system. However, opportunities exist to improve the modeling framework and the data set that drives the modeling analyses.

Introduction

The Central Groundwater Basin (Central Basin, fig. 1), located in southern Los Angeles County, is one of the most heavily used groundwater basins in southern California. The main aquifers within the ~280 mi^2 of the Central Basin provide at least one-third of the drinking water supply to more than two million residents. The northeastern part of the basin, referred to here as the Santa Fe Springs–Whittier–Norwalk area (fig. 1) is highly urbanized. There are multiple sites in this part of the basin where contaminated groundwater is being investigated and (or) remediated under the oversight of Federal and State regulatory agencies, including the U.S. Environmental Protection Agency (EPA), California Department of Toxic Substances Control (DTSC), and the Los Angeles Regional Water Quality Control Board (RWQCB).

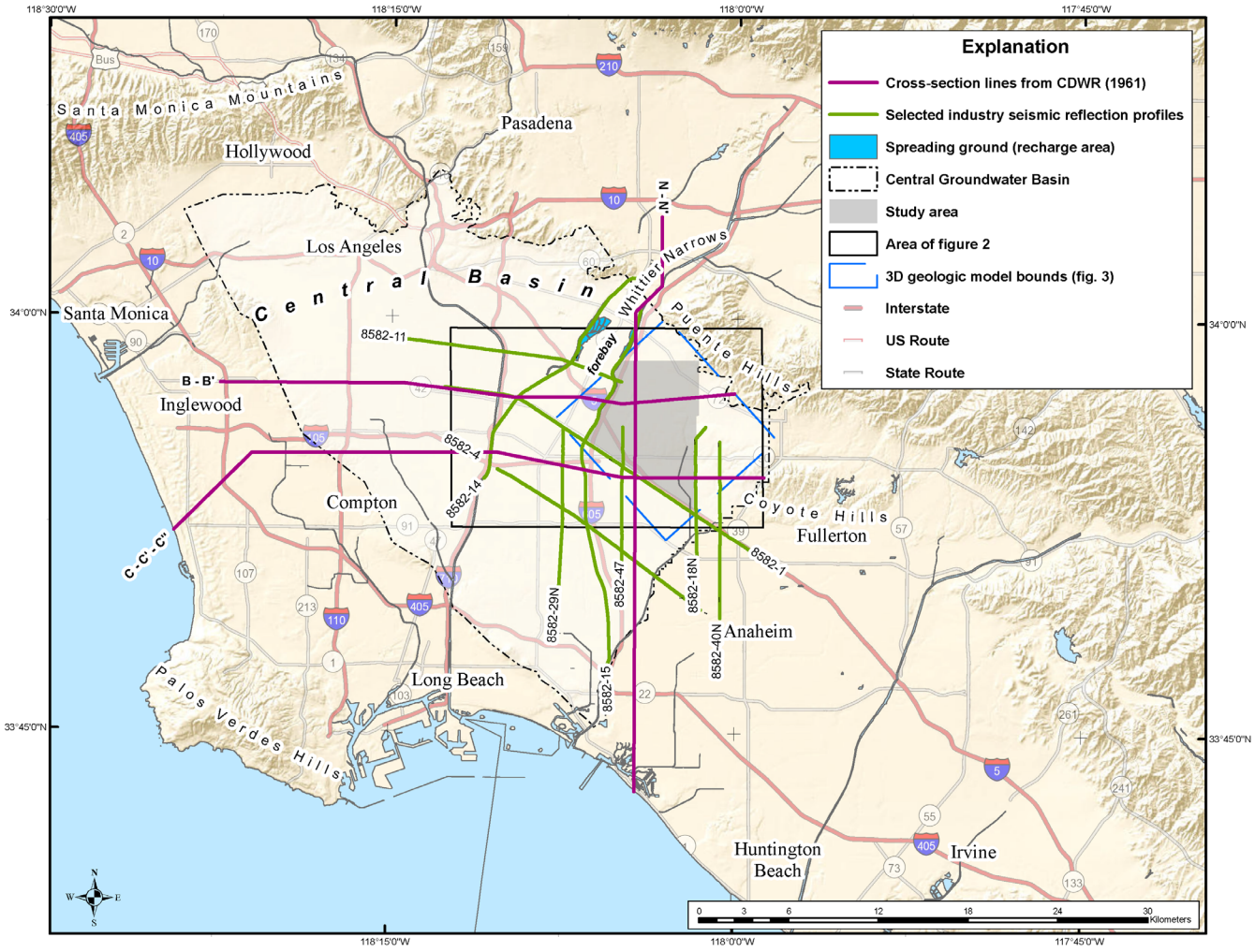

Figure 1. Map showing Los Angeles Coastal Plain and location of study area (shaded). Selected industry seismic reflection lines (green) are those relevant to determining the geologic structure in the Santa Fe Springs area. CDWR, California Department of Water Resources; 3D, three dimensional.

One of the sites where contamination occurs within the study area is the Omega Chemical Corporation Superfund Site. The former Omega Chemical Corporation was a refrigerant and solvent recycling facility located in Whittier, California, that operated from ~1976–91 (EPA, 2000). The EPA

manages the Omega Chemical Corporation Superfund Site as three operable units (OUs)—OU1 includes the contaminated soil and groundwater beneath the former Omega facility and in the immediate vicinity, OU2 covers a region that contains a groundwater plume that extends ~4.5 miles south-southwest (downgradient) from the former Omega facility, and OU3 addresses indoor-air contamination. It is inferred that contamination from other downgradient sites such as Angeles Chemical, McKesson Chemical, the former CENCO Refinery, and also possibly the former Ashland Chemical, has commingled with contamination from the former Omega facility in the OU2 plume (Ferguson and others, 1996; EPA, 2010; Murex Environmental Inc., 2011). High concentrations of volatile organic compounds (VOCs), including tetrachlorethene (PCE), trichloroethene (TCE), trichlorofluoromethane (Freon 11), trichlorotrifluoroethane (Freon 113), and 1,4-dioxane, as well as hexavalent chromium, have been detected in shallow monitoring wells [screen depths < 200 feet below land surface (bls)] located within the OU2 boundary.

Some public supply wells, screened at shallow (< 200 feet) depths, have been affected by VOCs in the study area (EPA, 2010). Current investigations, monitoring, and remediation at contaminated sites within the study area focus on the shallow groundwater system, but water managers and regulatory agencies have been concerned that groundwater contamination could migrate over time into deeper aquifers used for public drinking water supplies. A multifaceted investigation of the study area has been conducted to assess the possible transport rates and migration pathways of contaminants that occur within the shallow groundwater system, and the cumulative threat to aquifers that supply drinking water.

Purpose and Scope

The primary purpose of this study is to improve understanding of the potential hydrogeologic connections between shallow, contaminated aquifers in the Santa Fe Springs–Whittier–Norwalk area and the main drinking water aquifers of the Central Basin. This report describes a new sequence-stratigraphic framework for the study area and develops a two-dimensional groundwater flow and particle-tracking model constrained by analysis of existing and newly collected geochemical data. The report also identifies and prioritizes additional information and data collection needed for informing water management efforts to protect the Central Basin.

Although other sources of VOCs exist within the study area, co-occurring detections of PCE, TCE, Freon 11, Freon 113, and 1,4-dioxane, are considered to represent the presence of contaminants within the OU2 plume that likely originated from the former Omega facility (EPA, 2010). For the purpose of this study, these co-occurring detections are referred to as the characteristic Omega source contaminants (OSCs). This study does not have the information nor the intent to definitively determine whether an OSC signature in particular wells is in fact derived solely from the former Omega facility and (or) other specific contamination sources. Evaluation of individual sources of contamination to shallow groundwater is beyond the scope of this study. Rather, the spatial distribution of OSCs are used to define the shallow groundwater boundary conditions within OU2 for evaluating the potential for contamination, from any source, to move into aquifers used for public water supply. This study is a conceptual and numerical evaluation of the potential for shallow groundwater contamination to move into the deeper zones predominantly used for public-water supply, but it is not a specific evaluation of contaminant movement from a particular source.

Study Area

The study area lies within the northeastern margin of the Los Angeles Coastal Plain and Central Basin (fig. 1). It is ~19 mi^2 in area and is approximately centered upon the OU2 boundary (fig. 2). The

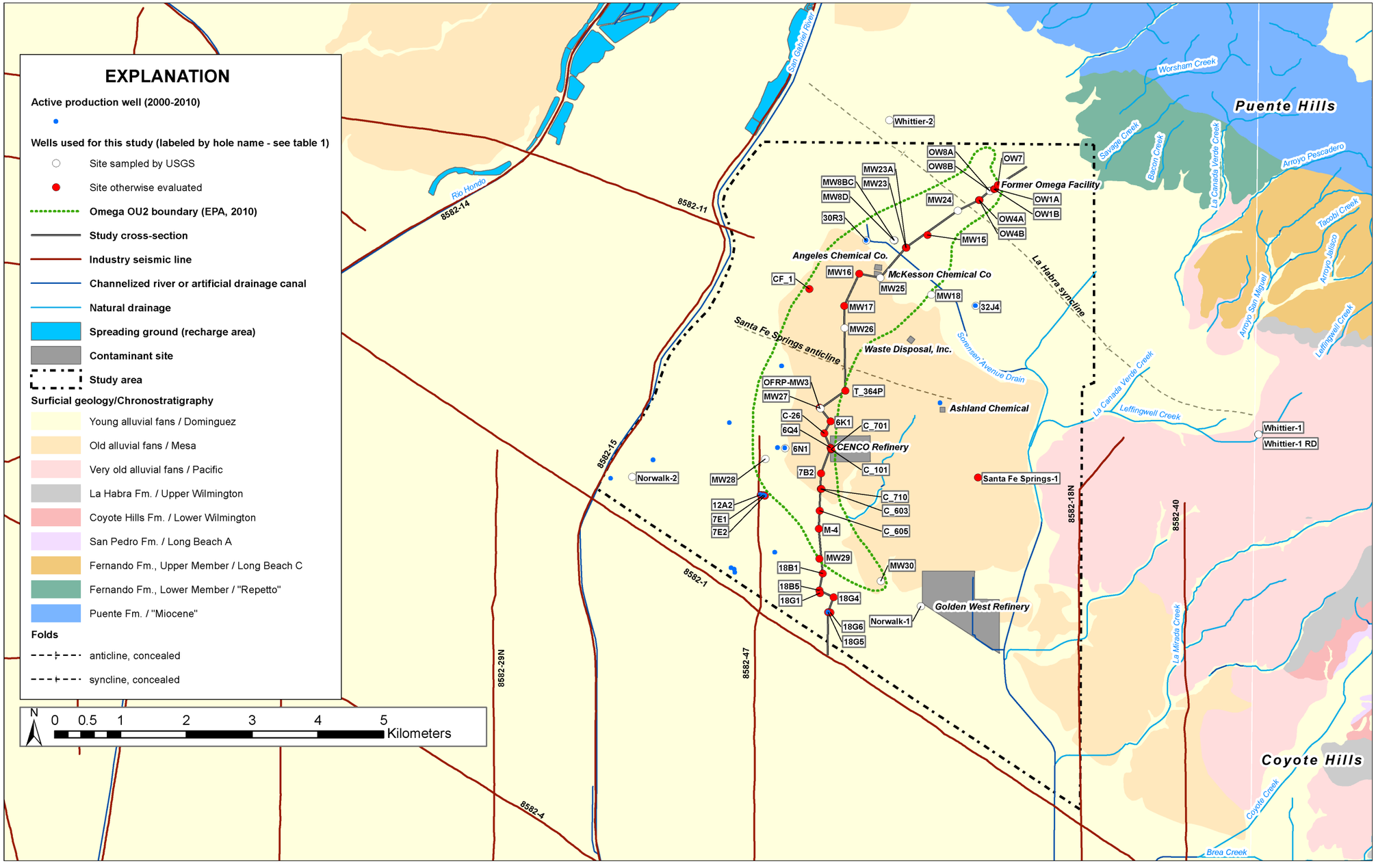

Figure 2. Map showing physiography and the generalized surficial geology and chronostratigraphy of the Santa Fe Springs–Whittier–Norwalk area. Surficial geology and nomenclature generalized from Saucedo and others (2003) and Morton and Miller (2006). Chronostratigraphic nomenclature interpreted from geologic map units discussed in the text. EPA, U.S. Environmental Protection Agency.

area is entirely urbanized, and most of the land has been used for industrial and commercial purposes since the 1950s, although the southern part of the study area also contains residential areas.

The climate is semiarid with moderate temperatures. The warmest temperatures generally occur during the months of July, August, and September and average ~76 °F (1979–2011 average temperature for the City of Montebello; Western Region Climate Center, 2014). Rainfall occurs primarily during the winter and spring months, with an annual average of about 14.3 in per year (1949–2013 average rainfall for the City of Whittier; Western Region Climate Center, 2014). The 50-year mean annual infiltration rate varies between 1.6 to 2.1 in per year in the Los Angeles Basin (Reichard and others, 2003).

Pliocene-age Fernando Formation bedrock (Yerkes, 1972; fig. 2) crops out at the extreme northeast corner of the study area, but the rest of the study area is overlain by unconsolidated sediment of Holocene and Pleistocene age (identified as young alluvial fans and old alluvial fans, respectively, see fig. 2). Young alluvial fans deposited from drainages in the Puente Hills have produced a broad piedmont that slopes gently to the southwest, where the former Omega facility is located. Further southwest, in the center of the study area, the topography flattens above a broad alluvial plain that is largely underlain by older (late Pleistocene) alluvial material. This older sediment is exposed at the surface as a result of folding and uplift above the Santa Fe Springs segment of the Puente Hills Thrust (Shaw and Shearer, 1999; Shaw and others, 2002; Plesch and others, 2007), an active blind-thrust fault that lies buried beneath much of the eastern Central Basin. The Santa Fe Springs Anticline (fig. 2) is one manifestation of this fold-and-fault system; its axial surface cuts through the center of the study area and trends west-northwest across the OU2 plume. To the west and southwest of this area of exposed older sediment, the land surface again slopes gently southwest, and the older Pleistocene sediment is buried by young alluvial-fan and basin sediments deposited primarily by the San Gabriel River. The river is a major drainage that originates to the north in the San Gabriel Mountains, and enters the basin north of the study area by way of the Whittier Narrows. Land surface elevations generally rise from the center of the study area toward the Coyote Hills, evidence that uplift and deformation above the Puente Hills Thrust increases to the east-southeast.

The San Gabriel River marks the west edge of the study area. It has, and continues to be, a major source of groundwater recharge to the Central Basin (Reichard and others, 2003), although at the present time much of the recharge comes from imported and treated water that infiltrates the subsurface at the San Gabriel River Spreading Grounds (spreading grounds) located along the river to the north of the study area. Smaller drainages with headwaters in the Puente Hills extend across the northern and eastern parts of the study area. These drainages likely contribute some recharge to the basin locally, along with recharge from precipitation (Reichard and others, 2003). As discussed later, local recharge is an important source of the groundwater in the study area, especially at shallow depths. The courses of smaller drainages, such as the Sorensen Avenue Drain, Leffingwell Creek, and several unnamed drainages that originate in the late Pleistocene deposits (fig. 2) appear to reflect recent deformation associated with the Puente Hills Thrust. An exception is La Canada Verde Creek, an antecedent stream that has maintained a north-south course through older, folded sediments near the eastern margin of the study area.

Production wells in the study area are generally screened over long intervals and draw water from multiple aquifers. Seventeen production wells within the study area were in active production during the period of 2000–10 (fig. 2). Several of these wells are screened at shallow depths (<200 feet bls), and as such, may be more at risk from contamination; some of these wells have already had VOC detections. Owing to uplift and ensuing erosion, growth of the Santa Fe Springs Anticline is potentially significant to groundwater flow in the study area because of its likely effects on the thickness, geometry, and lithologic character of the underlying sediment. Earlier models of the subsurface aquifers by the

California Department of Water Resources (CDWR, 1961) suggest that the major producing aquifers in the area are at shallower depths as a result of uplift along the anticline. The models also suggest the aquifers merge at some locations near the anticline crest, thus potentially enhancing the potential for shallow contaminated water to enter the producing systems.

Geologic and Hydrologic Framework

Objectives and Approach

One of the principal objectives of this study was to reevaluate the stratigraphy and geologic structure within the study area to refine our understanding of the region's aquifer architecture. The geology was then evaluated in relation to contaminant observations along a flow path that was parallel to the OU2 plume to assess whether geologic structures could allow for migration of contaminants from near-surface aquifers into those that are actively being pumped for drinking water. We applied the concepts of sequence stratigraphy to interpret available subsurface information and developed a chronostratigraphic, or time-based, framework for the water-bearing sediment of the Santa Fe Springs–Whittier–Norwalk area.

Sequence stratigraphy subdivides and links sedimentary deposits into unconformity-bound units that are genetically related and controlled by variations in base level (sea level), sediment supply, and available accommodation space (Van Wagoner and others, 1990; Catuneanu, 2006). Within depositional sequences, facies and lithologic properties can change both laterally and vertically. These changes result from depositional processes that are mappable and predictable, thus the lateral distribution of coarse-grained aquifers and their fine-grained, confining aquitards can be more realistically represented. Hydrologic connections among coarse-grained facies that serve as aquifers are likely to be extensive within a sequence. Connections develop naturally as sequences form and as facies transition laterally and vertically in response to changes in base level and sediment supply. Hydrologic connections between sequences tend to be localized, however, as they are controlled by (1) how sequences stack on top of one another, and (2) how tectonic deformation along faults and folds, as well as erosion, might influence facies distribution and preservation, or serve to juxtapose different sequences laterally. In contrast to the lithostratigraphic units that have previously been defined in the basin by their lithologic characteristics (for example, CDWR, 1961), sequences are defined by their bounding discontinuities. Within the study area, the identified sequences are bounded on top and bottom by regionally unconformable surfaces, upon which there appears to be evidence for erosion or a depositional hiatus. While the sequence-bounding unconformities are not strictly isochronous surfaces, they are significant because sediment deposited above an unconformity is everywhere younger than sediment that underlies that unconformity. Thus, sequence-bounding unconformities separate genetically unrelated packages of sediment that are deposited within distinct time intervals.

In the Los Angeles Coastal Plain, the geologic sequences of Quaternary age generally formed in response to sea-level changes resulting from worldwide glaciation cycles (Imbrie and others, 1984). In the study area, most sediment accumulation likely occurred during interglacial periods when sea levels were high and coastlines prograded across the shelf. During glacial periods when sea levels were low, erosion on the exposed shelf occurred, and thus produced the bounding unconformities. The sequences and their boundaries can be identified by characteristic cycles of coarsening or fining upward packages that reflect sediment progradation and retrogradation. These cycles are often recognized and correlated as characteristic vertical patterns in electric and lithologic well logs, even where specific electric and lithologic log signatures are quite different. Evidence for bed truncation and onlap at sequence

boundaries can also be observed in seismic-reflection profiles. In this study, a combination of borehole logs and seismic data were used for sequence identification and correlation.

Sequence stratigraphy is a useful approach for this study because it provides a robust means for defining geologic structure, hydraulic properties, and aquifer connectivity. Within a given sequence, coarse-grained deposits that may serve as productive aquifers might, for example, transition toward the coastline from river channel sands and gravels, to coastal dunes and tidal-channel sands, to intertidal and neritic-marine sands. Groundwater, controlled by the hydraulic properties of these various facies, would be expected to flow naturally between the coarse-grained deposits within a sequence because they are genetically connected. Movement of groundwater between sequences can certainly take place as well, but movement will most readily occur locally where the coarse-grained facies of two sequences are juxtaposed and where the groundwater gradients drive flow between the sequences. Such occurrences can occur vertically where coarse-grained deposits are juxtaposed across a stratigraphic boundary or laterally due to incision, onlap, or faulting. Once the overall aquifer architecture within sequences is understood, likely interconnections among sequences can be estimated and incorporated into flow and transport models.

Geologic Setting

The Los Angeles Coastal Plain region is a complexly faulted basin, primarily filled with marine sediment. It began forming during the late Miocene on a continental margin that had previously undergone Mesozoic and early Paleogene subduction, Paleogene terrane accretion, and mid-Miocene rifting and block rotation (Wright, 1991). Late Miocene subsidence evolved into a major phase of early Pliocene basin subsidence due to transtensional deformation that accompanied the opening of the Gulf of California, and an eastward shift in the southern San Andreas Fault. During the middle Pliocene (~3.9–3.5 Ma), in association with a change in relative plate motion, the basin began to experience north-south shortening that resulted in uplift of the Transverse Ranges, the propagation of blind thrusts beneath the basin, and basin filling (Wright, 1991). The transpressive tectonic regime that was initiated during the middle Pliocene continues to the present day.

Previous Work and Formal Stratigraphic Nomenclature

The sediment that records the evolution of the Los Angeles Basin has been extensively mapped and studied since the late 1800s, and the regional lithostratigraphic framework and stratigraphic nomenclature of the Los Angeles Basin and the Puente Hills region has been formalized since the mid 1960s (Durham and Yerkes, 1964; Yerkes and others, 1965). The formal stratigraphic nomenclature for Pleistocene age deposits (which contain most of the producing aquifers) was developed from work on the Palos Verdes Peninsula by Woodring and others (1946). They recognized three lower Pleistocene formations of marine origin (the Lomita Marl, Timms Point Silt, and San Pedro Sand), unconformably overlain by a series of upper Pleistocene marine-terrace deposits, the youngest of which was named the Palos Verdes Sand. This framework and nomenclature were first extended into the subsurface of the western Los Angeles Basin in two groundwater geology investigations by Poland and others (1956, 1959). The various Pleistocene marine and marine-terrace formations recognized on the Palos Verdes Peninsula could not be readily distinguished in the subsurface, so the Lomita Marl, Timms Point Silt, and San Pedro Sand of Woodring and others (1946) were combined into the marine San Pedro Formation, whereas the upper Pleistocene marine-terrace deposits and the Palos Verdes Sand were included with paralic and nonmarine deposits identified in the subsurface and called the Unnamed Upper Pleistocene. This subsurface framework was then extended into the Central Basin by the California Department of Water Resources (CDWR, 1961). The CDWR maintained the term “San

Pedro Formation" to represent the shallow marine deposits of Pleistocene age, but reassigned Poland's Unnamed Upper Pleistocene to the informally named Lakewood Formation.

In their mapping of the Puente Hills region, Durham and Yerkes (1964) and Yerkes (1972), defined three Pleistocene-age formations; in succession from oldest to youngest and separated by unconformities. These formations are the (1) the early Pleistocene San Pedro Formation, of shallow-water marine origin, which they correlated to the subsurface San Pedro Formation of Poland and others (1956, 1959), (2) the early late-Pleistocene Coyote Hills Formation, consisting of intertidal and nonmarine sediment, correlated to the lower part of the Unnamed Upper Pleistocene of Poland and others (1956, 1959), and (3) the late Pleistocene La Habra Formation, a nonmarine unit correlated to the upper part of the Unnamed Upper Pleistocene and the marine-terrace deposits on the Palos Verdes Peninsula. The La Habra and older units do not crop out in the study area, but we infer that their chronostratigraphic equivalents underlie the Santa Fe Springs–Whittier–Norwalk area.

More recent paleontological work on the San Pedro Formation in the Coyote Hills (Powell and Stevens, 2000), indicates that the formation is significantly older than the San Pedro Sand in the Palos Verdes Peninsula (and by analogy, much of the subsurface San Pedro Formation). Analysis for this study suggests that the La Habra and Coyote Hills Formations are likely older than inferred for most of the upper Pleistocene deposits in the subsurface (Unnamed Upper Pleistocene or Lakewood Formation) as well.

Durham and Yerkes (1964) and Yerkes (1972) also mapped younger alluvial fan deposits that overlie the La Habra and older Pleistocene formations. These are referred to informally as old (Pleistocene) and young (Holocene) alluvium. Recent surficial mapping by Saucedo and others (2003) and Morton and Miller (2006) have further subdivided the fans by relative age, as well as average grain size. These alluvial fan deposits nearly extend across the entire study area and are derived from the San Gabriel River, as well as local drainages that have their headwaters in the Puente Hills (fig. 2). In the north half of the study area, the young surficial Holocene deposits that are derived from the Puente Hills tend to be fairly fine grained (silt and fine sand), and are of moderate to low permeability. Surficial Holocene alluvium in the western part of the study area near the present location of the San Gabriel River, and in the southern part of the study area, is sandier and more permeable. Deposits within and adjacent to the river channel itself consist of coarse sand or gravel, and have high permeability. Alluvial deposits of Pleistocene age (mapped as old and very old alluvial fans; fig. 2) occur in the central and southeastern part of the study area. These units consist dominantly of silty sand at the surface, but tend to contain more sand at depth, and are therefore likely to vary from low to high permeability.

As previously described, the Pleistocene-age alluvial fan deposits are exposed at the surface as a result of uplift and folding above the Puente Hills Thrust. The axis of the Santa Fe Springs Anticline (fig. 2) occurs within the uplifted region. To the northeast, the Pleistocene alluvium dips northeast into the La Habra Syncline, and to the southwest, the beds plunge into the southern Central Basin. The CDWR (1961) shows that the San Pedro and Lakewood Formations thin over the axis of the anticline, and this observation indicates fold growth has been ongoing throughout the Quaternary. Analysis of subsurface data compiled for this study, including interpretation of industry seismic-reflection data, confirms syndepositional deformation and thinning of stratigraphic units over the anticline crest since at least early Pleistocene time.

In the hydrostratigraphic subsurface framework developed for the Santa Fe Springs–Whittier–Norwalk region by CDWR (1961), sand and gravel-filled river channels near the base of the young Holocene deposits constitute the Gaspur aquifer. Within the OU2 boundary, however, this young Holocene unit is largely unsaturated (EPA, 2010). Pleistocene alluvial and intertidal deposits that constitute the Lakewood Formation of CDWR (1961) contain, with increasing depth, the Exposition,

Artesia, Gardena, and Gage aquifers. These permeable zones probably represent coarser-grained fluvial and tidal-channel facies. Because of their shallow depth (less than 200 ft) and lithologic heterogeneity, the Lakewood Formation aquifers tend to have poor water quality and low yields (EPA, 2010). The marine San Pedro Formation is inferred by CDWR (1961) to extend to a depth of ~1,000 ft and contains, with increasing depth, the Hollydale, Jefferson, Lynwood, Silverado, and Sunnyside aquifers. These aquifers probably reflect coastal beach, dune, nearshore sand, and deltaic channel deposits. These types of deposits tend to be more laterally homogeneous than nonmarine sediments and therefore are the more productive aquifers typically exploited for public water supply.

Methodology

Existing Sequence Stratigraphic Models

To develop the new chronostratigraphic framework for the study area we relied on work initially performed in the Long Beach area (Ponti and others, 2007). The Long Beach study involved detailed analyses and age dating of continuously cored boreholes to identify key unconformities and to define major sequences. Through analysis of available well and seismic data within the new stratigraphic context, the authors constructed a digital three-dimensional (3D) structural model. Ten sequences spanning the Holocene through latest-Pliocene epochs were identified (Ponti and others, 2007).

Over the last several years, the USGS has been developing a regional sequence-stratigraphic model for the entire Los Angeles Coastal Plain subsurface through analysis of existing oil- and water-well logs, new water-well drilling logs, and medium- to high-resolution seismic-reflection data collected by the U.S. Geological Survey (USGS) and the oil industry. The regional model under development utilizes the same stratigraphic sequences as developed in Long Beach, although two of the sequences have been subdivided in the Central Basin, where they reach considerable thicknesses, to allow groundwater-flow models to better capture hydrologic variations that are observed in these units. From the available data, we cannot determine if these subdivided units are bounded by unconformities, and therefore represent different depositional packages, or if these boundaries are simply conformal within the original sequence from which they are subdivided. The regional model also extends to greater depth than that in the Long Beach area (-6 km elevation vs. -0.9 km elevation for Long Beach), in order to capture the base of the oldest water-bearing sequence within the Central Basin.

An early version of the regional structural model was completed prior to the initiation of work in the Santa Fe Springs–Whittier–Norwalk area, and it was used as a starting point for construction of the higher-resolution model for this study. This preliminary regional model incorporated data from more than 500 wells and 500 km of seismic lines within the Central Basin, but data coverage within the Santa Fe Springs–Whittier–Norwalk area was limited within the OU2 boundary, especially at shallow depths.

Data Collection and Compilation

This study relies on existing data collected and reported by others. To enhance coverage within the study area, well-log data from over 250 wells drilled in the region were compiled and evaluated. Most of these records are drillers' logs from water wells drilled by hydraulic rotary methods. With a few exceptions, these logs are quite general in nature and lack descriptive information useful for sequence-stratigraphic analysis. Some older water wells, typically drilled by the cable tool method, have more reliably described contacts that are less likely to be contaminated by infall. Geophysical logs from water wells are rare. Although of limited utility, several water well drillers' logs were selected for inclusion in our analysis because they extend to depths considerably below the typical investigation depth within the OU2 boundary (~200 ft).

Well-log data derived from geoenvironmental boreholes that were drilled as monitoring wells to characterize the OU2 plume or other contaminated regions, are of much higher quality, but they are fewer in number and are of more limited depth (generally <200 ft) than water well driller logs. Most of the geoenvironmental borehole logs were made by geologists or engineers, and were derived from examination of core samples either collected continuously or at regularly spaced intervals of 10 ft or less. In a few cases, however, descriptions came from drill cuttings supplemented by interpretation of geophysical logs. With few exceptions, lithologies from geoenvironmental boreholes were classified in the field using the Unified Soil Classification System (ASTM, 1985), which provides consistency when comparing data from multiple holes and different investigations. Many of these logs also contain constituent information (for example, color, mineralogical components, and fossils) that can be useful for identifying potential unconformities. Some of these wells also have geophysical logs, which are valuable for identifying fining- or coarsening-upward sediment packages and bounding unconformities.

A third set of well logs describe oil wells filed with the California Department of Oil, Gas, and Geothermal Resources. These wells extend to great depths, but they have no recorded data in the upper few hundred feet, and only a few logs contain data recorded in the upper 1,000 ft. Oil wells are typically described by electrical resistivity and spontaneous potential logs. These logs are valuable for determining stacking patterns and general lithologic character, but no geologic descriptions of the sediment are typically available.

To refine the regional chronostratigraphic model within the study area, 39 well logs were selected on the basis of the quality, depth, and areal distribution of the data being suitable for stratigraphic control. Emphasis was also placed on obtaining the best quality geological data within the OU2 boundary, where geologic interpretations can be compared to observed contaminant distribution. These well sites are shown on figure 2, and well-construction details are presented in table 1.

Table 1. Site identification and well-construction information, Central Basin groundwater contamination study, Los Angeles County, California (available as a .xlsx file only online at *http://pubs.usgs.gov/of/2014/1087/*).

In addition to the well data, figures 1 and 2 show the location of oil industry seismic-reflection lines located near the study area that have been interpreted for the regional model. The data analyzed were shot in the 1980s in the Central Basin by Texaco. These data are proprietary but have been obtained by the Southern California Earthquake Center (SCEC) for research purposes. The digital data are housed at Harvard University and were made available for interpretation onsite by Professor John Shaw. Unconformities can be observed in the seismic data, based on the occurrence of onlap, downlap, toplap, and truncation of seismic reflectors. Unconformities and seismic reflectors correlative with these surfaces were identified and digitized using Landmark® seismic interpretation software in the time-domain, and then converted to elevations using the SCEC CVM-H velocity model (Suess and Shaw, 2003; Plesch and others, 2011). Seven horizons within the upper 2.5 seconds were identified and mapped within the Central Basin, and the shallowest 6 horizons were correlated to sequence tops in the Long Beach model (Ponti and others, 2007). The seventh horizon is likely of Pliocene age and is assigned to the top of a unit defined in the geologic model ("Repetto") that is described later in this report.

Some uncertainties are inherent in the time-to-depth conversions of the seismic data, and in some instances, computed seismic horizon depths do not agree precisely with the chronostratigraphic sequence boundary depths identified from boreholes. In most cases, however, the depth discrepancies appear to be less than 10 percent. Where borehole control exists near the seismic lines, chronostratigraphic boundaries defined from the seismic data were locally adjusted to conform with the borehole depths.

Analysis and Model Construction

To facilitate interpretation of selected borehole data and to identify key boundaries and fining- or coarsening-upward sediment packages, the descriptive geologic log data were reclassified and a median grain-size for each described geologic layer was estimated from the descriptions. For geologic logs with Unified Soil Classification System assignments, the classifications were kept as assigned, and median grain sizes were estimated from the Unified Soil Classification group and other descriptive information as available. For water-well logs and other logs where geologic descriptions were more generic and did not use a prescriptive classification system, described geologic layers were classified into a simple 5-level classification scheme–gravelly sediment, coarse sands, medium to fine sands, silty and clayey sands, and silts/clays. The resulting classifications and estimated median grain sizes were plotted graphically (appendix A) and inferred sequence boundaries were identified, using stacking patterns identified from the graphic logs and any associated geophysical logs, nearby seismic horizons, and available descriptive data. When identifying sequence boundaries from borehole descriptions, attention was paid to (1) color changes in the sediment, (2) the presence of organic material and (or) carbonate or other cementation, (3) changes in density or stiffness, and (4) changes in drilling behavior, as possible indicators of buried soils or other unconformities.

Another aspect of model construction was to correlate mapped surficial geologic units with the sequences identified from subsurface data. For the mapped young, old, and very old alluvial fans, this process is fairly straightforward, because the original depositional surfaces of these deposits are preserved and geologists have subdivided them by relative stratigraphic position, not on their lithologic character. These map units are therefore chronostratigraphic units and the exposed depositional surfaces of these fans are sequence boundaries that can be projected with confidence into the subsurface.

For the La Habra Formation and older map units that are defined lithostratigraphically, the associations between them and the sequences identified in the subsurface are less clear. However, these older Pleistocene deposits are unconformity bound according to Durham and Yerkes (1964) and Yerkes (1972). Therefore, the ages of the mapped La Habra, Coyote Hills, and San Pedro Formations likely do not overlap (at least within our study area), and these formations can be reasonably assigned to subsurface sequences in a fashion similar to the younger deposits. Correlation of the mapped surficial deposits to the subsurface sequences is shown in the explanation of figure 2 and in table 2.

Chronostratigraphic unit tops identified from seismic and borehole data, along with surficial map assignments, were then incorporated back into the regional model framework, which was constructed using Dynamic Graphics EarthVision® software. A new, finer-scale model was built for a small region around the study area (fig. 1) using Dynamic Graphics' minimum tension grid algorithm (2009) on 21- by 31-m horizontal grid centers, as opposed to the regional model's 150- by 200-m cell size. A visualization of the resulting 3D digital structure model is shown in figure 3 with the colored layers representing the various chronostratigraphic units (sequences).

Table 2. Modeled chronostratigraphic units, Central Basin groundwater contamination study, Los Angeles County, California.

[Unit names and age estimates derive from Ponti and others (2007) and McDougall and others (2012). Long Beach A, B and C units are renamed here from original Pliocene A, B, and C (Ponti and others, 2007) as a result of recent redefinition in the age of the Pliocene-Pleistocene boundary (Gibbard and others, 2010). <, less than; >, greater than; ~, approximate; AAR, amino acid racemerization/epimerization; ka, thousand years, Ma, million years; OSL, optically stimulated luminescence; TL, thermoluminescence]

Unit	Estimated age range	Epoch	Age controls	Subsurface constraints in vicinity of study area	Probable correlative surficial map units in study area vicinity (after Saucedo and others, 2003; Morton and Miller, 2006)	Inferred depositional environments in study area vicinity
Dominguez	<15 ka	Holocene	Radiocarbon, OSL	Very good; contains basal sand or gravel in many areas	Young alluvial fan and valley deposits; alluvial wash deposits, active channel and wash deposits	Alluvial fan, flood basin and stream channel
Mesa	~20–80 ka	late Pleistocene	OSL, possible Laschamp magnetic polarity event (~40ka) present; AAR on marine-terrace outcrops	Good; top surface usually marked by basal gravel of overlying Dominguez sequence	Old alluvial fan and valley deposits *(also mapped as Lakewood Fm. by CDWR, 1961)*	Alluvial fan and flood basin
Pacific A	~30–80 ka	late Pleistocene	Lower subdivision of Mesa sequence in Central Basin to account for variations in hydraulic character within the sequence	Fair to poor; upper boundary arbitrary in some areas	No known exposures	Nonmarine (probably alluvial fan)
Pacific	110–130 ka	late Pleistocene	OSL, Blake magnetic polarity event (~115 ka); AAR estimates on marine-terrace outcrops	Fair, top surface seen in seismic reflection data, but often difficult to pick due to poor resolution at depths where this typically occurs	Very old alluvial fan deposits *(also mapped as Lakewood Fm. of CDWR, 1961)*	Nonmarine (alluvial fan) may become paralic to inner neritic marine near south end of study section
Harbor	~160–200 ka	middle Pleistocene	AAR estimates from shallow boreholes; macrofossils, TL; possible Pringle Falls magnetic polarity event (~200 ka)	No clear seismic reflector; unit often is marked by coarse-grained base and top with intervening fine-grained interval	No known exposures	Nonmarine (alluvial fan) may become paralic- to inner-neritic marine near south end of study section
Bent Spring	~200–450 ka	middle Pleistocene	TL; AAR estimates on terrace outcrops; Possible Pringle Falls magnetic polarity event (~200 ka) south of Pacific Coast Highway fault; otherwise unit appears to be older than ~300 ka	Good, clear seismic reflector at top of unit in most areas	No known exposures; seismic data show that unit pinches out in the subsurface and is not present under most of study area	Unknown, probably inner neritic in vicinity of study section
Upper Wilmington	~475–580 ka	middle Pleistocene	Possible Big Lost magnetic polarity event (~525–550 ka)	Good, clear seismic reflector at top of unit in most areas	La Habra Formation	Nonmarine (fluvial) where exposed, probably inner neritic in vicintiy of study section
Lower Wilmington	~580–<780 ka (Long Beach); probably <1.0 Ma elsewhere	middle/early Pleistocene	Contains Lava Creek "B" ash (~0.64 Ma) in Long Beach area; Bishop ash (~0.76 Ma) and magnetically reversed sediment (>0.78 Ma) in a northern portion of the Central Basin is inferred to belong to this unit (Quinn and others, 2000)	Top surface is marked by a clear seismic reflector in in most areas. Poorly defined lower boundary is likely older in Central Basin	Coyote Hills Formation *(also mapped as Lakewood Fm. of CDWR, 1961)*	Paralic where exposed, probably inner- to outer-neritic in vicinity of study section
Long Beach A[1]	~2.0 Ma or >2.6 Ma	early Pleistocene (?)	Apparent lower Pleistocene planktic fauna; but normal polarity paleomagnetic signature; may be younger in the study area	Poorly defined–not often distinguishable from Long Beach B or Lower Wilmington	San Pedro Formation	Inner-neritic marine where exposed; neritic to bathyl(?) marine in vicintiy of study section
Long Beach B[2]	~2.0 Ma or >2.6 Ma	early Pleistocene (?)	Apparent lower Pleistocene planktic fauna; but normal polarity paleomagnetic signature	Fair, generally marked by thick sands in elogs, top marked by clear seismic reflector	No known exposures	Neritic to bathyl(?) marine
Long Beach BC	> 2.6 Ma (?)	late Pliocene (?)	Upper subdivision of Long Beach C sequence in Central Basin to account for variations in hydraulic character within the sequence	Fair to poor. Upper boundary arbitrary in some areas	No known exposures	Bathyl(?) marine
Long Beach C[3]	>2.6 Ma	late Pliocene	Probable Pliocene age based on microfossil and paleomagnetic constraints in overlying Long Beach B unit	Good, clear seismic reflector marks top of unit in most areas	Fernando Formation, Upper Member	Neritic where exposed; probably bathyl in vicinity of study section
"Repetto"	~3–5 Ma	Pliocene	Benthic fauna	Based on cross-sections in Wright (1991) and clear seismic horizon in Central Basin; seismic horizon appears correlative with biostratigraphic Repetto near margins of the basin, but may be younger elsewhere	Fernando Formation, Lower Member	Bathyl marine
"Miocene"	5.3–23 Ma	Miocene, probably extending into early Pliocene	Benthic fauna	Based on sections and structure contours in Wright (1991)	Puente Formation	Bathyl marine

[1]Upper-, [2]Middle-, and [3]Lower-Long Beach of McDougall and others (2012)

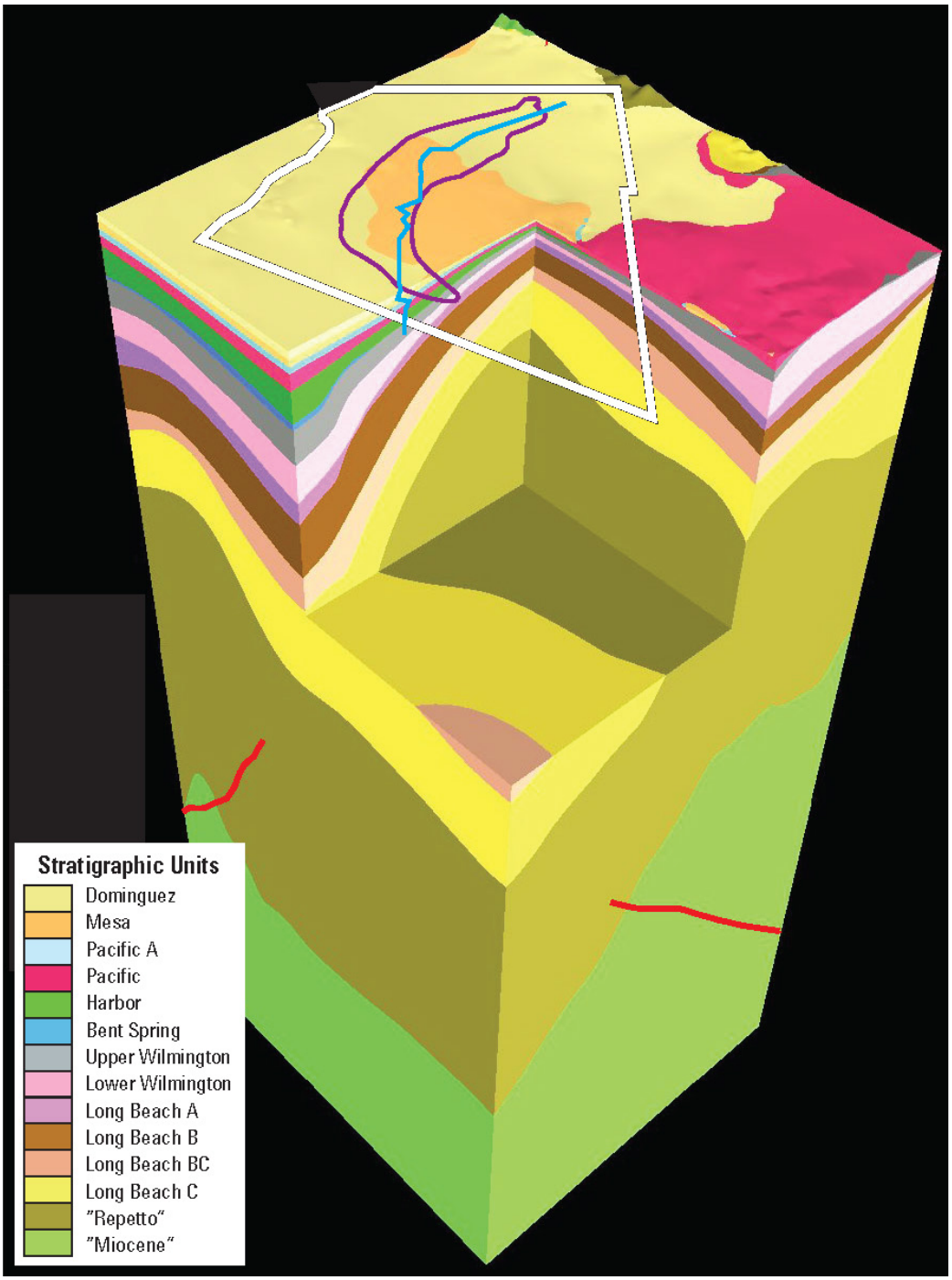

Figure 3. Three-dimensional stratigraphic model of the Santa Fe Springs–Whittier–Norwalk area. View to the north with look angle of 45°; vertical exaggeration is 4 to 1. The model extends from the ground surface to an elevation of -6 km. Red lines are traces of the Santa Fe Springs segment of the Puente Hills Thrust as represented by the Southern California Earthquake Center Community Fault Model (Plesch and others, 2007). The specific study area boundary (white), OU2 plume boundary (purple), and study cross-section line (blue) are shown draped onto the ground surface. The chair-cut into the model extends to an elevation of -1.5 km (the depth of the study cross section) and reveals steep dips of the southwest flank of the Santa Fe Springs Anticline.

A study cross section was selected to assess contaminant distribution in the context of the stratigraphy, and it was used for subsequent groundwater-flow and particle-tracking modeling. Consequently, it was important to align the section to be (1) generally parallel to the direction of groundwater flow, (2) through well sites where contaminant data exist, and (3) through well sites with good information on the distribution of lithologies within sequences. The resultant study cross section alignment is shown on figures 2 and 3. The section starts upgradient of the former Omega facility and is located mostly within the OU2 boundary, except for the southern part of the line where it extends south beyond OU2 through a production well (18G5) and ends at seismic line 8582-1 (fig. 2).

The selected cross section was used to cut the 3D model to reveal the geology along the alignment for further investigation. The resultant section and the unit boundaries within it were manually edited to remove geologically unreasonable interpolation artifacts that are not supported by observation. These discrepancies were minor and were generally associated with pinchouts of units near the north end of the section. The final cross section, along with supporting geologic data and relevant contaminant information, is shown on plate 1.

Modeled Stratigraphic Units

Because the chronostratigraphic framework differs from the previously defined lithostratigraphic formations and aquifer framework, Ponti and others (2007) introduced a set of informal names for Pliocene- and Pleistocene-age chronostratigraphic units that they then correlated to the paleomagnetic and marine oxygen-isotope records. Those names are used here, since most of the Long Beach area sequence boundaries have been mapped into the study area using oil-industry seismic reflection profiles interpreted as part of to the ongoing development of a regional geologic model for the entire Los Angeles Basin. Age estimates for the various sequences derive from Ponti and others (2007) and McDougall and others (2012).

Beneath the study area, 14 stratigraphic units are identified; a summary of the their ages, inferred depositional environments, and probable correlative surficial map units is provided in table 2. The lower two units defined in the table are consolidated rocks of mid-Pliocene and older age (“Miocene” and “Repetto” in table 2), referred to here as “bedrock units”. They are included in the regional model to provide structural context and constraints for the overlying units that are the primary focus of this study. Data used to define the bedrock units within the model come primarily from published sources, except as noted (Wright, 1991; Saucedo and others, 2003; Morton and Miller, 2006). The overlying 12 units are unconformity-bound sequences (or subdivisions within sequences) that range in age from latest Pliocene through Holocene. These units contain, at least in part, water-bearing sediments that are considered to be within the active groundwater flow system in the Los Angeles region.

“Bedrock” Units

“Miocene”

We use the term “Miocene” to represent a unit that serves as the base of the regional geologic model. Its upper surface is derived from structure contours and cross sections at the base of the Repetto Formation of Wright (1991) and is thought to be ~4.5 Ma. We do not subdivide the rocks below this surface, so the volume of the “Miocene” unit incorporates older rocks as well. The top of the “Miocene” reaches a maximum elevation of ~ -2,600 ft at the extreme northeast corner of the study area. Below the study cross section, its maximum elevation is ~ -6,700 ft. The rocks that lie just below the “Miocene” boundary are roughly age-equivalent to the Puente Formation, exposed in the Puente Hills to the east of the study area, where the unit consists of micaceous shale, siltstone, sandstone, and pebble conglomerate

of marine origin, and were likely deposited at bathyl depths (Yerkes, 1972). Wells that penetrate this unit within the study area have not been evaluated.

"Repetto"

The term Repetto Formation is an unofficial name that has been used to describe rocks of Pliocene age encountered in the subsurface of the Los Angeles Basin (for example, Reed, 1933; Kew, 1937). The rocks are defined on the basis of microfaunal zones (for example, Natland, 1953; Natland and Rothwell 1954; Blake, 1991). As described by those workers, the Repetto Formation is not a lithostratigraphic unit nor, due to the time-transgressive nature of the microfaunal zones, is it a chronostratigraphic unit. Durham and Yerkes (1964) have argued for the term "lower member of the Fernando Formation" to describe these rocks in outcrop. We use the informal term "Repetto" in this study to label the rocks that lie between the "Miocene" surface defined above, and an apparent unconformity identified by seismic reflection profiles in the Central Basin (djp-hor4; fig. 4). This horizon appears correlative with the top of the Repetto presented in cross sections around the basin margins (including the study area) by Wright (1991), but lies above (is younger than) Wright's top of the Repetto elsewhere.

The "Repetto" is found beneath the entire study area. The top of this unit occurs at a depth of ~700 ft bls at the north end of the study cross section and is found at a depth of 1,650 ft bls near the crest of the Santa Fe Springs Anticline, based on a change in electric log character at site T_364P (fig. 2; pl. 1). The "Repetto" is presumed to be correlative with the lower member of the Fernando Formation (Durham and Yerkes, 1964; Yerkes, 1972) where it crops out at the northeast edge of the study area. The exposed lower member of the Fernando Formation is composed of siltstone, sandstone, and conglomerate of marine origin. It was likely deposited as deep as 8,200 ft below sea level at the base of a steep submarine slope (Yerkes, 1972).

Late Pliocene and Quaternary Chronostratigraphic Units

Long Beach C

The Long Beach C sequence (Lower Long Beach unit of McDougall and others, 2012) was identified and characterized in the Long Beach area by a thin, fining-upward sand at its base, overlain by sediment that generally coarsens upward (Ponti and others, 2007). A similar composition is observed in the Long Beach C sequence in the study area, as determined by its electric log character at site T_364P on the study cross section (pl. 1). The sequence varies in thickness from ~170 ft at the crest of the Santa Fe Springs Anticline, to more than 1,500 ft at the southend of the cross section. Depth to Long Beach C at the anticline crest is ~1,150 ft bls. The top of the sequence is marked by a well-defined seismic reflector (djp-hor3_7; fig. 4) that can be correlated throughout the Central Basin.

Long Beach C is inferred to be of latest Pliocene age, (> 2.6 Ma) based on microfossil and paleomagnetic constraints from the overlying Long Beach B sequence (McDougall and others, 2012). It is likely correlative, in part, with the upper member of the Fernando Formation that crops out to the east of the study area. Where exposed, the upper member of the Fernando Formation consists of a basal conglomerate, overlain by sandstone and pebbly sandstone. The upper member of the Fernando is inferred to be of marine (neritic) origin, deposited in water <600 ft deep (Yerkes, 1972), but in the study area, west of the basin margin, water depths may have been somewhat greater.

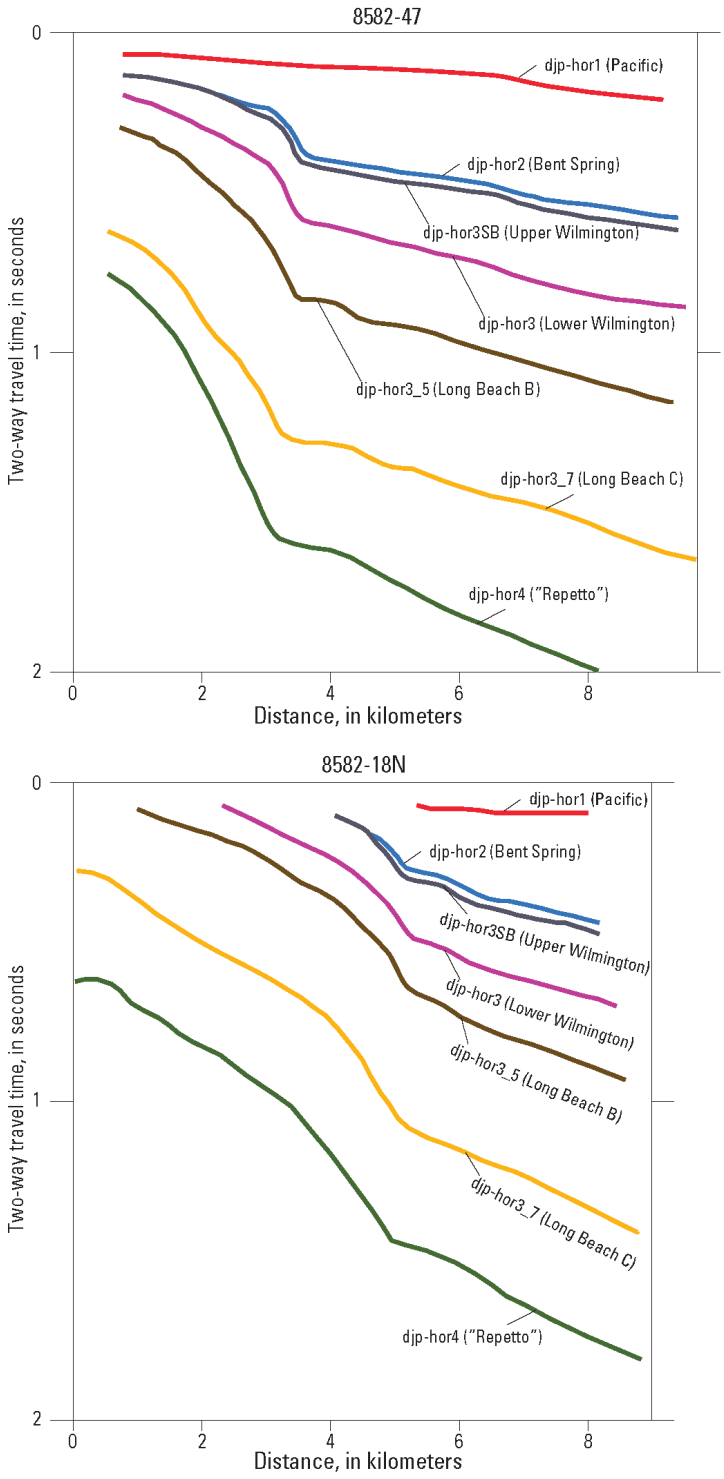

Figure 4. Sequence boundaries interpreted from selected seismic reflection data in the Santa Fe Springs–Norwalk–Whittier area. See figures 1 and 2 for location; north is to the left. Horizons shown represent the top surfaces of correlative sequences. The original seismic images, from which these interpretations derive, are made available for research purposes, but remain proprietary.

Long Beach BC

The Long Beach BC unit is defined as the upper part of the Long Beach C sequence in the eastern Central Basin. It was not subdivided in the Long Beach area, but such a subdivision is made in the Central Basin, based on a character change in electric log signatures. Moreover, some hydrographs from wells screened in this unit have a different character from wells screened deeper in the Long Beach C sequence or the overlying Long Beach B sequence, so the subdivision proves useful for groundwater-flow modeling. Evidence for erosion, onlap, or toplap at the base of the unit has yet to be discerned from seismic reflection data, so it is unclear if Long Beach BC is bounded by unconformities or if it is a conformal unit that composes the uppermost part of the Long Beach C sequence.

In the study area, Long Beach BC is indistinguishable from the Long Beach C sequence at the north end of the study cross section; it reaches a maximum thickness of ~950 ft at the south end of the section (pl. 1). Based on its electric log character at site T_364P, the unit appears considerably sandier than Long Beach C, and displays a coarsening-upward character consistent with a prograding coastline or delta. Because this unit is considered to be part of the Long Beach C sequence, its age is inferred to be the same as Long Beach C.

Long Beach B

The Long Beach B sequence (Middle Long Beach unit of McDougall and others, 2012) was described in the Long Beach area as a generally fining-upward package, possibly reflective of a marine transgression, with a sandy base eventually grading up into silt (Ponti and others, 2007). In much of the Central Basin, the sequence consists of a basal fining-upward section overlain by a generally coarsening-upward package indicative of high-stand progradation. The coarsening-upward section of Long Beach B typically is very coarse-grained and several production wells in the study area are screened within these sands. The top of Long Beach B is defined by a strong reflector (djp-hor3_5; fig. 4) in the seismic data that exhibits evidence of local truncation.

On the study cross section, Long Beach B ranges in thickness from ~120 ft at the northend of the cross section to >1,100 ft at the south end (pl. 1). Depth to the top of the sequence at the anticline crest is ~500 ft bls. The characteristic stacking pattern of the Long Beach B sequence is evident in electric logs from sites T_364P and 6Q4 (pl.1; appendix A).

Microfossil and paleomagnetic data from two core holes in the Long Beach area indicate an early Pleistocene to late Pliocene age for Long Beach B. Planktic foraminifers suggest correlation with Northern Hemisphere glaciation (2.75 to ~2.0 Ma) and an early Pleistocene warm period (~2 Ma). However, paleomagnetic analysis correlates this sequence with the Olduvai Normal Polarity Subchron (1.9–1.8 Ma) and thus overlaps with the ages predicted by the planktic foraminifers, but significantly restricts the age range of this sequence in that area (McDougall and others, 2012). While it is possible that the Long Beach B sequence could be of late Pliocene age (>2.6 Ma) based on the microfossils, fossil reworking may have occurred, and the younger age for the sequence (~2 Ma) appears more likely.

No outcrop of Long Beach B is recognized near the study area, but based on its age, it is possible that some portions of the upper member of the Fernando Formation may be time-correlative with Long Beach B. A marine depositional environment, probably neritic to bathyl water depths, is inferred for this sequence in the study area.

Long Beach A

The Long Beach A sequence (Upper Long Beach unit of McDougall and others, 2012) is identified in the Long Beach area based on a distinctive electric log signature and a strong, regionally extensive reflector located offshore in San Pedro Bay (Ponti and others, 2007). However, in the Central

Basin, the top of this sequence is difficult to discern in industry seismic reflection data, and no clear seismic horizon corresponding to the top of this sequence is recognized. At site 6Q4 (pl. 1), the Long Beach A sequence is marked by a coarse base and top, with apparent finer-grained sediment in the middle. This pattern is not as clearly recognized at site T_364P, where Long Beach A is separated from the underlying Long Beach B sequence by a thin clay or fine-grained unit based on electric logs. In the study area, Long Beach A appears to be ~170 ft thick and is inferred to pinch out against the Long Beach B sequence at the northern end of the study cross section. Depth to the top of the sequence at the anticline crest is estimated to be ~350 ft.

Microfossil and paleomagnetic data from the Long Beach A sequence in the Long Beach area indicate an age similar to that of Long Beach B (for example, ~2.0 Ma or >2.6 Ma; McDougall and others, 2012). However, in Long Beach, the top of Long Beach A represents a major hiatal surface and there is a significant section missing above this horizon. In the Central Basin and the southern part of the study area, where the basin is deeper and more of the section presumably is preserved, it is likely that much of the Long Beach A is younger than the portion of the sequence preserved in Long Beach. We tentatively infer the Long Beach A sequence in the subsurface of the Santa Fe Springs–Whittier–Norwalk area to be correlative with exposures of San Pedro Formation in the Coyote Hills, where analysis of macrofossils and a strontium isotope age determination of 1.4±0.4 Ma from a *Patinopecten caurinus* (Gould) collected from the upper part of the San Pedro Formation indicates a lower Pleistocene age (Powell and Stevens, 2000). If this correlation is valid, the Long Beach A sequence reflects an inner neritic environment in the Coyote Hills, and somewhat deeper water deposition in the vicinity of the study area.

Lower Wilmington

The Lower Wilmington sequence in the Long Beach area consists of blocky, basal sands capped by thick muds and an overall coarsening-upward character (Ponti and others, 2007). In seismic reflection profiles, the top of the sequence is marked by a clear seismic reflector (djp-hor3; fig. 4) and the sequence shows internal clinoform structure. On the study cross section, the Lower Wilmington has a thickness of ~500 feet at the south end of the section, and thins to ~160 ft at the anticline crest. Depth to the Lower Wilmington at the crest of the anticline is ~165 ft.

In the study area and along the study cross section, only a few boreholes with high-quality logs intersect the sequence. The best descriptions of the sequence come from sites MW17 and MW26 near the crest of the Santa Fe Springs Anticline. These wells penetrate only the upper portion of the sequence, that it is characterized by sand that caps an overall coarsening-upward package. The log for site MW17 describes oxidation at the top of the sequence, suggestive of a buried soil or subaerial weathering. Gley colors described for the sequence at site MW26, coupled with the presence of marly clay, suggest a marine origin.

The ages and paleoecologic interpretations from cores in Long Beach indicate deposition in both warm- and cool-water intervals. Paleomagnetic interpretation places this entire sequence in the Brunhes Normal Polarity Chron, that restricts the age to 0.78 Ma or younger. In one corehole, the Lava Creek B ash (639±2 ka) occurs in the lower part of the Lower Wilmington sequence, and biostratigraphy suggests an age >0.6 Ma (McDougall and others, 2012). In the northern Central Basin, marine deposits of similar character that contain the Bishop ash (~0.76 Ma) and have reversed magnetic polarity (Quinn and others, 2000), suggest that the base of the Lower Wilmington may extend into the lower Pleistocene in the study area.

We correlate the subsurface Lower Wilmington sequence with outcrops of the Coyote Hills Formation in the Coyote Hills (Durham and Yerkes, 1964; Yerkes, 1972). There, the Coyote Hills

Formation is of paralic and nonmarine origin. However, in the study area, descriptions of the subsurface Lower Wilmington suggest that it may be of shallow marine origin.

Upper Wilmington

The Upper Wilmington sequence in the Long Beach area contains the type Silverado aquifer, which is the primary producing aquifer in the basin (Ponti and others, 2007). Electric log signatures and well logs from across the basin indicate that the Upper Wilmington was primarily deposited in shallow marine waters (inner- to outer-neritic) and records an episode of significant delta progradation across a shelf from the Whittier Narrows area toward Long Beach. The top of this sequence is defined by a well-expressed seismic reflector (djp-hor3SB; fig. 4), and like the underlying Lower Wilmington sequence, the Upper Wilmington displays internal clinoform structure. Coarse-grained axial channel deposits and shallow-marine sands make excellent aquifers and the sequence is extensively pumped within the basin. In the study area, the Upper Wilmington sequence is off-axis from the main delta channels, so it tends to be fairly fine-grained. However, it still maintains the coarsening-upward pattern of stacked beds characteristic of marine progradation and is typically capped by a sand. The Upper Wilmington sequence reaches a maximum thickness at the south end of the study cross section of ~400 ft, and thins to ~50 ft over the crest of the Santa Fe Springs Anticline (pl. 1). Depth to the top of the Upper Wilmington at the crest of the anticline is ~120 ft.

The age of the Upper Wilmington is constrained to <600 ka and > 470 ka based on the age of the underlying Lower Wilmington sequence, and analysis of microfossils in the Long Beach area. Estimates for the age of the Upper Wilmington from correlation to marine oxygen-isotope stages is between 475–580 ka (Bassinot and others, 1994).

We correlate the Upper Wilmington sequence in the study area to exposures of nonmarine sands, gravels, and silts of the La Habra Formation in the Coyote Hills. The stacking pattern, gley colors, and the presence of marly clay within the Upper Wilmington beneath the study area suggest a shallow marine origin, such that the Upper Wilmington shoreline was likely situated not far to the east of the study cross section.

Bent Spring

In the Long Beach area, the Bent Spring sequence is correlated by Ponti and others (2007) to the type San Pedro Sand, Timms Point Silt, and Lomita Marl of Woodring and others (1946). The sequence of deposits represents a prograding shallow-marine delta that was deposited into a subsiding trough adjacent to the Palos Verdes Peninsula. However, over much of the Central Basin the sequence is quite thin, as evident in seismic reflection profiles (djp-hor2; fig. 4). Within the study area the Bent Spring sequence is largely absent; seismic reflection data show it pinches out around the margins of the Santa Fe Springs Anticline. On the study cross section, the Bent Spring is inferred to be present at the southern end of the section, where it is ~40 ft thick. In this area it is likely of paralic or shallow-marine origin.

Data from the Long Beach area provide an age estimate of 200–500 ka for the Bent Spring sequence (McDougall and others, 2012). Bounding constraints from the underlying Upper Wilmington sequence and thermoluminescence (TL) ages suggest that the age of Bent Spring is more likely between 300–450 ka. No correlative surface outcrops are known in the study area.

Harbor

In the Long Beach area, the Harbor sequence is an areally extensive series of deposits that record a coastal progradation, and consist of a number of sedimentary environments from marine-shelf to

coastal beach, tidal flats, lagoons, and possibly fluvial channels and floodplains (Ponti and others, 2007). In the Central Basin, electric log signatures and well log descriptions suggest that the Harbor sequence is mostly of shallow-marine origin. The top of the Harbor sequence is not clearly distinguishable in seismic reflection profiles. In the study area, the Harbor sequence is modeled to reach a maximum thickness of ~380 ft at the south end of the study cross section, but thins to ~35 ft at the crest of the Santa Fe Springs Anticline (pl. 1). Depth to the top of the Harbor sequence at the crest of the Santa Fe Springs Anticline is ~60 ft.

North of and near the crest of the Santa Fe Springs Anticline, the Harbor sequence is typically olive-colored, and shows a fining-upward character that often consists of a basal gravelly sand that grades upward to a silt at the top of the unit. South of the anticline crest the unit's character changes, with either aggradational stacking or a possible coarsening-upward sequence, and gley colors are noted locally (site MW27). Although not definitive, this apparent change in character within the Harbor sequence suggests a facies transition from a dominantly fluvial environment to the north, to a paralic or shallow-marine depositional environment to the south.

The age of the Harbor sequence, based on macrofossils and TL dates from the Long Beach area, (McDougall and others, 2012) is constrained between 100–275 ka, with a best estimate inferred from ages of underlying and overlying sequences of between ~160–200 ka. No outcrops of correlative deposits are known near the study area.

Pacific

In the Long Beach area, the Pacific sequence consists of shallow marine, marine terrace, paralic, and nonmarine deposits, and is correlated in part with the Palos Verdes Sand (Ponti and others, 2007). Like the Harbor sequence, the Pacific appears to be dominantly of shallow-marine origin in the Central Basin. In the study area, the Pacific sequence reaches a maximum thickness of ~180 ft at the south end of the study cross section, but thins to ~25 ft at the anticline crest, and appears to pinch out at the north end of the cross section. Its top is defined by a distinctive seismic reflector in the Central Basin, but this reflector is often difficult to correlate on lines where the horizon reaches shallow depths. Depth to the top of the Pacific unit at the crest of the anticline is ~30 ft.

In the northern part of the study area, the sequence is characterized by fining-upward beds, typically with a basal sand that grades up to a silt or silty clay that caps the unit. To the south, gley colors are noted in some logs, and changes in the stacking pattern suggest that the unit may be transitioning basinward from a nonmarine, alluvial fan origin, to a paralic or even shallow-marine origin.

In the Long Beach area, the Pacific sequence is believed to have resulted from a marine high-stand progradation during early $\delta^{18}O$ stage 5 (~97–122 ka; Bassinot and others, 1994), based on TL dates, macrofossil data, amino-acid racemization age estimates on marine-terrace deposits, and the presence of the Blake paleomagnetic event (Ponti, 1989; McDougall and others, 2012). McDougall and others (2012) report optically stimulated light (OSL) dates from the same sequence that are as young as 28–33 ka, but these ages appear to be too young, as they are contradicted by the weight of other evidence. The Pacific sequence appears to correlate with very old alluvial fans that crop out at the east end of the study area (fig. 2).

Pacific A

The Pacific A unit is a subdivision thought to represent the lower portion of the overlying Mesa sequence and is not recognized in the Long Beach area. In the Central Basin, it is subdivided to accommodate observed variations in water levels and hydrograph character that are apparent within the

Mesa sequence, where the Mesa thickens significantly. The top of Pacific A is usually identified as the base of a fining-upward package that is often seen within the Mesa sequence, but in some cases, the top of the Pacific A is ambiguous in borehole or electric logs. As with the Long Beach BC unit, it is unclear whether the top Pacific A represents a true unconformity or is a conformal boundary that represents a change in character within the Mesa sequence. In the study area, the Pacific A reaches a maximum thickness of ~100 ft at the south end of the study cross section. It appears to pinch out to the north and is missing over the crest of the Santa Fe Springs Anticline, but reappears in the La Habra Syncline, where the unit appears to be ~25 ft thick (pl. 1).

Based on age estimates for the Mesa sequence, the Pacific A unit is late Pleistocene in age, most likely <80 ka. The fining-upward nature of this unit in the study area suggests that it is of fluvial origin. There are no known outcrops that correlate with the Pacific A unit, although as the basal unit within the Mesa sequence, Pacific A deposits may correlate with some old alluvial fan exposures within the study area (fig. 2).

Mesa

The Mesa sequence is the youngest of the Pleistocene-age sequences in the Los Angeles Basin. In the Long Beach area, the Mesa is composed of marine-terrace, paralic, and nonmarine deposits, but in the study area it appears to be entirely of fluvial origin. As expressed in borehole and electric logs, the sequence fines upward; it typically has a sandy base that is inferred to have been deposited within fluvial channels, and is capped by probable overbank or flood-basin silts and clays. It is exposed at the surface at the crest of the Santa Fe Springs Anticline and is likely correlative with other surficial units mapped as old-alluvial-fan-deposits by Saucedo and others (2003) and Morton and Miller (2006). In the subsurface, the top of the unit is readily picked at the base of a coarse-sand or gravel deposit that marks the beginning of the Holocene progradation. The Mesa sequence reaches a maximum thickness of ~120 ft at the south end of the study cross section, but is only ~30 ft thick on the anticline crest.

Young marine-terrace deposits in the Long Beach area assigned to the Mesa sequence are inferred to be ~80 ka old based on amino-acid racemization data (Ponti, 1989; Ponti and others, 2007), but OSL, TL, and radiocarbon dates on fluvial deposits, and the occurrence of the Laschamp paleomagnetic event within the sequence, indicate that much of the sequence is probably on the order of 20–40 ka (McDougall and others, 2012).

Dominguez

The Dominguez sequence is the result of deposition that occurred in response to worldwide climate change that initiated the Holocene epoch and ended the last major glacial stage (McFadden, 1982; Bull, 1991). This transition destabilized the landscape and exposed the soil mantle to erosional processes. Resultant erosion caused mountain streams to aggrade rapidly and push sediment out onto the coastal plain, ultimately filling the eroded channels and blanketing the coastal plain with flood deposits (Bull, 1991).

In the study area, the Dominguez sequence reaches a thickness of >100 ft at the south end of the study cross section. It is not present over the crest of the Santa Fe Springs Anticline, but is present in the La Habra Syncline, where it rarely exceeds 30 ft in thickness. The Dominguez sequence typically is comprised of a sandy or gravelly basal unit that grades up into silt. In some areas, such as northeast of the anticline, the basal channel deposits are thin or missing, and the bulk of the sequence is fine grained. OSL, TL, and radiocarbon dates, as well as macrofossil evidence from the Long Beach area, indicate that the Dominguez sequence is younger than 18 ka (McDougall and others, 2012).

Geologic Structures

The prominent structure exposed in the study area is the Santa Fe Springs Anticline, a simple elongate dome with an axis that trends ~N 70° W. across OU2 (Winter, 1943; see fig. 2). This fold occurs within the center of the study area and is one of a series of west-northwest trending structures inferred to reflect activity on the blind Puente Hills Thrust (Shaw and Shearer, 1999; Shaw and others, 2002;). Oil was first discovered within middle Pliocene to upper Miocene sediment ("Repetto" and "Miocene" chronostratigraphic units, respectively) in 1919, and the resulting Santa Fe Springs Oil Field is projected to ultimately produce 622 million barrels of oil, the fourth largest oil field in the Los Angeles Basin (Wright, 1991).

Bounding unconformities interpreted from north-south seismic lines 8582-47 and 8582-18N (fig. 4; locations shown on figures 1 and 2) and correlated to Pleistocene- and Pliocene-age sequences, clearly show (1) the steep southwest limb of the Santa Fe Springs Anticline to the north (left) end of the lines, (2) thinning of the stratigraphic section toward the crest of the anticline, (3) pinchout to the north of the Bent Spring sequence on the fold's flank, (4) a well-defined axial surface where the plunges of reflectors decrease abruptly south of the anticline, and (5) continued thickening of the stratigraphic section (especially in the younger sequences) as the reflectors plunge deeper into the southern Central Basin. On the southwest limb, dips reach a maximum of ~36° on the top of the "Repetto" sequence, 20° on the top of the Upper Wilmington sequence, and ~4° on the top of the Pacific sequence. These relations indicate that folding has been ongoing from "Repetto" depositional time to at least the late Pleistocene. Exposed Mesa sequence near the fold axis and recent seismicity attributed to the Puente Hills Thrust suggest that deformation is continuing (Shaw and Shearer, 1999; Pratt and others, 2002; Shaw and others, 2002).

Available seismic data do not extend completely across the fold, so we do not have as clear a picture of the stratigraphy and structure at the anticlinal crest or within the La Habra Syncline (which occurs northeast of the anticline and southwest of the Puente Hills; fig. 2), nor does the seismic data resolve well above ~300 ft depth bls. Plate 1 shows the modeled crest of the anticline and the trough of the syncline clearly defined by the top of the "Repetto" unit, as derived from small-scale maps in Wright (1991). The geometry of overlying units is not well constrained, however, until ~200 ft bls, where high-quality borehole data exist. Based on these controls, the crest of the Santa Fe Springs Anticline is much gentler and broader in the Upper Wilmington through Mesa sequences than it is at depth, and it appears that the axial surface that defines the crest of the Santa Fe Springs Anticline may be shifted to the north ~3,000 ft relative to its position at the top of the "Repetto" unit (and relative to the anticline axis displayed on fig. 2, that is derived from oil field data). This shift may represent recent northward vergence of the fold, but could be an artifact in the cross section that results from inaccuracies related to different scales of input data.

Available seismic data and sequence boundary correlations in borehole data reveal an important characteristic about the geologic structure in the study area—sequences that occur at significant depths at the south end of OU2 and to the west of the plume boundary occur at much shallower depths in the vicinity of the anticline and the OU2 plume.

Comparison to Current Hydrostratigraphic Framework and Aquifer Nomenclature

The hydrostratigraphic framework and nomenclature of CDWR (1961) that is the standard currently used in groundwater investigations, derives from Quaternary mapping and subsurface correlation by Woodring and others (1946), and Poland and others (1956, 1959). These workers cast the Quaternary geology of the Los Angeles Coastal Plain into a lithostratigraphic framework, where units were defined and correlated according to their lithologic character, which is reflective of depositional

environment. Water-bearing zones occur in both Holocene- and Pleistocene-age deposits. The Holocene series is composed of surficial alluvial fans, channels, and valley deposits that are easy to distinguish from older sediments based their geomorphology. The Pleistocene-age deposits in the basin are divided into upper and lower series. The lower series, of marine origin, is represented by the San Pedro Sand, Timms Point Silt, and Lomita Marl of Woodring and others (1946) and the San Pedro Formation of Poland and others (1956, 1959). The upper series (Terrace Deposits, Unnamed Upper Pleistocene) is largely of nonmarine and paralic origin. The transition from marine Lower Pleistocene to nonmarine Upper Pleistocene is consistent with our understanding that the Los Angeles Basin has been shoaling since the onset of transpressive tectonic deformation during the Pliocene. These lithostratigraphic units, because of their distinctive facies, fossils, and lithologic characteristics, are easy to distinguish in outcrop and in the subsurface from drillers' and electric logs.

Following these early workers, CDWR (1961) identified and correlated water-bearing zones – sandy facies – within this lithostratigraphic framework. The Gaspur aquifer, included in a unit named Recent Alluvium by CDWR (1961) was placed within the Holocene series defined by Poland and others (1956, 1959). The next older (deeper) aquifers, the Exposition, Artesia, Gage, and Gardena, are of nonmarine origin and were therefore placed into the Lakewood Formation (Unnamed Upper Pleistocene of Poland and others, 1956; 1959) and correlated in the subsurface based on stratigraphic position. Next, the aquifers of marine origin (Hollydale, Jefferson, Lynwood, Silverado, and Sunnyside, in stratigraphic order from top to bottom), were placed within the Lower Pleistocene San Pedro Formation.

The classic subdivision within the Pleistocene-age units into upper and lower series gives rise to the notion of "shallow" and "deep" groundwater systems. The "shallow" systems consist of nonmarine aquifers of the Holocene series and Lakewood Formation— all of which may be interconnected and are younger everywhere in the basin than the "deep" system. The "deep" system consists of marine sands, which, because of their greater homogeneity, tend to be more productive sources of groundwater. Because the two systems reflect different depositional settings, and were considered to be separated in time, historical reasoning suggested there would be little opportunity for connectivity between the systems (mergence of aquifers), except in the forebay area (fig. 1) where recharge into both systems occurs (CDWR, 1961).

Figure 5 shows how our chronostratigraphic structural model in the Santa Fe Springs–Whittier–Norwalk area compares to the lithostratigraphic model of CDWR (1961). Figures 5*A*-*C* show parts of CDWR (1961) cross sections B-B′, C-C′-C′′, and N-N′ respectively, where they cross the region of the 3D chronostratigraphic model (fig. 1). The 3D model was cut along these section traverses and the unit tops revealed in those cross sections are superimposed on the CDWR interpretation.

We observe good agreement between the youngest sequences (Dominguez and Mesa) and the youngest aquifers (Gaspur and Exposition), both on the crest and the southwest flank of the Santa Fe Springs Anticline. This relation is not unexpected because in the CDWR model, original depositional surfaces of Holocene and late Pleistocene alluvial-fan and valley deposits are mostly preserved, and are mapped using geomorphology and stratigraphic position, so these units are essentially chronostratigraphic units.

However, the close association between the chronostratigraphic units and aquifer boundaries breaks down in the older units, as one moves from the fold crest into the Central Basin (fig. 5). The aquifers, as represented in the CDWR model, cross time-lines defined by the chronostratigraphic model and the actual structural relief of the Central Basin is under-represented by the lithostratigraphically-based aquifer stratigraphy. The chronostratigraphic sequences contain genetically related packages of sediment that form in response to base-level change. At the basin margin, nonmarine deposits transition into coastal deposits basinward, and these deposits in turn transition basinward into marine deposits

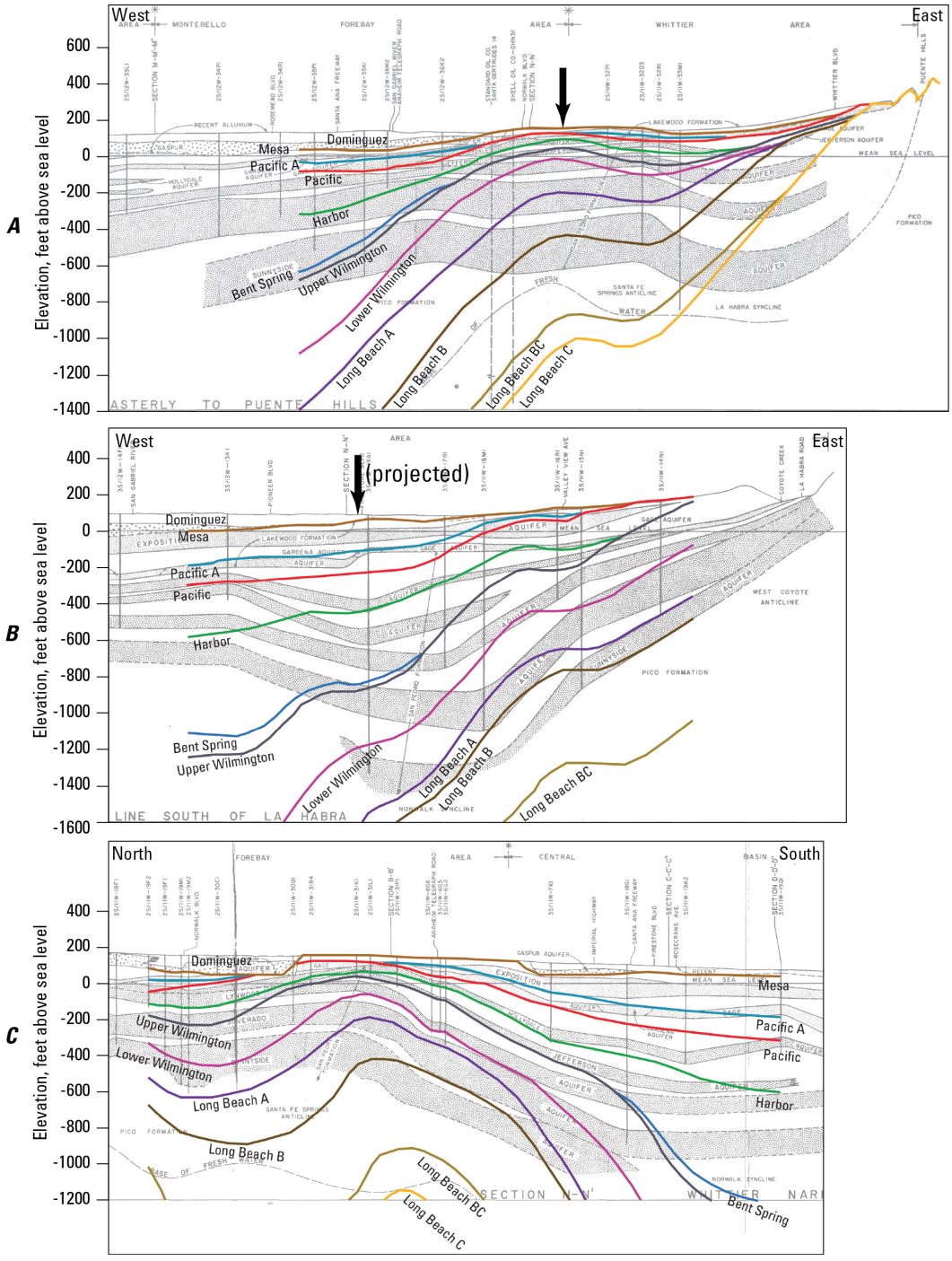

Figure 5. Boundaries of chronostratigraphic units compared to classical aquifer geometry derived from lithostratigraphic correlations. *A*, Part of cross section B-B′, *B*, part of cross section C-C′-C′′, *C,* part of cross section N-N′ from CDWR (1961). See figure 1 for location; vertical exaggeration is ~10:1. Chronostratigraphic boundaries shown are the tops of the units described in this report and were extracted directly from the 3D digital geologic model along the CDWR section lines and modified to remove geologically unreasonable modeling artifacts. Approximate intersection of these sections with the study cross section (arrows) as seen in fig. 2. Section *C* lies slightly west of, and parallels the north-south portion of study cross section.

within the same sequence. As the basin shoals, the nonmarine facies of subsequent sequences would prograde further into the basin center. If one correlates this architecture lithostratigraphically, the marine facies of different sequences would be correlated across sequence boundaries, as would overlying nonmarine facies. The effect of this interpretation not only artificially reduces the structural relief of the basin, but the lithostratigraphic correlations cannot represent the true architecture of the aquifer system.

By placing the stratigraphy of the Santa Fe Springs–Whittier–Norwalk area into a chronostratigraphic context, the notion of separate "shallow" and "deep" aquifer systems in the east Los Angeles Basin is dispelled. The cross sections in figure 5 show it is possible to associate chronostratigraphic units with the CDWR aquifers in the vicinity of the Santa Fe Springs Anticline crest and the southwest flank of the fold (table 3). From this, we can see that water flowing within a single chronostratigraphic unit might appear to be migrating between shallow and deep aquifers, when in fact no such migration between units is occurring.

Hydrologic Characteristics and Contaminant Occurrence Along Study Cross Section

This section discusses the association between contaminant occurrence, geology, and hydrology along a two-dimensional cross section through the study area (pl. 1; fig. 2). The trend of the OU2 plume is inferred to parallel the shallow groundwater gradient (EPA, 2010), which trends southwest from the former Omega facility, turns to the south at about the location of the Santa Fe Springs Anticline crest, and then trends slightly to the southeast, south of site C_603. The regional groundwater gradient, derived from deeper, producing aquifers, does not show the same southeastward bend (Water Replenishment District of Southern California (WRD), 2013), and instead maintains a south-southwest trend across the entire study area. As shown on figure 2, the study cross section begins just northeast of the former Omega facility and approximately follows the trend of the OU2 plume downgradient to the southwest and south until site MW29, where it continues approximately due south through the site of active production well 18G5. This alignment is therefore approximately flow-parallel to both the inferred shallow and regional groundwater systems along most of the section.

The modeled chronostratigraphy along the study cross section (pl. 1) is derived from the 3D structure model, and is therefore informed by stratigraphic data both on and off of the cross-section alignment. Plate 1 also shows generalized lithologies and electric log curves for boreholes along the alignment, the location of well screens, and a representation of contaminant occurrence from wells where VOC data are available.

This discussion focuses on the distribution of five target constituents—tetrachlorethene (PCE), trichloroethene (TCE), trichlorofluoromethane (Freon 11), trichlorotrifluoroethane (Freon 113), and 1,4-dioxane. As discussed previously, the co-occurrence of all 5 target constituents (OSCs) is suggestive of contamination that originates from the former Omega facility (EPA, 2010). Table 4 summarizes the concentrations of these five compounds measured in recent water samples collected along the study cross section (EPA 2010; Murex Environmental, Inc., 2011; CH2M HILL, 2012; T. Perina, CH2M Hill, written commun., 2012).

General Observations

The data from Table 4 are represented graphically on plate 1 by colored circles placed adjacent to the well screens where the water samples were obtained. In general, the highest concentrations observed are for tetrachloroethene (PCE) and trichloroethene (TCE) and the concentrations of these two compounds are reflected in the sizes of the circles on plate 1. The color of each circle indicates the number of target constituents that have been detected historically at each well. If a target constituent was not detected in a recent round of sampling, but was detected historically, that constituent is

Table 3. Comparison of chronostratigraphic units and major aquifers in two parts of the study area, Central Basin groundwater contamination study, Los Angeles County, California.

Chronostratigraphic unit	Santa Fe Springs Anticline crest		Southwest flank of Santa Fe Springs Anticline	
	Associated major aquifers (CDWR, 1961)	Subsurface Formation (CDWR,1961)	Associated major aquifers (CDWR, 1961)	Subsurface Formation (CDWR,1961)
Dominguez	Gaspur	Recent Alluvium	Gaspur	Recent Alluvium
Mesa	Exposition	Lakewood Formation	Exposition	Lakewood Formation
Pacific A	Gage	Lakewood Formation	Gage, Gardena	Lakewood Formation
Pacific	Exposition-Gage	Lakewood Formation	Hollydale, Jefferson	San Pedro Formation
Harbor	Hollydale, Jefferson	San Pedro Formation	Jefferson, Lynwood, Silverado	San Pedro Formation
Bent Spring	not present	--	Silverado, Sunnyside	San Pedro Formation
Upper Wilmington	Jefferson, Lynwood	San Pedro Formation	Lynwood, Silverado, Sunnyside	San Pedro Formation
Lower Wilmington	Silverado	San Pedro Formation	Silverado, Sunnyside	San Pedro Formation
Long Beach A	Silverado, Sunnyside	San Pedro Formation	Silverado, Sunnyside	San Pedro Formation/Pico Formation
Long Beach B	Sunnyside	San Pedro Formation	Sunnyside	San Pedro Formation/Pico Formation
Long Beach BC	not in active groundwater system	Pico Formation	Pico	Pico Formation
Long Beach C	not in active groundwater system	Pico Formation	Pico	Pico Formation
"Repetto"	not in active groundwater system	Repetto Formation	not in active groundwater system	Repetto Formation
"Miocene"	not in active groundwater system	Puente Formation	not in active groundwater system	Puente Formation

Table 4. Compilation of selected volatile organic compounds, reported 2004–10, from wells along study cross section, Central Basin groundwater contamination study, Los Angeles County, California (available as a .xlsx file only online *at http://pubs.usgs.gov/of/2014/1087/*).

considered present for the purpose of the presentation on plate 1. This was done to assess the likelihood that a particular well screen is within the path of a plume that may have originated at or near the former Omega facility. In some wells, one or more of the target constituents have never been analyzed for; in those instances, the compounds are represented on plate 1 as if they have never been detected, but are recorded in table 4 as "nc" (not collected). In many of the wells where only 3 of the 5 target constituents co-occur, the missing two compounds are Freon 11 and Freon 113. Freon 11 and Freon 113 are considered by the EPA (2010) to be tracer compounds used to map the extent of VOCs in groundwater that have migrated from the former Omega facility. Also shown with the contaminant data on plate 1 are arrows that represent results of a Mann-Kendall trend analysis performed by CH2M HILL (2012). Upward pointing arrows show where there is a statistically significant trend of increasing contaminant concentration from 2006 through first quarter 2011, and downward pointing arrows show where contaminant concentrations appear to be decreasing. Wells with no arrow symbols do not show any statistical trends or were not evaluated.

The highest concentrations of PCE and TCE are observed at fairly shallow depths near the former Omega facility (for example, at well OW1A, screened between 63–78 ft bls; at well OW8A screened between 60–80 ft bls). Concentrations decrease rapidly downgradient, but high concentrations of PCE and TCE [>10 times the maximum contaminant level (MCL)] are observed as far downgradient as the location of well C_603 (screened between 70–100 ft bls), ~4 mi from the former Omega facility. OSCs are observed in almost all wells along the the study cross section where the sum of PCE and TCE concentrations are high (>50 µg/L). The only exceptions are well MW27B (screened between 144–164 ft bls), and possibly well OFRP-MW3 (screened between 64–109 ft bls). Both of these wells are located ~3 mi downgradient of the former Omega facility. OFRP-MW3 is screened in the Pacific sequence. It has detections of PCE, TCE and Freon 11, but has never been analyzed for 1,4-dioxane or Freon 113. However, OSCs are observed in nearby well MW27A, which is also screened in the Pacific sequence. It is therefore reasonable to infer that OFRP-MW3 would have detections of both Freon 113 and 1,4-dioxane if analyzed. Well MW27B is screened in the Harbor sequence. This well has a high concentration of TCE (280 µg/L), and a moderately high PCE concentration (9.6 µg/L), but no measureable Freon 11 or Freon 113.

Where the sum of measured PCE and TCE concentrations is <50 µg/L, OSC observations are limited to wells occurring at or upgradient from site MW23, located ~1.25 mi from the former Omega facility. Thus, at distances greater than 1.25 mi downgradient of the former Omega facility, there is a direct association between the concentration of PCE and TCE, and the likelihood that all five target constituents co-occur.

Both OSC occurrence and high PCE- and TCE-concentrations (pl. 1) are confined to the young Mesa sequence upgradient of site MW23, located ~1.25 mi downgradient of the former Omega facility. Downgradient of site MW23, OSCs with high concentrations of PCE and TCE are observed in progressively older stratigraphic units, such that by site MW16, ~0.5 mi farther downgradient, OSCs are observed in well MW16C (screened between 149–164 ft bls) within the upper part of the Upper Wilmington sequence. It is over this same distance that the modeled chronostratigraphic units are inferred to rise onto the crest of the Santa Fe Spring Anticline.

In general, OSCs are observed farthest downgradient in the youngest units, and the downgradient extent of OSCs appears to be progressively less in the older units. Within the Mesa

sequence and the Pacific A unit, OSCs are observed as far as ~4 mi downgradient at site C_603. Within the Pacific sequence, OSCs are observed as far downgradient as site MW27, ~3 mi from the former Omega facility. Unfortunately, the downgradient extent of OSCs in the Pacific sequence is not well constrained, as no monitoring wells are screened in Pacific sequence aquifers downgradient of site MW27. In the Harbor and Upper Wilmington sequences, OSCs as observed as far downgradient as site MW26, ~2.2 mi from the former Omega facility.

Only two monitoring wells are screened within the Lower Wilmington sequence on the study cross section. Both wells, MW17C (screened from 172–182 ft bls) and MW26D (screened from 185–205 ft bls), occur along the crest of the Santa Fe Springs Anticline. OSCs are not observed in these wells, but measured concentrations above laboratory reporting limits for both Freon 11 and Freon 113 have historically been detected in well MW26D (table 4). If the Freon compounds are indeed tracers indicative of contaminants that originate from the former Omega facility, then contaminants from the former Omega facility may extend as far downgradient as site MW26 within the Lower Wilmington sequence, as well as within the overlying Upper Wilmington and Harbor sequences. Interestingly, no detections of Freon compounds have ever been measured in well MW17C, located ~1,100 ft upgradient of site MW26. This suggests that Freon compounds are migrating downward into the Lower Wilmington sequence from the Upper Wilmington sequence at some point between the two wells. Such an inference is speculative, however, as it does not consider the potential for flow into the section from paths that are out of plane, or other processes that could affect Freon migration.

Detections of PCE, TCE and 1,4-dioxane, but not Freon compounds, are observed in both the Harbor and Upper Wilmington sequences as far downgradient as site MW27, ~3 mi from the former Omega facility, at depths as great as 210 ft bls (well MW27D, screened from 200–210 ft bls). Detections of target constituents PCE, TCE and 1,4-dioxane at low concentrations are also observed in production well 18G5, ~5.5 mi downgradient from the former Omega facility (pl. 1; fig. 2). The screened interval in this well is from 200 to 402 ft bls, but on the basis of a dynamic flow profile that was performed (A. Chakmak, Golden State Water Company, written commun., January 2012), about 85 percent of the total flow occurs at depths between 300 and 350 ft. This would suggest that target constituents are entering the well from the upper portion of the Pacific sequence. We cannot establish with certainty whether contaminants are migrating within the Pacific sequence directly between well MW27A (where OSCs and high measured PCE and TCE concentrations occur) and production well 18G5, but we cannot discount it. Additional monitoring wells and (or) depth-dependent sampling in production wells screened within the Pacific and adjoining sequences will be needed to establish whether contaminants within the Pacific sequence upgradient in the OU2 plume may be moving into production well 18G5.

In summary, the observed distribution of target constituents along the study section, in relation to the modeled chronostratigraphy, shows that OSCs occur within progressively older units downgradient of the former Omega facility. In the vicinity of the northern flank and crest of the Santa Fe Springs Anticline (near and downgradient of site MW16), all units above the Lower Wilmington show evidence of contamination by OSCs, with at least locally high concentrations of PCE and TCE. Downgradient of the anticlinal crest, units that contain OSCs near the fold crest plunge into the southern Central Basin, and small concentrations of PCE, TCE and 1,4-dioxane have been detected from within what appears to be the upper part of the Pacific sequence in production well 18G5, located near the south end of the study cross section. The occurrence of OSCs in units older than Pacific A are not observed more than 3 miles downgradient from the former Omega facility, but data are lacking from older units downgradient of site MW27 that could clarify whether contaminants within the Pacific sequence and older units might be migrating to deeper depths downgradient.

Hydrologic Conditions and Occurrence of Inter-sequence Flow

Despite limitations inherent in evaluating contaminant distribution along a two-dimensional profile, consistent patterns in the relations of contaminant distributions to geology can be discerned. Moving southwest from the former Omega facility, high concentrations of all OSCs appear to advance downgradient within the near-surface units (for example, Mesa sequence and Pacific A), but also appear to progressively migrate into older sequences, moving into at least the Upper Wilmington sequence, and possibly the upper portion of the Lower Wilmington sequence. Although our data are limited, most of the migration into older sequences appears to be occurring near the crest and northeast flank of the Santa Fe Springs Anticline, where these units are at shallow depths.

Vertical flow between sequences is supported by water level measurements along the study cross section (fig. 6) that show a downward vertical-gradient exists between units and that, with few exceptions, this pattern has been persistent over time. At the north end of the profile, hydrographs from multilevel monitoring sites indicate that most of the downward vertical-gradient occurs between the Mesa and Pacific sequences (site MW24; fig. 6). Near the north flank and crest of the anticline (sites MW23, MW23A, MW17, MW26) downward vertical-gradients appear to exist between all of the sequences, with overall head differences of between ~8 and 25 ft (fig. 6). At site MW16, where OSCs are first observed within the Upper Wilmington sequence, head differences are small (<5 ft between the Pacific and Upper Wilmington sequences). This may be an indication of interconnection (mergence) among aquifers near site MW16. On the southwest flank of the fold (site MW27), there appears to be a strong vertical gradient (~20 ft head difference) between the Harbor and Upper Wilmington sequences, but little vertical gradient between the Pacific and Harbor sequences. The nature of the vertical gradients is unclear in the southern part of the study area, because water-level measurements confined to individual sequences (and within the older sequences) are not available south of site MW27. Relative vertical gradients south of site MW27 must be determined to ascertain whether groundwater flow will migrate downgradient within sequences, continue to move downward into older sequences, or migrate upward into younger sequences. It is also not known whether the pattern of vertical gradient occurrence along the cross section alignment persists elsewhere in the study area.

While the hydrologic conditions near the anticline crest could permit vertically-downward migration of contaminants and inter-sequence flow in this area, water-level measurements also show that a strong gradient exists along the section within each sequence, and that this pattern persists over time (fig. 7). Water levels fall more than 100 ft within the Mesa sequence between the north end of the profile (site OW4A) and site MW29. Over a distance of <3 mi, water levels decrease ~50–60 ft from north to south within each of the Pacific, Harbor, and Upper Wilmington sequences (fig. 7). These flow gradients would permit a conceptual model where most of the groundwater flow stays within a sequence where aquifer facies are expected to be genetically connected. Given that all of the units plunge into the southern Central Basin south of the anticline crest, groundwater flow parallel to the sequence boundaries would serve to transport contaminants to greater depths to the south without further requirement for inter-sequence flow.

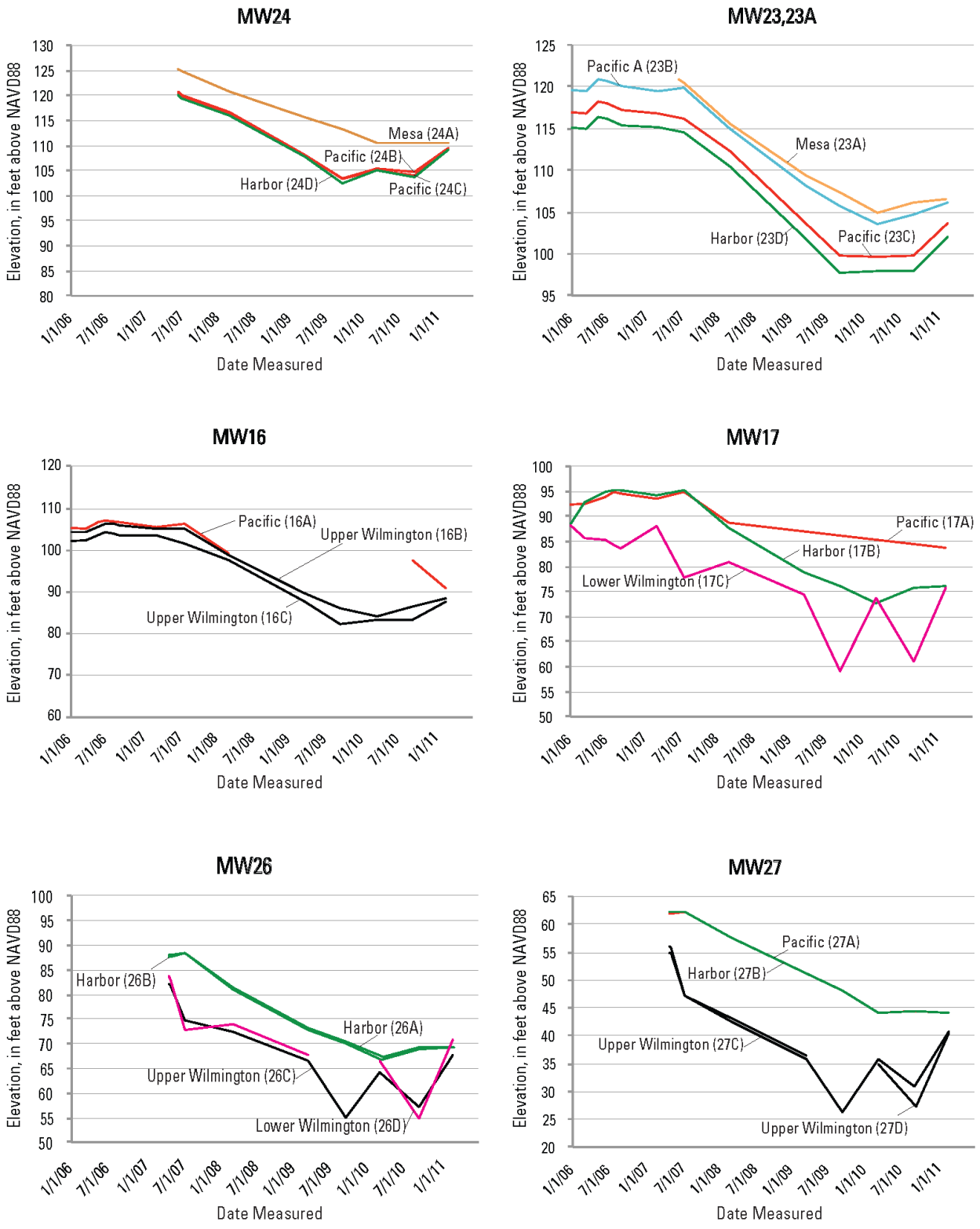

Figure 6. Hydrographs for selected wells along the study cross section. See table 1 and appendix A for well construction details.

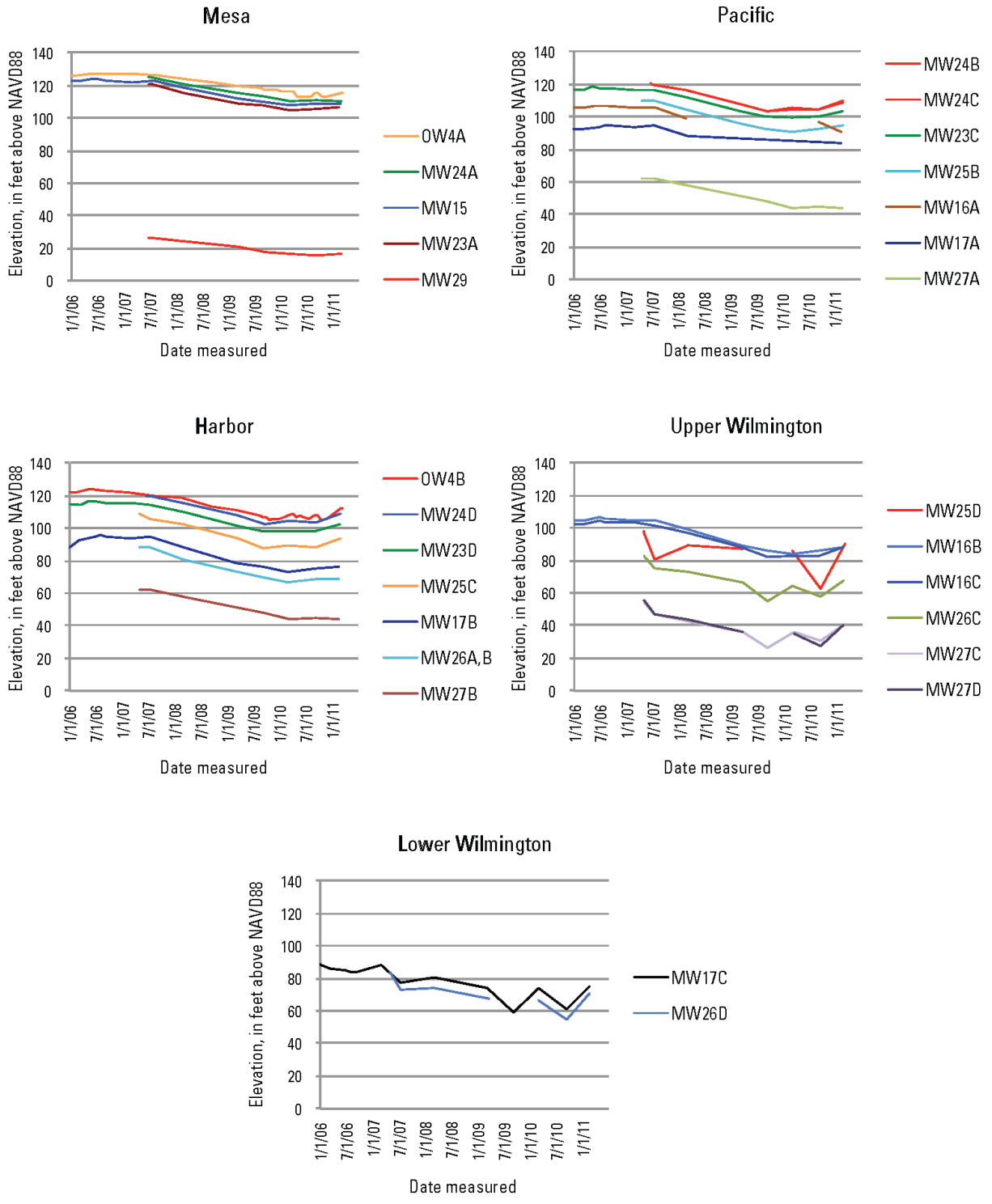

Figure 7. Hydrographs for study cross section wells, grouped by chronostratigraphic unit. Hydrographs colored by well. The explanation lists wells in order from north (upgradient) to south (downgradient). In nearly all cases, hydrographs show water levels systematically decreasing from north to south along the section within each chronostratigraphic unit.

One possible conceptual model for groundwater flow in the vicinity of the anticline crest is shown in figure 8. The distribution of likely aquifer and aquitard material is based on borehole log descriptions, electric logs, and the recognition that these dominantly fluvial packages tend to fine upwards. Bed-level correlations are tenuous in this setting because of the complex internal architecture of alluvial fan material, the wide spacing between boreholes, and the orientation of the study cross section, which is oblique to the dominant northeast-southwest trend of drainages and alluvial fan axes south of site MW25. Thus, individual facies, such as channel sands, may not persist for significant distances along portions of the section.

Finer-grained facies that are generally associated with the uppermost portions of the sequences are shown in blue (silt/clay dominant) and gold (silt and fine sand dominant) in figure 8. South of site MW23, near the anticline crest, these "capping aquitards" tend to consist of silts and fine sands rather than clays, and the silt/clay zones are quite rare and thin. As such, the finer-grained caps to the sequences may be "leaky" in the anticline region, and could provide a pathway for inter-unit flow (purple arrows in the figure), given the overall downward gradient that is observed in this area. The occurrence of more permeable, or thinner, low-permeability zones at the tops of sequences adjacent to the anticlinal crest is likely not a coincidence. Because uplift and folding are syndepositional, thinner units and more extensive erosion during periods of low base-level would be expected near the fold crest relative to the flanks. If more extensive erosion were to have occurred near the fold crest, this would preferentially remove the topmost and finest-grained portions of the sequences, providing opportunities for groundwater to more readily flow between units.

There may be other preferential pathways leading to inter-unit flow that are unrecognized or occur off of the profile alignment. These pathways can occur locally beneath channel deposits that are incised through the finer-grained tops of underlying sequences. If these channel deposits are present in the study area, they would likely occur along northeast-southwest trends that would cross the study cross section and might not be discernible in our present model because the cross-sectional widths of these channels would likely be small. A better representation of facies distribution in three-dimensions would be required to identify the likely physical pathways for inter-unit flow, but based on the structural setting of the study area, these natural pathways would most likely be concentrated near the fold crest.

Within some aquifer systems, it has been documented that water and contaminants can be distributed between zones with different heads by ambient flow through wellbores intersecting multiple aquifers (Santi and others, 2006; Landon and others, 2010). The study area includes hundreds of oil and agricultural wells of various ages (EPA, 2010). It is possible that some of these wells could have leaky wellbores that would permit water and contaminants to move vertically along preferential pathways. It is beyond the scope of this study to examine the potential effects of preferential pathways on contaminant transport. However, if wellbore leakage was a predominant transport pathway, it is expected that contaminants from shallow zones would be ubiquitous throughout deeper stratigraphic units beneath the defined OU2 plume, and this does not appear to be the case. Instead, observed contaminant distribution in the aquifer system along the study section more reasonably supports a model of contaminant transport controlled by natural movement of water through layered sediments with the geometry as modeled from available borehole and seismic data. Therefore, while possible effects of wellbore leakage on contaminant transport cannot be dismissed, this mechanism is likely localized and not considered to be of primary importance in controlling contaminant distributions in the study area.

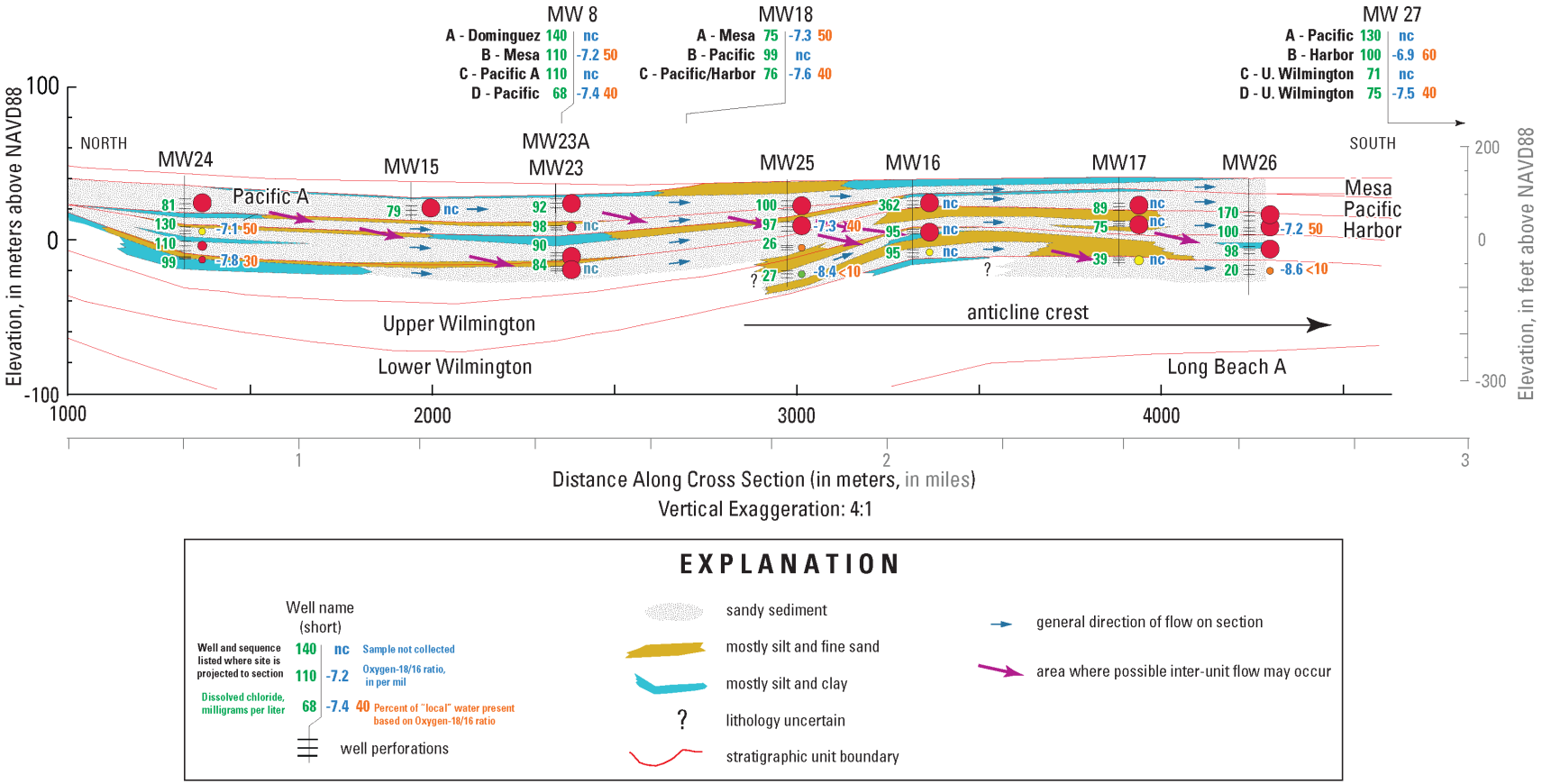

Figure 8. Conceptual model for groundwater flow near the Santa Fe Springs Anticline crest. Conceptual model for groundwater flow showing possible fluid flow pathways that can explain observed water quality and contaminant distribution along a section near the Santa Fe Springs Anticline crest. Colored circles next to well screen symbols represents contaminant distribution (see pl. 1). Dissolved chloride data are from EPA (2010); all other data shown from this study. The percentage of local water present in the water samples (orange) assumes mixing occurs only between water derived directly from nearby drainages with an assumed $\delta^{18}O$ of -5.8 per mil (based on samples from well W1-5), and water derived from the San Gabriel Mountains and entering the basin from the Whittier Narrows, with an assumed $\delta^{18}O$ of -8.5 per mil (similar to water from well MW25D). Site MW8 is projected from ~690 ft west of the section, while site MW18 is projected from ~1/2 mi east of the section. Site MW27 occurs on the study cross section about 0.9 mi south of well MW26.

In the study area vicinity, there are 17 production wells known to have been active between 2000–10 (fig. 2). Of these 17 wells, 14 are screened between the Lower Wilmington and Pacific A units. The remaining three wells are screened within the older Long Beach units. We observe on our study cross section that the Upper Wilmington through Mesa sequences are locally contaminated with OSCs and have PCE and (or) TCE concentrations >10 times the MCL. We infer that this contamination reflects inter-unit flow controlled by the stratigraphic architecture in the vicinity of the Santa Fe Springs anticlinal crest. Although contaminant concentrations are low, two monitoring wells on the study cross section screened within the Lower Wilmington sequence have yielded detections of some of the target constituents. Thus, the 14 production wells screened within the Lower Wilmington and younger units are pumping from zones that are stratigraphically connected to contaminated zones within OU2. Several of these wells, including well 18G5 discussed above, have experienced VOC detections. We cannot directly attribute these detections to contaminants from OU2, but we can conclude that there are likely direct stratigraphic pathways that would allow migration of contaminants to these wells from shallow zones near the Santa Fe Springs Anticline, should appropriate hydraulic conditions exist.

Groundwater Sampling and Geochemistry

New water-chemistry data were collected and analyzed as part of this study, and integrated with previously collected information (tables 5–7). The new groundwater chemistry, isotope, and age-tracer information was used to further understanding of groundwater-flow patterns in the study area. Specifically, water chemistry signatures in wells distributed along, or near, the study cross section were compared to evaluate the connections between contaminated shallow groundwater and deeper parts of the groundwater system used for water supply. This section describes well selection, sample collection and analysis methods, and use of the data to evaluate the distribution of different groundwater sources in the study area. The final part of this section discusses our understanding of the groundwater-flow system determined from a combination of new and existing water-chemistry data.

Methods of Analysis

Well-location and construction data were compiled from the Los Angeles County Department of Public Works, EPA, Water Replenishment District of Southern California (WRD), and the USGS into a geographic information system. These data provided an inventory of potential sampling wells. After contacting well owners, selected wells were visited to confirm suitability for sampling and to record site characteristics.

Samples collected from wells were analyzed for dissolved inorganic constituents (major and minor ions, trace elements, and nutrients), VOCs, stable isotopes of oxygen and hydrogen, and groundwater-age tracers tritium and carbon-14. The dissolved inorganic constituent data provides information on geochemical signatures in different parts of the groundwater system that can be used to evaluate groundwater flowpaths. The VOC samples were collected for comparison with VOC data from other sources and to fill data gaps. The isotopic data were used to compare and contrast groundwater recharge sources for different parts of the flow system. Age-tracers were used to estimate travel times from recharge areas for young and old components of the groundwater system.

Table 5. Well identification and sample information for wells sampled, 2010–11, Central Basin groundwater contamination study, Los Angeles County, California.

[Well name in first column appears in table 1 and indicates location of well shown in figure 2. Samples from all 36 wells were analyzed for stable isotopes of water; samples from 16 wells were analyzed for volatile organic compounds; samples from 6 wells were analyzed for tritium and selected inorganic constituents; seven samples were analyzed for carbon isotopes; nc, not collected. Purge method: ap, active pumping production well; db, dedicated bladder pump; ps, portable submersible pump.]

Well name (short)	State well number	Sample date	Purge method	Type of sample collected				
				Stable isotopes of water	VOC	Inorganic	Tritium	Carbon isotopes
6N1	003S011W06N001S	9/29/2010	ap	x	x	x	x	x
32J4	002S011W32J004S	9/29/2010	ap	x	x	x	x	x
30R3	002S011W30R003S	9/29/2010	ap	x	x	nc	nc	nc
MW8B	002S011W29N004S	9/9/2010	db	x	nc	x	nc	nc
MW8D	002S011W29N002S	9/9/2010	db	x	nc	x	nc	nc
MW18A	002S011W32G006S	9/10/2010	db	x	nc	x	nc	nc
MW18C	002S011W32G004S	9/10/2010	db	x	x	x	nc	nc
MW24B	002S011W29J004S	9/10/2010	db	x	nc	nc	nc	nc
MW24D	002S011W29J002S	9/10/2010	db	x	nc	nc	nc	nc
MW25B	002S011W32E004S	9/9/2010	db	x	nc	nc	nc	nc
MW25D	002S011W32E002S	9/9/2010	db	x	x	nc	nc	nc
MW26B	002S011W31Q005S	9/9/2010	db	x	nc	nc	nc	nc
MW26D	002S011W31Q003S	9/9/2010	db	x	nc	nc	nc	nc
MW27B	003S011W06G015S	9/8/2010	db	x	nc	nc	nc	nc
MW27D	003S011W06G013S	9/8/2010	db	x	nc	nc	nc	nc
MW28	003S011W06N005S	9/8/2010	db	x	nc	nc	nc	nc
MW30	003S011W17D005S	9/8/2010	db	x	nc	nc	nc	nc
N1-5	003S011W17F005S	5/26/2011	ps	x	x	nc	x	x
N1-4	003S011W17F004S	5/26/2011	ps	x	x	nc	x	x
N1-3	003S011W17F003S	5/26/2011	ps	x	x	nc	x	x
N1-2	003S011W17F002S	5/26/2011	ps	x	nc	nc	nc	nc
N1-1	003S011W17F001S	5/26/2011	ps	x	nc	nc	nc	nc
N2-6	003S012W11A012S	4/20/2011	ps	x	nc	nc	nc	nc
N2-5	003S012W11A011S	4/20/2011	ps	x	nc	nc	nc	nc
N2-4	003S012W11A010S	4/20/2011	ps	x	x	nc	nc	nc
N2-3	003S012W11A009S	4/20/2011	ps	x	x	nc	nc	x
N2-2	003S012W11A008S	4/20/2011	ps	x	x	nc	nc	nc
N2-1	003S012W11A007S	4/20/2011	ps	x	nc	nc	nc	nc
W1-5	003S011W02K007S	9/28/2010	ps	x	x	nc	nc	nc
W1-3	003S011W02K008S	9/28/2010	ps	x	x	nc	nc	nc
W2-6	002S011W20N006S	4/20/2011	ps	x	nc	nc	nc	nc
W2-5	002S011W20N005S	4/20/2011	ps	x	nc	nc	nc	nc
W2-4	002S011W20N004S	4/20/2011	ps	x	x	nc	x	x
W2-3	002S011W20N003S	4/20/2011	ps	x	x	nc	nc	nc
W2-2	002S011W20N002S	4/20/2011	ps	x	x	nc	nc	nc
W2-1	002S011W20N001S	4/20/2011	ps	x	nc	nc	nc	nc
Total				*36*	*16*	*6*	*6*	*7*

Table 6. Major sources of groundwater recharge and descriptive information, Central Basin groundwater contamination study, Los Angeles County, California.

Source of recharge (study-area end member)	Isotopic composition[1,2,4]	Relative age[1,4]	Dissolved chloride[1-5]	Example	Comment
Local	about -5.8 per mil δO^{18} and -42 per mil δH^2 (ranges from -6.5 to -5.8, and -43 to -37, respectively), and on or above the global meteoric water line	pre-modern	variable, depending on location and depth; 80–280 mg/L (1)	Whittier-1 #3 (W1-3)	Principally runoff from Puente Hills; probably some precipitation within the study area
San Gabriel native	about -8.5 per mil δO^{18} and -56 per mil δH^2 (ranges from -8.7 to -8.1, and -58 to -53, respectively), and above the global meteoric water line	pre-modern	20–30 mg/L for this study; can range from 10–60 mg/L (2,3,5)	Whittier-2 #2 (W2-2); Norwalk-1 #4 (N1-4)	Natural, pre-development drainage from the San Gabriel Valley through Whittier Narrows
Artificial / engineered	variable; -8.8 to -7.6 per mil δO^{18} and -66 to -56 per mil δH^2 found in water from wells near spreading grounds; always below the global meteoric water line	modern	variable; about 40–120 mg/L (3,4)	Whittier-2 #5,6 (W2-5,6)	Includes a mixture of imported-, storm-, and recycled-water diverted into the San Gabriel River spreading grounds

[1] This study, and other regional USGS sampling events, 2000–08; accessed March 2011 at http://waterdata.usgs.gov/ca/nwis/qw.

[2] Reichard and others (2003)

[3] Water Replenishment District of Southern California (2012; 2013)

[4] Anders and Schroeder (2003)

[5] Piper and Garrett (1953)

Table 7. Summary of selected well-construction information, as well as chemical and isotopic data (available as a .xlsx file only online at *http://pubs.usgs.gov/of/2014/1087/*).

Selection of Wells

To enhance the set of existing water-quality data utilized in this study, samples were collected from 36 wells and analyzed for selected chemical and isotopic constituents. The wells selected for sampling (tables 1, 5, and 7) reflect the combination of three selection strategies.

First, 14 monitoring wells located at 8 single- or multiple-well monitoring sites operated by the EPA were selected for sampling to gain additional detail on groundwater conditions within the OU2 plume. At multiple-well monitoring sites, samples were collected from the deepest well and a shallow or intermediate-depth well to help identify changes in water chemistry with depth at a single location.

Second, three active production wells in the study area were available for sampling. All three production wells have multiple screened intervals and tap several stratigraphic units. Water samples collected from these wells likely include water from all of the screened units, and provide a contrast to the discrete, depth-specific observation wells. One production well (30R3) is located in the upgradient portion of the study area, ~1 mi from OU1. Another production well (6N1) is located downgradient of the regional anticline feature. The third production well (32J4) was chosen as a background well for the study area as it is located somewhat upgradient to the east, ~1/2 mi from edge of the OU2 plume (fig. 2).

Third, 19 wells from 4 regional multiple-well monitoring sites owned by the WRD were selected for sampling to characterize groundwater conditions in or near the study area, especially at greater depths than contaminated, shallow groundwater zones. Inclusion of these wells provides a context for observed variations in groundwater conditions with depth in the regional-flow system.

Well locations were verified using a global positioning system (GPS), 1:24,000-scale USGS topographic maps, comparison with existing well information in USGS and other databases, and information provided by well owners, drillers' logs, and (or) other sources of construction information. Well location and information were recorded on field sheets. All information was verified and uploaded into the USGS National Water Information System (NWIS) database. For some wells, information describing the well location and construction was submitted to CDWR so that an official state well name could be assigned and recorded.

Previous water-chemistry data collected by USGS in the regional monitoring wells were incorporated in the analysis. Data collected from these wells prior to the study sample collection in 2010–11 are footnoted in table 7.

Sample Collection and Analysis

USGS field personnel collected water samples from wells listed in table 5 from September 2010 through April 2011. Except for the three production wells, arrangements were made with the well owner or designee for collection of a 'split' sample during a regularly scheduled sampling event by other agencies (WRD or EPA) with dedicated sampling equipment. At all wells, field parameters (temperature, specific conductance, pH, dissolved oxygen, and dissolved sulfide) were measured. Samples were also collected for analysis of stable isotopes of oxygen and hydrogen, data that were otherwise lacking in the study area. From selected wells, samples were collected for analysis of inorganics, VOCs, tritium, and carbon isotopes based on the need to fill data gaps (table 7).

At the regional multiple-well monitoring sites, a portable positive-displacement pump was used to purge the well until three casing volumes of water were removed, and measured field parameters stabilized. A check valve was placed between the sample pump and tubing to minimize flow from the

hose into the well casing. A pre-cleaned, double-check valve bailer was used to retrieve a sample for VOCs; the bailer was secured 1 ft below the portable pump using stainless-steel wire. Immediately after purging concluded, the bailer was rapidly lowered an additional 5 ft and then retrieved for processing.

Each monitoring well selected for sampling within the OU2 area had a dedicated bladder pump and pump tubing to allow sampling using low-flow sampling techniques, as described by the EPA (2010). Low-flow sampling is the process of purging and sampling wells at low-flow rates from within the well screen zone to minimize the volume of extracted water. During well purging, continuous, closed-cell measurements of field parameters were used to assess when purged water had reached equilibrium. Each well was pumped until specific conductance, pH, and temperature measurements stabilized within 10 percent over three successive readings prior to collecting samples.

Water samples from production wells were collected from a designated faucet at (or near) the wellhead, and prior to any pressure tank or distribution pipe, following methods detailed by Mathany and others (2008).

Following collection, samples were processed according to procedures outlined by the USGS National Field Manual (variously dated). Major ions, trace elements, and nutrients were analyzed by the USGS National Water Quality Laboratory (NWQL) in Denver, Colo., using standard methods outlined by Fishman and Friedman (1989), Faires (1993), Fishman (1993), and Jones and Garbarino (1999). Stable isotopes of oxygen and hydrogen were analyzed by the USGS Isotope Laboratory in Reston, Va., using methods described by Révész and Coplen (2008a, 2008b). The ratio of oxygen isotopes, $\delta^{18}O$, is expressed as the ratio of oxygen-18 (^{18}O) to the more common isotope, oxygen-16 (^{16}O), relative to the ratio in a standard reference material, Vienna Standard Mean Ocean Water (VSMOW), in per mil. The ratio of hydrogen isotopes, $\delta^{2}H$, is expressed as the ratio of hydrogen-2 (^{2}H) to the more common isotope, hydrogen-1 (^{1}H), relative to the ratio in VSMOW, in per mil (Coplen, 2011). Tritium was analyzed at the USGS Menlo Park Isotope Tracer Laboratory using electrolytic enrichment and gas scintillation (Thatcher and others, 1977). The activity of tritium is reported in terms of tritium units (TU); each tritium unit equals one atom of ^{3}H in 10^{18} atoms of hydrogen. Carbon-14 was analyzed by the Woods Hole Laboratory in Woods Hole, Mass., using methods described by McNichol and others (1994). The activity of carbon-14—expressed as percent modern carbon (pmc)—is reported relative to the 1950 National Bureau of Standards (NBS) oxalic acid standard (Stuiver and Polach, 1977). Analytical results of samples collected and analyzed as part of this study are presented in tables 8–10 and selected results discussed in the text are summarized in table 7.

Study-specific quality assurance and quality control samples were not collected for this study investigation due to practical or physical sampling limitations. The method uncertainties for $\delta^{18}O$ and $\delta^{2}H$ data are 0.2 and 2 per mil, respectively (Révész and Coplen, 2008a,b). These values are much less than the isotopic contrasts in environmental samples discussed in this report. For all other constituents discussed in this report (chloride, tritium, carbon-14, and selected VOCs), results of historical analyses of replicate samples (for example, Mathany and others, 2008) show uncertainties in results are many times less than ranges in environmental concentrations in the study area. Analyses of hundreds of field-blank samples collected for VOCs by the USGS in California during 2005–10 indicate concentrations of PCE, TCE, Freon 11, and Freon 113 are rarely detected, and reporting levels for these VOCs in groundwater samples can be considered statistically equivalent to the laboratory reporting levels (Fram and others, 2012). Reporting levels for VOC analyses in this study are listed in table 10. Concentrations of VOCs below or near the reporting levels need to be regarded with caution. However, in this study, noted concentrations of VOCs were many times larger than reporting levels. In 7 of 16 well samples collected and analyzed for VOCs in this study, there were no VOC detections (table 10). These results indicate that VOC samples were collected for this study without systematic sample bias (contamination

Table 8. Results for analyses of stable isotope ratios, carbon-14 activities, and tritium in samples collected, 2010–11, Central Basin groundwater contamination study, Los Angeles County, California.

[Well name in first column appears in table 1 and indicates location of well shown in figure 2. The five-digit USGS parameter code below the constituent name is used to uniquely identify a specific constituent or property. Stable isotope ratios are reported in the standard delta notation (δ), the ratio of a heavier isotope to the more common lighter isotope of that element, relative to a standard reference material; TU, tritium unit; 1 TU is approximately equal to 3.19 picocuries per liter; nc, not collected; <, less than]

Well name (short)	State well number	$\delta^{2}H$ (per mil) (82082)	$\delta^{18}O$ (per mil) (82085)	$\delta^{13}C$ (per mil) (82081)	Carbon-14 (percent modern) (49933)	Tritium (TU) (07000)
W2-6	002S011W20N006S	-52.50	-7.62	nc	nc	nc
W2-5	002S011W20N005S	-58.50	-8.35	nc	nc	nc
W2-4	002S011W20N004S	-46.30	-6.92	-17.08	38.43	1.3
W2-3	002S011W20N003S	-56.00	-8.46	nc	nc	nc
W2-2	002S011W20N002S	-58.10	-8.70	nc	nc	nc
W2-1	002S011W20N001S	-53.80	-8.19	nc	nc	nc
MW24B	002S011W29J004S	-46.84	-7.06	nc	nc	nc
MW24D	002S011W29J002S	-51.20	-7.80	nc	nc	nc
30R3	002S011W30R003S	-55.90	-8.14	nc	nc	nc
MW8B	002S011W29N004S	-49.90	-7.21	nc	nc	nc
MW8D	002S011W29N002S	-49.90	-7.40	nc	nc	nc
MW25B	002S011W32E004S	-48.80	-7.32	nc	nc	nc
MW25D	002S011W32E002S	-55.60	-8.43	nc	nc	nc
MW18A	002S011W32G006S	-49.10	-7.30	nc	nc	nc
MW18C	002S011W32G004S	-50.20	-7.55	nc	nc	nc
32J4	002S011W32J004S	-43.40	-6.66	-14.47	50.64	0.1
MW26B	002S011W31Q005S	-47.40	-7.14	nc	nc	nc
MW26D	002S011W31Q003S	-56.50	-8.63	nc	nc	nc
MW27B	003S011W06G015S	-46.84	-6.87	nc	nc	nc
MW27D	003S011W06G013S	-48.80	-7.48	nc	nc	nc
W1-5	003S011W02K007S	-37.80	-5.81	nc	nc	nc
W1-3	003S011W02K008S	-42.00	-6.24	nc	nc	nc
6N1	003S011W06N001S	-53.30	-8.14	-14.71	63.53	0.1
MW28	003S011W06N005S	-51.50	-7.53	nc	nc	nc
N2-6	003S012W11A012S	-54.70	-7.78	nc	nc	nc
N2-5	003S012W11A011S	-61.60	-8.60	nc	nc	nc
N2-4	003S012W11A010S	-57.40	-8.53	nc	nc	nc
N2-3	003S012W11A009S	-55.80	-8.47	-13.25	70.19	nc
N2-2	003S012W11A008S	-52.10	-7.99	nc	nc	nc
N2-1	003S012W11A007S	-54.80	-7.90	nc	nc	nc
MW30	003S011W17D005S	-51.40	-7.50	nc	nc	nc
N1-5	003S011W17F005S	-50.30	-7.59	-18.39	43.36	0.5
N1-4	003S011W17F004S	-55.30	-8.46	-13.96	39.37	0.2
N1-3	003S011W17F003S	-56.70	-8.37	-17.61	17.20	<0.1
N1-2	003S011W17F002S	-62.30	-9.17	nc	nc	nc
N1-1	003S011W17F001S	-48.10	-7.23	nc	nc	nc

Table 9. Concentration of selected inorganic constituents in samples collected, 2010–11, Central Basin groundwater contamination study, Los Angeles County, California.

[Well name in first column appears in table 1 and indicates location of well shown in figure 2. The five-digit USGS parameter code below the constituent name is used to uniquely identify a specific constituent or property; °C, degrees Celsius; E, estimated concentration value; µg/L, micrograms per liter; mg/L, milligrams per liter; nc, not collected or available; µS/cm, microseimens per centimeter; >, greater than; <, less than]

Well name (short)	State well number	Water temperature, °C (00010)	Dissolved oxygen, mg/L (00300)	Sulfide, field, mg/L (99119)	Specific conductance, µS/cm at 25°C (00095)	pH, field, standard units (00400)	Dissolved solids, dried at 180°C, mg/L (70300)	Calcium, mg/L (00915)	Magnesium, mg/L (00925)	Potassium, mg/L (00935)	Sodium, mg/L (00930)
MW8B	002S011W29N004S	nc	>2.0	<0.2	1500	nc	1010	153	40.9	4.10	102
MW8D	002S011W29N002S	nc	1.3	<0.2	1220	nc	832	144	37.8	4.03	64.7
MW18A	002S011W32G006S	nc	2.0	<0.2	2610	nc	1650	231	68.3	5.21	155
MW18C	002S011W32G004S	nc	0.2	<0.2	968	nc	589	92.3	31.0	3.59	45.1
32J4	002S011W32J004S	21.7	0.3	<0.2	1690	7.2	1170	152	53.2	4.45	116
6N1	003S011W06N001S	22.4	<0.2	1.3	724	7.7	455	48.6	8.00	3.18	89.2

Well name (short)	State well number	Alkalinity, mg/L as $CaCO_3$ (29801)	Bromide, mg/L (71870)	Chloride, mg/L (00940)	Fluoride, mg/L (00950)	Silica, mg/L as SiO_2 (00955)	Sulfate, mg/L (00945)	Iron, µg/L (01046)	Manganese, µg/L (01056)	Boron, µg/L (01020)	Iodide, mg/L (71865)
MW8B	002S011W29N004S	410	0.726	94.0	0.31	38.4	238	<6.0	<0.20	368	0.004
MW8D	002S011W29N002S	259	0.339	71.6	0.44	28.2	268	<6.0	0.34	129	0.003
MW18A	002S011W32G006S	351	0.436	94.9	0.27	34.6	686	<12.0	3.91	515	0.045
MW18C	002S011W32G004S	141	0.471	106	0.41	27.8	168	<6.0	0.63	78	0.004
32J4	002S011W32J004S	218	0.616	137	0.32	26.3	446	<6.0	0.26	260	0.015
6N1	003S011W06N001S	191	0.188	38.5	0.25	26.1	115	E3.6	12.2	122	0.014

Table 10. Volatile organic compounds detected in samples collected, 2010–11, Central Basin groundwater contamination study, Los Angeles County, California.

[Well name in first column appears in table 1 and indicates location of well shown in figure 2. The five-digit USGS parameter code below the constituent name is used to uniquely identify a specific constituent or property; E, estimated concentration value; <, less than; VOC, volatile organic compounds]

Well name (short)	State well number	Number of VOC detections per well	Number of tentatively identified compounds, by GCMS (99871)	1,2-Dichloroethane, µg/L (32103)	1,2--Dichloropropane, µg/L (34541)	1,4-Dichlorobenzene, µg/L (34571)	1,1,2-Trichloro-1,2,2-trifluoroethane, µg/L (77652)	1,1-Dichloroethane, µg/L (34496)	1,1-Dichloroethene, µg/L (34501)	1,2-Dichlorobenzene, µg/L (34536)	1,3-Dichlorobenzene, µg/L (34566)
W2-4	002S011W20N004S	3	0	<0.08	<0.0260	<0.026	<0.034	0.014	<0.022	<0.028	<0.024
W2-3	002S011W20N003S	0	0	<0.08	<0.0260	<0.026	<0.034	<0.044	<0.022	<0.028	<0.024
W2-2	002S011W20N002S	0	0	<0.08	<0.0260	<0.026	<0.034	<0.044	<0.022	<0.028	<0.024
30R3	002S011W30R003S	8	0	<0.08	<0.0260	<0.026	2.69	0.057	1.34	<0.028	<0.024
MW25D	002S011W32E002S	1	0	<0.08	<0.0260	<0.026	<0.034	<0.044	<0.022	<0.028	<0.024
MW18C	002S011W32G004S	2	0	<0.08	<0.0260	<0.026	<0.034	<0.044	<0.022	<0.028	<0.024
32J4	002S011W32J004S	1	0	<0.08	<0.0260	<0.026	<0.034	<0.044	<0.022	<0.028	<0.024
W1-5	003S011W02K007S	0	0	<0.08	<0.0260	<0.026	<0.034	<0.044	<0.022	<0.028	<0.024
W1-3	003S011W02K008S	0	0	<0.08	<0.0260	<0.026	<0.034	<0.044	<0.022	<0.028	<0.024
6N1	003S011W06N001S	7	2	<0.08	<0.0260	<0.026	<0.034	0.106	0.518	<0.028	<0.024
N2-4	003S012W11A010S	3	0	<0.08	<0.0260	<0.026	<0.034	<0.044	<0.022	<0.028	<0.024
N2-3	003S012W11A009S	0	2	<0.08	<0.0260	<0.026	<0.034	<0.044	<0.022	<0.028	<0.024
N2-2	003S012W11A008S	0	1	<0.08	<0.0260	<0.026	<0.034	<0.044	<0.022	<0.028	<0.024
N1-5	003S011W17F005S	11	2	0.17	0.0432	3.26	<0.034	<0.044	<0.022	4.74	0.490
N1-4	003S011W17F004S	0	0	<0.08	<0.0260	<0.026	<0.034	<0.044	<0.022	<0.028	<0.024
N1-3	003S011W17F003S	1	2	<0.08	<0.0260	<0.026	<0.034	<0.044	<0.022	<0.028	<0.024

Table 10 Volatile organic compounds detected in samples collected, 2010-11– Continued

[Well name in first column appears in table 1 and indicates location of well shown in figure 2. The five-digit USGS parameter code below the constituent name is used to uniquely identify a specific constituent or property; E, estimated concentration value; µg/L, micrograms per liter; <, less than; VOC, volatile organic compounds]

Well name (short)	State well number	Benzene, µg/L (34030)	Chloro-benzene, µg/L (34301)	*cis*-1,2-Dichloro-ethene, µg/L (77093)	Dichloro-difluoro-methane, µg/L (34668)	Ethyl methyl ketone, µg/L (81595)	Tetrachloro-ethene, µg/L (34475)	*trans*-1,2-Dichloro-ethene, µg/L (34546)	Trichloro-ethene, µg/L (39180)	Trichloro-fluoro-methane, µg/L (34488)	Trichloro-methane, µg/L (32106)
W2-4	002S011W20N004S	<0.026	<0.026	<0.022	<0.10	<1.6	0.100	<0.018	<0.022	<0.06	0.01
W2-3	002S011W20N003S	<0.026	<0.026	<0.022	<0.10	<1.6	<0.026	<0.018	<0.022	<0.06	<0.03
W2-2	002S011W20N002S	<0.026	<0.026	<0.022	<0.10	<1.6	<0.026	<0.018	<0.022	<0.06	<0.03
30R3	002S011W30R003S	<0.026	<0.016	0.118	<0.10	<1.6	2.60	<0.018	4.76	0.88	0.28
MW25D	002S011W32E002S	<0.026	<0.016	<0.022	<0.10	<1.6	E0.010	<0.018	<0.022	<0.08	0.05
MW18C	002S011W32G004S	<0.026	<0.016	<0.022	<0.10	<1.6	E0.020	<0.018	E0.011	<0.08	<0.03
32J4	002S011W32J004S	<0.026	<0.016	<0.022	<0.10	<1.6	<0.026	<0.018	<0.022	<0.08	E0.01
W1-5	003S011W02K007S	<0.026	<0.016	<0.022	<0.10	<1.6	<0.026	<0.018	<0.022	<0.08	<0.03
W1-3	003S011W02K008S	<0.026	<0.016	<0.022	<0.10	<1.6	<0.026	<0.018	<0.022	<0.08	<0.03
6N1	003S011W06N001S	0.045	<0.016	1.70	<0.10	<1.6	E0.022	0.033	3.23	<0.08	<0.03
N2-4	003S012W11A010S	<0.026	<0.026	<0.022	<0.10	<1.6	0.276	<0.018	0.490	<0.06	0.06
N2-3	003S012W11A009S	<0.026	<0.026	<0.022	<0.10	<1.6	<0.026	<0.018	<0.022	<0.06	<0.03
N2-2	003S012W11A008S	<0.026	<0.026	<0.022	<0.10	<1.6	<0.026	<0.018	<0.022	<0.06	<0.03
N1-5	003S011W17F005S	<0.026	2.21	0.316	E0.26	1.8	0.087	<0.018	0.127	<0.06	<0.03
N1-4	003S011W17F004S	<0.026	<0.026	<0.022	<0.10	<1.6	<0.026	<0.018	<0.022	<0.06	<0.03
N1-3	003S011W17F003S	<0.026	<0.026	<0.022	<0.10	<1.6	<0.026	<0.018	0.014	<0.06	<0.03

of field samples by sampling procedures). Therefore, for the purposes of this study, the analytical data were of suitable quality.

Groundwater samples are assigned age classifications on the basis of the tritium and carbon-14 values of the samples, using the classification approach for the coastal Los Angeles basins described by Goldrath and others (2012). Groundwater with tritium activity greater than or equal to 1 tritium unit (TU, 3.19 picocuries per liter) and uncorrected carbon-14 greater than or equal to 90 percent modern carbon (pmc) was defined as "modern", and contains a substantial component of water recharged since 1952. Groundwater with tritium activity less than 1 TU and carbon-14 less than 90 pmc was defined as "pre-modern." Samples with tritium activity greater than 1 TU and modern carbon percentage less than 90 percent were classified as "mixed." Previous investigations have used a range of tritium values from 0.3 to 1.0 TU as a threshold for indicating the presence of water that has exchanged with the atmosphere since 1952 (Michel, 1989; Plummer and others, 1993; Michel and Schroeder, 1994; Clark and Fritz, 1997; Manning and others, 2005). By using a tritium value of 1.0 TU for the threshold in this study, the age classification scheme allows a larger fraction of modern groundwater to be classified as mixed or pre-modern than if a lower threshold were used. This higher threshold was considered more appropriate for this study because mixing of waters of different ages is likely to occur as a result of regional anthropogenic recharge and pumping. Measured carbon-14 values discussed in this study are referred to as "uncorrected" because they have not been adjusted to consider exchanges with sedimentary sources of carbon (Fontes and Garnier, 1979). When they occur, these exchanges result in lower carbon-14 values than would occur due to radioactive decay alone. Age-tracer concentrations and age classifications are listed in table 7.

Results of Groundwater Sampling

Stable isotope, age tracer, inorganic, and VOC data collected by USGS as part of this study were evaluated to discern geochemical evidence of relations between contaminated shallow groundwater and deeper parts of the groundwater flow-system downgradient that are used for public water supply. Previous work (Schroeder and others, 1997; Shelton and others, 2001; Dawson-Milby and others, 2003; Reichard and others, 2003) indicates that a combination of stable isotopic, inorganic, and age characteristics are required to distinguish between the three primary sources of recharge to the study area—local precipitation, water from the San Gabriel Mountains, and engineered recharge at the San Gabriel River spreading grounds (table 6). The discussion below includes new stable isotopic data and other selected data collected from 14 monitoring wells located along the study cross section, for comparison with historical VOC data. In addition, data from three supply wells and regional multiple-well monitoring sites (4 sites, 19 wells) located off of the study cross section are discussed to provide a regional geochemical context for information from the cross section.

Isotopes

The oxygen ($\delta^{18}O$) and hydrogen ($\delta^{2}H$) stable isotopic data indicate contrasts in recharge sources vertically and along the studied flowpath that suggest modern- or mixed-aged shallow groundwater is reaching deeper groundwater in places along the groundwater-flow section. Figure 9 shows $\delta^{18}O$ and $\delta^{2}H$ values of water from wells in the study area plotted along a global meteoric water line (GMWL; Craig, 1961). Variations in $\delta^{18}O$ and $\delta^{2}H$ along the GMWL primarily result from differences in the temperature of condensation, and is dependent on latitude, climatic conditions, and elevation. In and near the study area, water that condensed at cooler temperatures (associated with higher latitudes, cooler climatic regimes, or higher elevations such as drainage from the San Gabriel Mountains) is isotopically lighter (more negative) than water condensed at warmer temperatures (associated with lower latitudes,

warmer climatic regimes, or lower elevations such as drainage from the Puente Hills or rainfall within the study area) (Clark and Fritz, 1997; Land and others, 2004). Differences in the isotopic values of water can also result from mixing of discrete sources or evaporation. These occurrences would cause points on figure 9 to shift to heavier isotopic values and to the right of the GMWL.

The isotopic data from this study plot in groups that represent different recharge sources and mixtures, as discussed below (fig. 9).

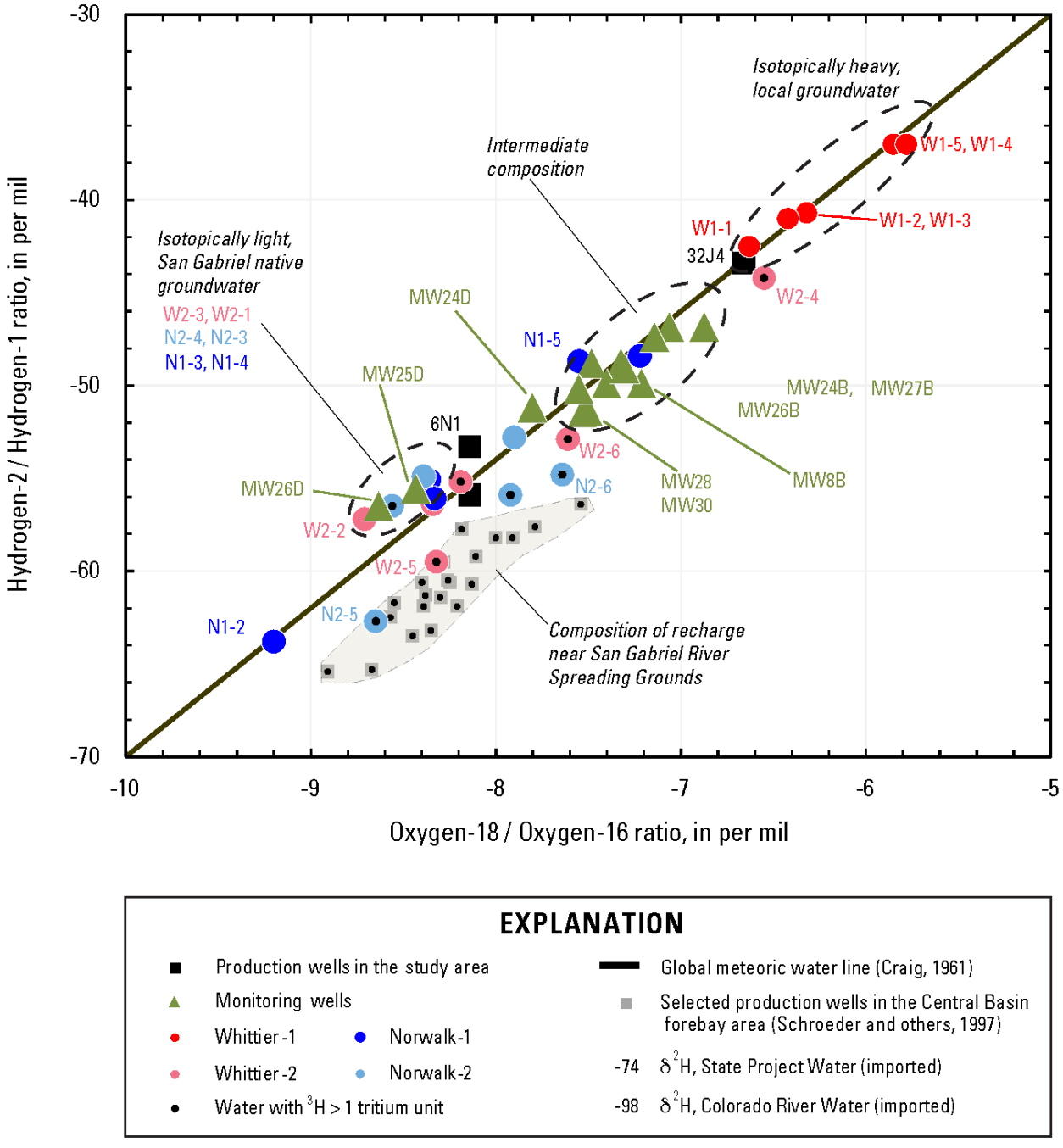

Figure 9. Plot of δ^2H and $\delta^{18}O$ values for water in study area.

Local water: A source of recharge to the study area is infiltration from precipitation falling directly within the study area or the nearby Puente Hills to the northeast. Isotopically heavy (less negative) water present at the Whittier-1 site is representative of the local water recharge to the groundwater-flow system (Reichard and others, 2003). The shallowest two wells at Whittier-1 (W1-4 and W1-5) have the least negative δ^2H and $\delta^{18}O$ values, but the deeper samples have only slightly more negative values (table 7). These local water end-member samples plot on the GMWL (fig. 9), consistent with little or no evaporative effect on the water. This water also has tritium and carbon-14 activities less than 1 TU and ~15 pmc (W1-3,4,5), respectively (table 7), indicative of water of pre-modern age (predominantly recharged before 1950 and up to thousands of years ago).

San Gabriel native water: Another source of water to the study area is water originating from the San Gabriel Mountains, which has recharged or passed through the Whittier Narrows area (fig. 1). The stable isotopic values of water from this recharge source have been previously described by Shelton and others (2001) and Reichard and others (2003). This San Gabriel native water is present at Norwalk-1 (N1-3 and N1-4; fig. 9). Deep monitoring wells MW25D and MW26D, located along the northern part of the cross section, are observed to have a similar composition (table 7; fig. 9) and are interpreted as having the same source of recharge. All the samples in this group plot slightly above the GMWL, indicating little or no evaporative modification and that the water may be derived from a local meteoric water line with a slightly different y-intercept (also referred to as the "deuterium excess" value). Local meteoric water lines of differing deuterium excess values, but with parallel slopes to the GWML, commonly occur as a function of recharge elevation and other factors (Kendall and Coplen, 2001). Thus, the slight offset of these samples from the GMWL may be consistent with water from precipitation falling at higher elevations in the San Gabriel Mountains.

Intermediate composition: Most monitoring wells on the study cross section plot between the isotopically heavy local and the isotopically light San Gabriel native end-members described above, and plot along or near the GMWL (fig. 9). A linear mixing calculation was made to estimate the fraction of local and San Gabriel native water present along the study cross section. The calculated fractions assume that mixing occurs only between local water as represented by the isotopic values of W1-5, and San Gabriel native water as represented by the isotopic values of well MW25D (table 7). Varying amounts of local water (~30 to 60 percent) are present in groundwater from the Mesa, Pacific, and Harbor sequences (fig. 8). In contrast, local water is generally not present or abundant (less than 10 percent) in the Upper or Lower Wilmington sequences upgradient of the anticline. However, downgradient of the anticline at monitoring well MW27D, the local fraction is ~40 percent.

Engineered recharge: Some groundwater in the study area may be mixed with engineered recharge from the San Gabriel River spreading grounds, but engineered recharge is unlikely to be a predominant source of water along the study cross section. Water recharged at the spreading grounds (engineered recharge) consists of a mixture of imported water from the State Water Project and the Colorado River, stormwater, and recycled water (WRD, 2011). The spreading grounds are located 2-4 mi north and northwest of the study area (fig. 1) and have been shown to be a primary source of groundwater to the south and southwest on the basis of stable isotopes, selected major elements, and VOCs diagnostic of the engineered recharge (Shelton and others, 2001; Anders and Schroeder, 2003; Reichard and others, 2003). In the study area, engineered recharge derived from the spreading grounds and perhaps the San Gabriel River becomes more prevalent in the groundwater system with proximity to the river, which forms the west edge of the study area. Recharge from the spreading grounds has $\delta^{18}O$ values that

overlap with San Gabriel native water, but plots below the GWML (fig. 9). Because most groundwater in the study area, particularly along the study cross section, has isotopic values plotting on or slightly above the GMWL, it is likely that engineered recharge is not widely present along the study cross section.

Off of the study cross section, wells at the regional multiple-well monitoring sites that have isotopic values, modern ages, and inorganic chemical signatures consistent with engineered recharge include the shallowest two wells at Norwalk-2 (N2-5 and N2-6), and the shallowest two wells at Whittier-2 (W2-5 and W2-6) (fig. 9; table 7). The occurrence of engineered recharge in the upper 500 ft of the groundwater system at Norwalk-2 is not surprising, since this site is located near the San Gabriel River and is hydrologically downgradient from the spreading grounds (fig. 2). Whittier-2 is located slightly upgradient (north) of the study area (fig. 2), and its position in the regional groundwater flow system is consistent with isotopic and other chemistry data indicating that groundwater at the location consists of a mixture of all three recharge sources discussed in this section (tables 6–7). However, since Whittier-2 is located north of the study cross section, the groundwater mixture at this location is not likely to be exactly analogous to those occurring on the study cross section. The eastward bend in the OU2 plume and the study cross section in the northern part of the study area is more consistent with groundwater coming from the Puente Hills (local water), rather than from the spreading grounds to the north. Wells having isotopic values that plot slightly below the GWML, and therefore could include some fraction of engineered recharge, include off-section wells MW8B, MW28, and MW30 (figs. 2 and 9, table 7). Wells MW8B and MW28 are located to the west of the study cross section and are more likely to include groundwater derived from engineered recharge than groundwater on the study cross section. Well MW30 has a nearly identical isotopic composition to that of MW28, but is located east of the section where mixing with engineered recharge would not be expected. Because of the limited data available, the presence and fractions of engineered recharge in samples from these wells cannot be definitively determined. However, isotopic and other chemical evidence along the study cross section are consistent with groundwater along the study cross section predominantly representing mixtures of local and San Gabriel native waters.

Inorganics

Inorganic data provide additional insights regarding the distribution of water from different recharge sources in the study area and along the study cross section. Chloride is a particularly valuable tracer because it generally moves conservatively (not affected by attenuation processes) with groundwater. Consequently, chloride was used as a proxy for inorganic signatures from different recharge sources in the study area. Previous work in the Los Angeles coastal basins has indicated that there are differences in chloride concentrations between various recharge sources (for example, Anders and Schroeder, 2003; Reichard and others, 2003; WRD, 2011). In particular, chloride concentrations are quite high in local water, low in San Gabriel native water, and variable in engineered recharge from the spreading grounds (table 6).

The combination of chloride and δ^2H data indicates that most groundwater in the study area, and along the study cross section, are mixtures of San Gabriel native water and local water of various ages. Groundwater from Whittier-1, representing the local recharge end-member, has more uniform δ^2H but widely variable chloride, with the lowest chloride values at the shallowest depths (wells W1-4 and W1-5) and increasing chloride values with increasing depth (wells W1-1 and W1-2; fig. 10). The increasing chloride values with depth likely reflects increasing interactions of local recharge with chloride sources in sediments, particularly marine deposits. Although all the samples from the monitoring wells at Whittier-1 have pre-modern ages and similar carbon-14 values, it is expected that the groundwater age

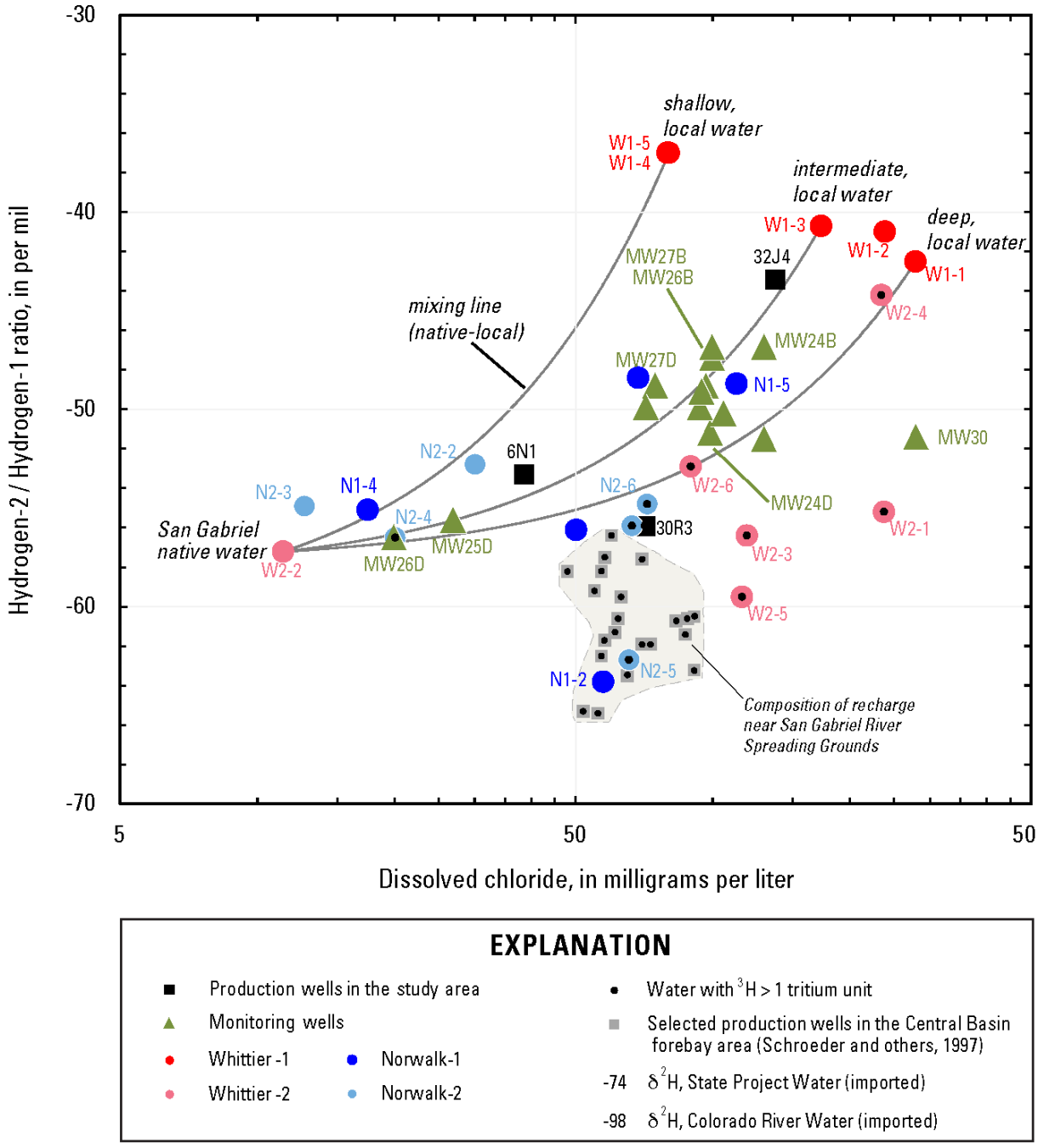

Figure 10. Plot of δ^2H and dissolved chloride in samples. Note log scale for chloride.

should generally increase with depth and the increasing chloride with depth is consistent with greater residence time and interactions of groundwater with sources in sediments. San Gabriel native waters, best represented by well W2-2, have more negative δ^2H and low chloride values (fig. 10). Because local groundwater has variable chloride values as a function of depth, theoretical mixing lines between San Gabriel native water and local waters appear to move toward different chloride concentrations for different depths (fig. 10). Many samples along the study cross section have values that plot near a mixing line between San Gabriel native water and intermediate-depth local water represented by well

W1-3 (screened from 600-620 ft bls; fig. 10). Supply well 32J4, with screened interval from 228 to 780 ft bls, also has δ^2H and chloride values consistent with a mixture of predominantly local water from intermediate depths (represented by well W1-3) and lesser amounts of San Gabriel native water (fig. 10). Engineered recharge water, based on data from the forebay area (Anders and Schroeder, 2003; Land and others, 2002), generally has intermediate chloride concentrations and lighter δ^2H values (fig. 10). The sample from well N2-5 is consistent with these waters (fig. 10). Samples from monitoring wells at several depths at the Whittier-2 site (wells W2-6, W2-5, W2-3, and W2-1) may represent variable mixtures of engineered recharge, San Gabriel native, and local water (table 7; fig. 10). However, most groundwater in the study area, and particularly along the study cross section, have chloride and isotopic values consistent with being mixtures of San Gabriel native and local groundwater, without a significant component of engineered recharge.

Volatile Organic Compounds

USGS sampled two wells for VOCs (MW18C and MW25D) where sampling by EPA (EPA, 2010) occasionally detected low levels of VOCs. The new samples, analyzed at low reporting levels, produced similar low-level detections. VOC samples collected by USGS from the production wells 30R3, 32J4, and 6N1, near, but not on, the study cross section identified VOC occurrence in different parts of the groundwater system. Well 30R3 is located near the west edge of the OU2 plume and is screened from 200 to 900 ft bls. Well 30R3 had detections of eight VOCs, including PCE, TCE, Freon-11, and Freon-113 (tables 7, 10); 1,4-dioxane (the other target Omega constituent) was not analyzed for. Concentrations of VOCs and the number of VOCs detected in this well increased from 2000–10 (Shelton and others, 2001; Mathany and others, 2008). The top of the screens in well 30R3 is only slightly below the screened intervals of upgradient monitoring wells (for example, well MW24C), in which elevated concentrations of VOCs are detected. These results indicate that production wells with shallow upper-screens are vulnerable to contamination from the shallow part of the groundwater system. In contrast, well 32J4, located east of the OU2 plume, had no detections of the VOCs associated with OU2 (table 7) despite having similar screen intervals (228 to 780 ft bls) to well 30R3. The only VOC detected in well 32J4 was chloroform, a constituent that is nearly ubiquitous in the Los Angeles Coastal Basin groundwater, at an estimated concentration of 0.01 µg/L (table 10).

Results of VOC sampling in production well 6N1, located downgradient (south) of the anticline and west of the section but within the OU2 plume, may be informative as an example of the potential for vertical movement of VOC contamination from shallow groundwater to deeper zones downgradient of the anticline. Well 6N1 had a trace detection of PCE and a TCE concentration of 3.23 µg/L (table 7). Well 6N1 is screened from 335 to 574 ft bls and is dominantly within the Upper Wilmington sequence, as represented in the 3D chronostratigraphic model. However, the screens are ~125 ft below that of upgradient, deep monitoring-well MW27D. MW27D is also screened within the Upper Wilmington (from 200 to 210 ft bls), and has VOC concentrations approximately an order of magnitude higher than those in 6N1 (table 7). VOC concentrations in well 6N1 may be lower than in upgradient monitoring wells because higher concentrations entering the well in the upper portion of the screened sections are diluted by water with lower VOC concentrations from screens located deeper in the well. Alternatively, it could indicate that high VOC concentrations at shallower depths in the Upper Willmington have not yet extended into deeper parts of the sequence that are screened by well 6N1. Whatever the local mechanisms are that explain the detections in well 6N1, the occurrence of TCE and PCE in well 6N1 suggests that movement of VOCs from shallower depths where VOC contamination is prevalent to greater depths used for public water supply is possible.

Results of VOC analyses in samples from regional monitoring wells at multiple depths follow expected patterns, indicating that the OSCs are not detected outside of the plume and that concentrations of target constituents are much lower than inside the plume. However, PCE and (or) TCE were detected in 4 of the 11 regional monitoring wells analyzed for VOCs by this study (table 7). Of these four wells, one was located upgradient of the OU2 plume (well Whittier-2-4), one was located to the west of the OU2 plume (well Norwalk-2-4), and two wells were located downgradient of the OU2 plume (wells Norwalk-1-3,1-5). The presence of TCE and PCE at wells downgradient of the mapped OU2 plume (Norwalk-1) may or may not be related to the OU2 plume. However, the presence of detections at sites upgradient and to the west of the OU2 plume indicates that there may be other sources of VOCs than the OU2 plume in or near the study area. Consequently, use of PCE and TCE data alone to trace movement of the OU2 plume in the groundwater system should be done with caution and be supported by other geochemical data.

Sources of Groundwater Recharge and Relation to Contaminant Occurrence

The previous section discussed water-chemistry data from wells off of the study cross section. In this section these results are compared to historical VOC results from the wells on the study cross section.

Along the study cross section, the occurrence of VOCs is associated with less negative isotopic values, indicating that the groundwater contains significant local water. For example, isotopic sampling at two depths in four multiple-well monitoring sites along the cross section (MW24, MW25, MW26, and MW27; fig. 2) indicates that both the concentrations and numbers of VOCs detected (historical regulatory data) are generally greater in wells having less negative isotopic values (figs. 10, 11; table 7). Detections and concentrations of VOCs, as well as the fraction of local water, were generally greater in shallower wells (“B” well at each location) than in deeper wells (“D” well at each location). Among the wells both with historical VOC and stable-isotopic data, deep monitoring well MW25D, upgradient of the anticline, has no recent VOC detections (only PCE at an estimated concentration of 0.01 µg/L in USGS VOC sample) and isotopic values consistent with San Gabriel native water. This well had regulatory sampling detections of 0.2 µg/L for PCE and 1.4 µg/L for TCE in 2007, but these detections still indicate that numbers and concentration of VOC compounds in this well are quite low. In contrast, shallow wells MW25B, MW26B, and MW27B were isotopically consistent with being primarily locally recharged and had 3 to 5 target constituents detected with total VOC concentrations >200 µg/L (fig. 11). However, there were variations in depth relations between the different monitoring well sites. At site MW24, closest to the OU1 source area, VOC detections and concentrations were low although local water was predominant or mixed with San Gabriel native water. Moreover, well MW26D, located near the anticline had two VOCs detected in association with isotopic values consistent with San Gabriel native water. In reality, relations of VOCs to groundwater source are likely to be more complex than the simple relations described here and are likely to be spatially variable as a result of aquifer characteristics and geometry, pumping stress, and other anthropogenic alterations to the system. These factors are discussed in more detail in the groundwater-flow and particle-tracking simulations discussed in the next section. Generally, VOC concentrations are greater in the shallow groundwater, and are associated with local water that mixes with San Gabriel native water deeper in the groundwater system. The extent of mixing of local water at depth varies by site. The presence of local recharge signals at depth, sometimes containing VOCs, typically suggests that vertically downward movement of contaminants from the shallow groundwater into deeper aquifers used for public supply is occurring in places and is likely to continue.

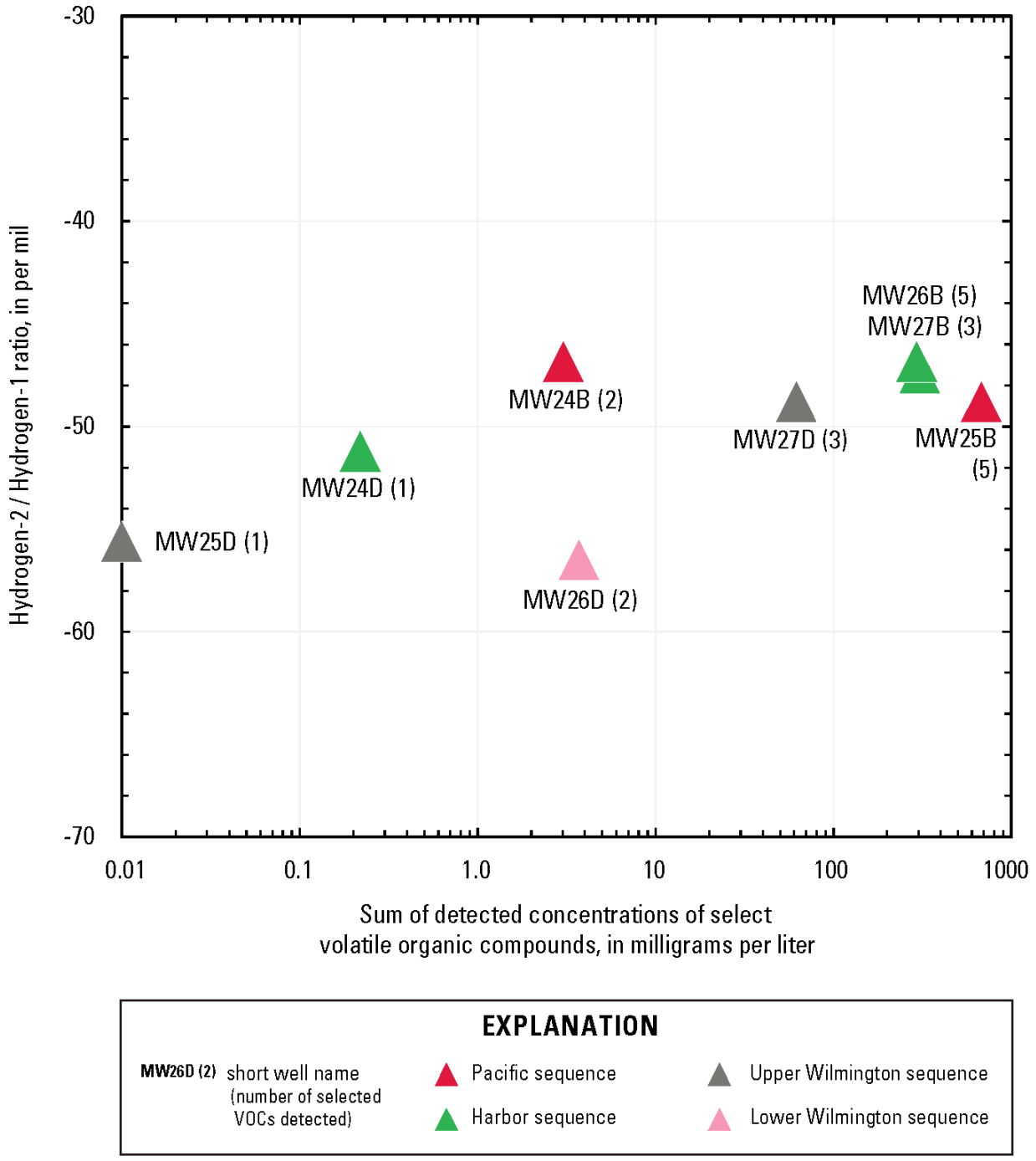

Figure 11. Plot of δ^2H and reported volatile organic compounds.

Groundwater-Flow and Particle-Tracking Model

This study seeks to provide an improved understanding of the patterns of groundwater flow in the study area and the potential for the movement of shallow, contaminated groundwater into deeper zones that provide drinking water to the public. We developed a two-dimensional (cross-sectional), steady-state groundwater-flow and particle-tracking model of the study area using the sequence stratigraphic model presented in plate 1. It is important to recognize that the groundwater-flow and particle-tracking model presented in this report is a simplified representation of the complex patterns of groundwater flow in the study area. The model considers groundwater flow along an approximate flow path that traces the pattern of groundwater movement in this area. The true groundwater-flow system, however, is three-dimensional, and groundwater-flow paths and travel times are likely affected by off-cross-section influences not included in this model. Moreover, the groundwater-flow and particle-tracking model simulates advective transport only. It does not simulate physical processes that may affect solute migration, such as hydrodynamic dispersion and diffusion, and also does not simulate chemical or biological processes that may affect the fate and transport of contaminants. An example application of a cross-section model that simulates transient, density-dependent groundwater flow and solute transport in the Dominguez Gap area of Los Angeles is available in Nishikawa and others (2009).

Model Description

Governing Equations and Model Code

The governing equation describing the movement of groundwater through porous media is based on Darcy's law and the conservation of mass (McDonald and Harbaugh, 1988). For steady-state, two-dimensional groundwater flow the governing equation is

$$\frac{\partial}{\partial x}(K_x \frac{dh}{dx}) + \frac{\partial}{\partial z}(K_z \frac{dh}{dz}) - \mathrm{W} = 0 \qquad (1)$$

where K_x is the value of hydraulic conductivity in the x direction along Cartesian coordinate axes, which are assumed to align with principal directions of hydraulic conductivity (LT^{-1}),

K_z is the value of hydraulic conductivity in the z direction along Cartesian coordinate axes, which are assumed to align with principal directions of hydraulic conductivity (LT^{-1}),

h is the hydraulic head (L),

W is a volumetric flux per unit volume and represents sources and/or sinks (T^{-1}), and

T is time.

Equation 1 generally cannot be solved analytically for practical applications involving complex groundwater systems. In this study, the USGS MODFLOW-NWT modeling software (Niswonger and others, 2011) was used to simulate groundwater flow in the study area. The MODFLOW-NWT program implements a finite-difference approximation of equation 1. The sedimentary deposits of the study area are assumed to be anisotropic with horizontal and vertical hydraulic conductivity values that vary throughout the model domain. Steady-state groundwater flow was simulated and assumed to be representative of long-term average conditions.

The groundwater-flow paths and travel times were obtained using MODPATH (Pollock, 1994) to track a parcel of water from a monitoring well backward to a recharge location. MODPATH is a particle-tracking post-processing program that uses the cell-by-cell flow rates calculated by MODFLOW-NWT to compute travel paths and travel times of groundwater moving through the simulated groundwater system. The calculation of groundwater flow paths and travel times requires the calculation of seepage velocity at each model cell-face, which is equal to the Darcian flux (the terms in parentheses in eq. 1) divided by the effective porosity of the porous material. Effective porosity is therefore a parameter that must be specified or estimated, along with hydraulic conductivity in eq. 1, as part of the groundwater-flow model's calibration. Discussions of the numerical techniques used in this study and the simulation codes MODFLOW-NWT and MODPATH can be found in McDonald and Harbaugh (1988), Anderson and Woessner (1992), Pollock (1994), and Niswonger and others (2011). Example applications of groundwater-flow and particle-tracking models are available in Kauffman and others (2001) and Sanford and others (2004).

Discretization

The method of numerical modeling requires that the model domain (fig. 12) be divided into discrete cells. For the model described in this report, the sequence stratigraphic cross section (pl. 1) has a horizontal extent of 32,800 ft and a vertical extent that ranges from ~700 ft at the upstream boundary to more than 5,900 ft at the downstream boundary. The elevation of the top of the domain varies from ~270 ft to ~100 ft above sea level. The domain of the cross-section model was divided into cells with a lateral dimension of 65.6 ft, aligned in a grid consisting of 500 columns that span the length of the domain. In the vertical dimension the model consists of 196 layers. The top layer was defined as the water table layer and extends from the land surface to a depth of ~60 to 120 feet, depending on the location along the x axis. The remaining layers range in thickness from ~5 ft in the upper 500 ft of the model domain to ~50 ft in the lower 1,800 ft of the model domain. The fine grid spacing in the upper model layers provides more accurate calculations of spatial changes in simulated hydraulic heads and particle trajectories in shallow regions where groundwater-elevation and contaminant-occurrence data are located. Figure 12 shows the model discretization at well MW27.

In this study, minor modifications were made to the stratigraphic section by removing a sequence when its thickness decreased to less than 10 ft. The impact of this change was negligible because there were a small number of points where a zone's thickness was less than 10 ft, and the vast majority of these thickness changes happened in areas that were located between the land surface and the water table and thus are not part of the active model. These modifications, along with the finer grid spacing in the upper layers, allows for characterization of thin stratigraphic sequences such as the shallow sequences that thin in the area of the anticline (pl. 1). With a model-cell thickness of 5 ft and a minimum sequence thickness of 10 ft, the thin, shallow stratigraphic sequences are represented with a minimum of two model cells.

Hydrologic characteristics of the aquifer were defined for each cell in the model using the Upstream Weighting (UPW) package of MODFLOW-NWT. The top three layers were formulated as unconfined using the wetting capability of MODFLOW-NWT; all other layers were simulated as confined. The resulting model has 98,000 finite difference cells, of which 68,716 are active cells (those cells for which groundwater flow is calculated).

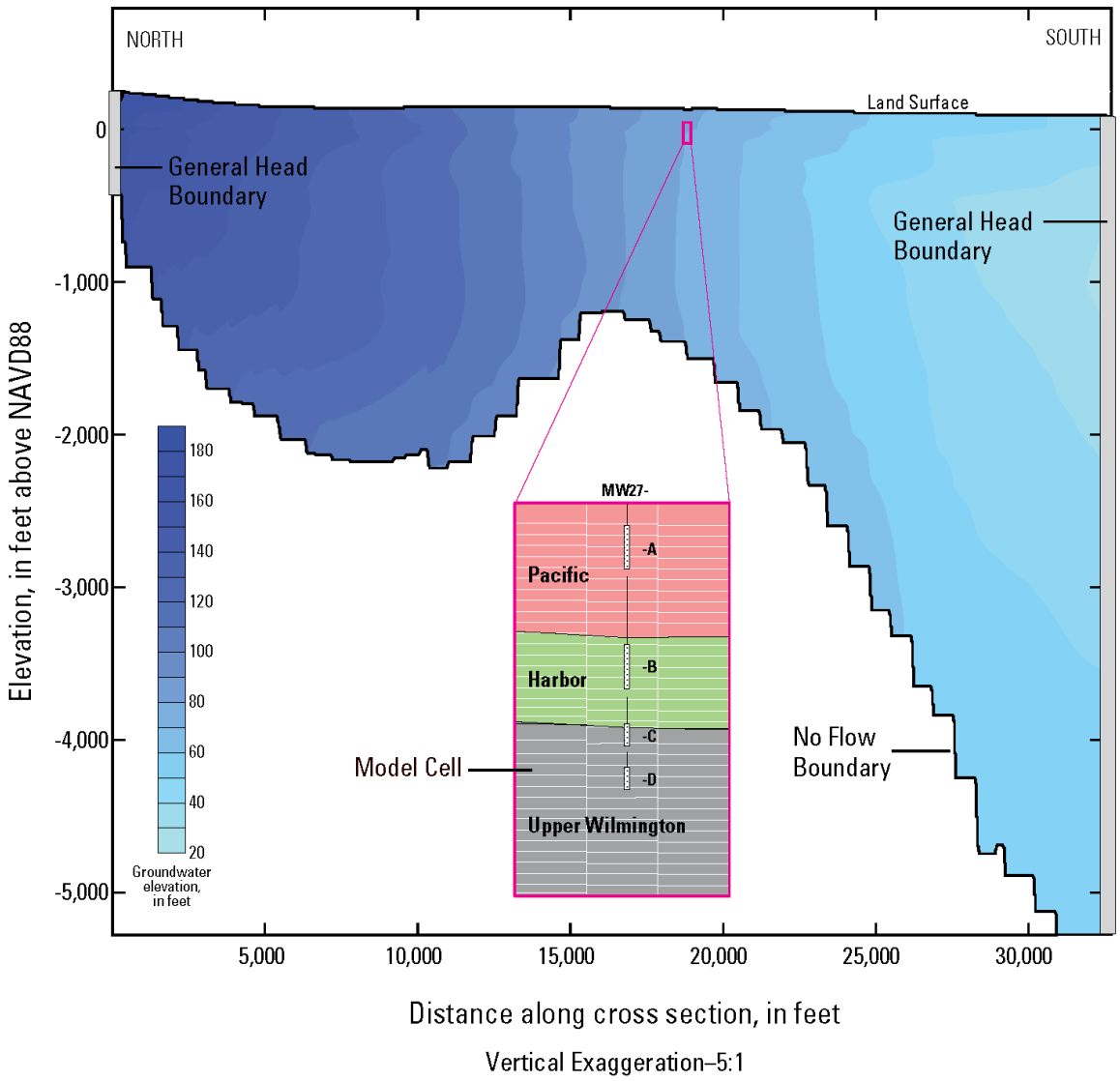

Figure 12. Schematic of cross-sectional groundwater model.

Parameterization of Subsurface Hydraulic Characteristics

The groundwater-flow model requires values of hydraulic conductivity and porosity throughout the model domain. The degree to which these properties vary is accounted for in the model by specifying parameter zones, with a single value of horizontal hydraulic conductivity, vertical hydraulic conductivity, and porosity specified for each zone. To create a realistic representation of the groundwater system, the model zone boundaries generally follow the sequence stratigraphic model shown in plate 1. The hydraulic conductivity and porosity values assigned to each zone are initially constrained based on independent information, such as aquifer tests, or literature values appropriate to the sediment types, and then are refined during model calibration.

Aquifer tests (slug tests and pumping tests) have been performed and analyzed to estimate the horizontal hydraulic conductivity of shallow deposits in the study area. While both methods provide in situ values of hydraulic conductivity, slug tests generally represent a small volume of the aquifer in the

vicinity of the well screen, whereas pumping tests provide information averaged over a much larger aquifer volume (Freeze and Cherry, 1979). Thirty-six aquifer tests, including 29 slug tests and 7 pumping tests, were conducted in observation wells within 100 ft of the model transect (EPA, 2010). These tests were performed at a maximum depth of ~200 ft below land surface, and at screened intervals with lengths that range from 5 to 20 ft. Hydraulic conductivity estimates from these tests (table 11) range from ~1.0 to ~340 ft/day. The hydraulic conductivity estimates obtained from pumping tests are generally larger than those obtained from slug tests; however, the estimates of hydraulic conductivity (obtained from pumping or slug tests) show no correlation with depth or stratigraphic zone.

Table 11. Estimates of hydraulic conductivity (reported), Central Basin groundwater contamination study, Los Angeles County, California

[Hydraulic conductivity in units of ft/day]

Stratigraphic unit	Hydraulic conductivity estimate from slug test	Hydraulic conductivity estimate from pumping test
Dominguez	2–15	213–342
Mesa	6–79	--
Pacific A	51–52	--
Pacific	2–45	--
Harbor	1–105	54–255
Bent Spring	--	45–316
Upper Wilmington	2–107	--
Lower Wilmington	1–7	--

The calculation of groundwater travel times by backward particle tracking requires that effective porosity be specified throughout the model domain. Porosities can be constrained based on values found in the literature with a degree of certainty that is substantially greater than that for hydraulic conductivity. Freeze and Cherry (1979), for example, provide estimates of porosity for unconsolidated sediments that range from 0.25–0.5 for sand and silt. For this reason, the effective porosity of the model was specified rather than estimated during the calibration process. In addition, it is well established that porosity decreases exponentially with depth in sedimentary deposits (Athy, 1930). Based on this information, the porosities were assigned by depth according to an exponential function, beginning with 30 percent at the land surface and decreasing to 20 percent at the deepest point in the model domain. These values were fixed in all modeling analyses presented in this report. The contaminant occurrence data used in this study are limited to shallow observation wells, and travel times to these wells will vary with changes in the value of porosity specified for the uppermost layers of the model.

Boundary Conditions

Boundary conditions define the manner in which water moves to or from the groundwater system. Boundary conditions for the groundwater-flow model include no-flow and general-head boundaries. An additional boundary condition for the particle-tracking model is the contaminant source location and period of activity.

No-flow boundaries correspond to contacts with low-permeability sediments across which groundwater-flow is considered negligible. For the model presented in this report, the base of model layer 196 (the contact between the “Repetto” and overlying Long Beach C stratigraphic unit) is

formulated as a no-flow boundary because it corresponds to the contact between the regional groundwater-flow system and the underlying sediments that have comparatively low permeability (fig. 12).

The upstream and downstream boundaries of the groundwater-flow model were simulated as general-head boundaries where water moves to or from the groundwater system based on the hydraulic head in the aquifer. General-head boundaries, simulated using the MODFLOW GHB package (Niswonger and others, 2011), simulate this process based on the difference between the head in the model cell and the head in the external system (boundary head). The rate of flow is proportional to the head difference between the model cell and the external source or sink. The constant of proportionality is determined by a conductance term that incorporates hydraulic conductivity, cell geometry, and distance. The conductance values were set based on the hydraulic conductivity of model cells at the boundaries and range from ~200 to 110,000 ft^2/day. Conductance values vary with depth depending on the hydraulic conductivity of the parameter zone at the boundary model cell and the thickness of the model cell. Sensitivity analyses showed that the results were insensitive to the conductance values; therefore, these values were fixed in all model runs.

The external heads at the upstream and downstream boundaries are the link between the groundwater domain modeled in this report and the regional groundwater system. The boundary heads vary with depth and were defined based on hydraulic heads simulated by the regional groundwater-flow model currently under development (S. Paulinski, U. S. Geological Survey, written commun., August 2013). These boundary heads impose vertical gradients at the upstream and downstream boundaries that developed in response to the regional geologic structure and stresses imposed on the system. At the upstream boundary, the boundary heads range from ~184 ft at the top of the model domain to ~146 ft at the bottom of the model domain. At the downstream boundary, the boundary heads range from ~34 ft at the top of the model domain to 12 ft at the bottom of the model domain.

The particle-tracking model includes a source area that is delineated as a recharge zone that spans a defined set of model cells. For the purpose of the particle-tracking model, it was assumed that parcels of water that carry the OSCs can originate only at the predefined source area and only during a specified time period. The particle-tracking model tracks the path and travel time of a parcel of water backward from a monitoring well to the point at which the parcel entered the groundwater system. If the point of recharge is within the source zone and the time of entry is within the source's active period, the parcel of water is assumed to be affected by the activity of the source and to carry the OSCs. The source zone was assumed to be active beginning in 1976 (EPA, 2010) and the contaminant occurrence data used to calibrate the particle-tracking model were collected in 2009; therefore, the maximum travel time for particles that move from the source zone to an observation well is 33 years. Contaminants that originate at or near the land surface can migrate downward through aqueous, nonaqueous, and vapor-phase transport to create a subsurface reservoir that serves as a long-term source of groundwater contamination (National Research Council, 1997). There is limited information about the occurrence and distribution of contaminants with depth at the source zone. Observation well OW1B (table 1) is located at the downstream end of the source zone with a screened interval from 110 ft to 120 ft bls, and groundwater-quality sampling at well OW1B identified the OSCs. This relation suggests that contaminants that reached the water table could be distributed to a depth of 90 ft above sea level or deeper; therefore, the source zone was assumed to extend from the water table to an elevation of 90 ft above sea level.

Evaluation of Alternative Model Parameters

Model calibration is the process in which model inputs, such as hydraulic properties and boundary conditions, are refined so that model output matches observed values as closely as possible. The parameters that are adjusted during the calibration process include the horizontal and vertical hydraulic conductivities of the stratigraphic zones. Table 12 is a list of the calibration parameters for the model described in this report. During calibration, the parameter values are adjusted within acceptable ranges to provide the best fit between observed hydraulic head and contaminant occurrence, and their simulated equivalents.

Table 12. Parameter ranges used in Monte Carlo sensitivity analysis of groundwater-flow and particle-tracking model along with calibrated parameter values, Central Basin groundwater contamination study, Los Angeles County, California.

[Hydraulic conductivity in units of ft/day]

Stratigraphic unit	Parameter ranges		Parameter values that provide the best fit to groundwater elevation observations		Parameter values that reproduce contaminant occurrence observations at sites MW23 and MW24	
	Horizontal hydraulic conductivity	Vertical hydraulic conductivity	Horizontal hydraulic conductivity	Vertical hydraulic conductivity	Horizontal hydraulic conductivity	Vertical hydraulic conductivity
Dominguez	1–1000	0.001–10	200.5	0.91	200.5	0.91
Mesa	1–1000	0.001–10	701.0	0.012	700.5	0.012
Pacific A	1–1000	0.001–10	40.0	0.014	40.5	0.014
Pacific	1–1000	0.001–10	101.0	0.017	101	0.017
Harbor	1–1000	0.001–10	100.4	0.0014	100.4	0.114
Bent Spring	1–1000	0.001–10	40.0	0.01	40.1	0.01
Upper Wilmington	1–1000	0.001–10	20.7	0.003	20.7	0.003
Lower Wilmington	40–1000	0.001–10	80.7	0.027	80.7	0.027
Long Beach A	40–1000	0.001–10	40.0	8.69	40	8.69
Long Beach B	40–1000	0.001–10	235.1	1.05	6.3	0.004
Long Beach BC	40–1000	0.001–10	50.7	10.0	50.8	10.1
Long Beach C	40–1000	0.001–10	52.4	1.09	2.4	0.11

Calibration Data

The parameters of the groundwater-flow and particle-tracking model are evaluated using groundwater-elevation, contaminant-occurrence, and groundwater travel-time data. Groundwater-elevation data used for the calibration include 32 observations (table 13). Groundwater elevations are assigned to a particular layer and longitudinal location in the model grid. During calibration, observed groundwater elevations are compared with simulated hydraulic heads at the given location and model layer. The groundwater-flow and particle-tracking model was evaluated for steady-state groundwater-flow conditions, which allows for a single groundwater-elevation observation at each observation location. Groundwater-elevation data obtained in 2007 are used for model calibration in this study. It

should be noted that model-calibration results could change if groundwater-elevation data from a different year were used.

Table 13. Comparison of observed and simulated groundwater elevation and contaminant occurrence, Central Basin groundwater contamination study, Los Angeles County, California.

[Groundwater elevation based on measurements in 2007; contaminant detection based on samples collected in 2009; shading used to identify observation locations where groundwater elevation or contaminant occurrence was not measured; Yes, all five characteristic constituents observed; No, particle trajectory did not originate at source zone; Dry, no simulated equivalent because model cell at observation location converted to dry]

Well name (short)	Longitudinal distance downstream from source zone (ft)	Screened interval, depth below land surface (ft)	Measured ground-water elevation (ft)	Characteristic Omega source contaminants detected	Simulation results with parameter values that provide best fit to groundwater elevation data		Simulation results with parameter values that reproduce contaminant occurrence observations at wells MW23 and MW24	
					Simulated ground-water elevation (ft)	Simulated groundwater travel time from source to measurement location (years)	Simulated ground-water elevation (ft)	Simulated groundwater travel time from source to measurement location (years)
OW7	0	71–91	139.5		144.4		130.6	
OW8A	295	60–80	134.5	Yes	137.5	0.2	116.0	0.1
OW8B	295	116–126	121.6		128.6		113.1	
MW24A	2,263	50–70	125.5	Yes	122.4	0.9	102.6	0.8
MW24B	2,263	110–125	120.4		120.5		101.4	
MW24C	2,263	140–160	120.0	Yes	116.3	No	97.1	2.9
MW24D	2,263	173–178	119.8		113.5		94.0	
MW15	4,297	50–70	123.1	Yes	119.1	3.1	98.6	2.2
MW23A	5,609	35–55	120.9	Yes	117.7	3.3	97.9	2.6
MW23B	5,609	82–97	120.1	Yes	113.9	11.1	92.8	11.5
MW23C	5,609	145–160	116.4	Yes	105.9	No	88.0	10.5
MW23D	5,609	175–185	116.0	Yes	102.2	No	86.5	12.8
MW25A	7,708	45–65	110.4	Yes	111.8	5.5	88.8	4.1
MW25B	7,708	90–110	110.2	Yes	107.7	10.6	86.8	7.8
MW25C	7,708	140–150	106.4		102.1		85.2	
MW25D	7,708	194–209	80.7		89.2		76.5	
MW16A	8,823	45–60	106.4	Yes	108.5	5.4	Dry	Dry
MW16B	8,823	106–116	105.2	Yes	104.3	15.0	83.7	11.9
MW16C	8,823	149–164	101.8		92.8		77.1	
MW17A	10,660	56–71	95.3	Yes	97.1	8.1	Dry	Dry
MW17b	10,660	94–104	95.7	Yes	95.7	12.2	74.4	7.8
MW17C	10,660	172–182	78.2		81.2		68.1	
MW26A	11,841	70–90	88.9	Yes	90.9	9.5	68.7	8.8
MW26B	11,841	105–120	88.9	Yes	88.8	14.4	68.9	10.4
MW26C	11,841	145–160	75.4	Yes	82.2	31.1	67.3	30.7
MW26D	11,841	185–205	73.5		76.2		64.6	
MW27A	18,860	90–110	62.5	Yes	68.1	20.0	50.6	16.6
MW27B	18,860	144–164	62.6		60.9		49.6	
MW27C	18,860	180–190	47.4		58.1		49.7	
MW27D	18,860	200–210	47.6		59.3		51.1	
MW29	27,191	90–100	26.3		36.8		36.4	
C_603	23,518	70–100	32.7	Yes	41.9	30.3	38.4	31.6

Contaminant-occurrence data used for model calibration include 19 observations (table 13). In this study, contaminant occurrence is defined based on the presence or absence of the OSCs. During calibration, observations of OSCs are compared to occurrences simulated by the particle-tracking model. A particle that travels from the source area to the positive occurrence location within the allowable travel time is defined as a correct fit. Contaminant-occurrence data provide inherent information on the possible path line from a source to an observation location. This path line information, however, is generally dependent on knowledge of the source location, the time period of source activity, and historical groundwater conditions.

Model calibration requires a comparison of observations with their simulated equivalents. For most observation locations, the well screen spans more than one model layer (fig. 12). In this case, a multi-layer hydraulic head value is calculated, as described in Hill and others (2000). The backward-tracking in MODPATH brings the particle to the location where that parcel of water would have intercepted the contaminant source zone or entered the groundwater system at the upstream boundary. In MODPATH one particle of water was tracked backward for each 0.25 ft of well screen. It could then be determined if that particle of water originated at the designated source area, along with the particle's travel time. An occurrence location that had at least one particle track backward to the source, with a travel time <33 years, was considered a positive calibration for that location.

Calibration Methods

Model calibration can be a challenge because (1) the simulated responses vary in a nonlinear manner as a function of the model inputs, and (2) there are interactions between parameters such that the best value of one parameter is dependent on the values of other parameters. The method of nonlinear least squares is widely used in groundwater-model calibration to estimate unknown model parameters (Hill and Tiedeman, 2007). The least-squares method, however, requires that simulated conditions be continuous functions of the model inputs. While this is the case for simulated hydraulic heads, it is not the case for contaminant occurrence, which is a binary function that can take on the values 1 (occurrence) or 0 (non-occurrence). In order to incorporate both types of data into the calibration process, a Monte Carlo parameter-estimation procedure was used. In this approach, (1) a large number of parameter realizations are generated (horizontal and vertical hydraulic conductivity in this case), (2) hydraulic head, contaminant occurrence, and travel times are simulated, and (3) the simulated and observed values are compared to identify the parameter values that provide an acceptable fit. The Monte Carlo parameter-estimation procedure was implemented using the sensitivity-analysis option of PEST (Doherty, 2005).

Model Fit

It is useful to have some mathematical measure of the goodness of model fit. In this study, two simple measures were used to evaluate and compare the ability of alternative parameter values to reproduce observed conditions. The first measures the model fit to hydraulic head observations and the second measures the model fit to contaminant occurrence observations.

$$S_h(b) = \sum_{i=1}^{nh} \left(h_i - h_i^{'} \right)^2 \tag{2}$$

$$S_{oc}(b) = \sum_{i=1}^{nc} \left(oc_i - oc_i^{'} \right) \tag{3}$$

where $\boldsymbol{b}$ is the vector containing the parameter values,
nh is the number of hydraulic head observations,
h_i is the ith hydraulic head observation,
h_i' is the simulated equivalent to the ith hydraulic head observation,
nc is the number of contaminant occurrence observations,
oc_i is the ith contaminant occurrence observation, and
oc_i' is the simulated equivalent to the ith contaminant occurrence observation.

Equations 2 and 3 are simple calibration measures that increase as the simulated values of h_i and oc_i diverge from the observed values. These measures were used to rank and compare model fits associated with alternative parameter sets, $\boldsymbol{b}$. The goal of the calibration process was to identify parameter values that provide an acceptable fit to both calibration measures. It is not possible, however, to guarantee that the calibrated parameter values provide the best fit across all possible parameter realizations.

The groundwater-flow and particle-tracking model was calibrated using a combination of Monte Carlo sensitivity analysis as it is implemented in PEST (Doherty, 2005), and manual adjustments of parameters. For this study, MODFLOW and MODPATH, with pre- and post-processing routines, were used by PEST to evaluate the ability of alternative parameter realizations to simulate the observed groundwater-elevation and contaminant-occurrence data. The sensitivity analysis evaluated ~40,000 parameter realizations. The parameter values in each realization were randomly generated assuming a uniform distribution with the upper and lower parameter limits defined in table 12. Each parameter realization was evaluated based on its ability to minimize the groundwater elevation and contaminant-occurrence objectives defined in equations 2 and 3.

After the PEST sensitivity analysis, individual parameter values were adjusted manually to improve the fit of simulated equivalents to observations. The calculations of particle movement by the PEST sensitivity analysis was limited by the discrete nature of the particle trajectories. Small changes in parameter values could cause trajectories to shift from one recharge area to another, with an associated shift in travel time. As a result, discrete changes in the contaminant-occurrence error were observed when parameter values were adjusted; the hydraulic-head calibration error varied in a continuous manner due to the continuous nature of the hydraulic heads simulated by the groundwater-flow model. Individual parameter values were adjusted and the effects on hydraulic-head and contaminant-occurrence errors were evaluated.

As a means to limit the parameter values considered in the calibration process, parameter values were restricted based on a broad range of hydraulic conductivity estimates obtained from aquifer tests and modeling studies summarized in table 11.

Calibration Results

Simulations of groundwater levels and particle trajectories were completed for more than 40,000 parameter sets. The results presented are for the simulation model that best reduced the hydraulic-head calibration errors.

The estimated values of hydraulic conductivity are presented in table 12. Hydraulic conductivity estimates range from 20.7 ft/day for the Upper Wilmington sequence to 701.0 ft/day for the Mesa sequence. These values are similar in magnitude to estimates from previous modeling studies (Reichard and others, 2003; EPA, 2010). However, a direct comparison to these earlier studies is not possible because of the differences between the conceptual hydrogeologic models used in those studies and the sequence stratigraphic model used in this study. The range of hydraulic conductivity estimates also compares well to the range of values obtained from slug and pumping tests (table 11) performed in the study area. The values of vertical anisotropy (the ratio of vertical to horizontal hydraulic conductivity) range from ~0.00001 to 0.2. The estimated values of hydraulic conductivity and vertical anisotropy are within the range of possible values for unconsolidated sediments (Freeze and Cherry, 1979).

The estimated hydraulic conductivity values presented in table 12 represent a single realization of model-parameter values identified from the more than 40,000 parameter realizations evaluated in the model-calibration process. The parameter values, along with the numerical results of the groundwater-flow and particle-tracking model, have an associated, but unquantified, uncertainty. While it is possible to quantify model-parameter and model-prediction uncertainty (Hill and Tiedeman, 2007), that analysis is not included in the scope of this report.

Groundwater Elevations

The simulated values of groundwater elevations are given in table 13. One of the features of the groundwater elevation data used in the model calibration is the presence of vertical gradients at the locations with multi-level observations. However, the groundwater-elevation data are limited to shallow (<200 ft bls) monitoring sites and it is not known if the vertical gradients persist with depth. The current model generally reproduces these shallow vertical hydraulic-head gradients along the cross section, although it tends to overpredict groundwater elevations near the upstream and downstream boundaries of the cross section, as can be seen in wells OW7, OW8, MW29, and C_603. Residual errors (the difference between the observed groundwater elevation and its simulated equivalent) range from <1 ft to a maximum of ~13 ft, with an average of ~6 ft.

The simulation model also provides information about the horizontal hydraulic-head gradients that move water laterally along the cross section. Simulated and observed water-table elevations from wells MW25A to C_603 exhibit a consistent horizontal hydraulic-head gradient of ~0.005 ft/ft. Over the distance of ~11,000 ft, the water table moves through stratigraphic units that have estimated horizontal hydraulic conductivities that range from 40 to 700 ft/day. Assuming a porosity of 0.30, we can estimate that groundwater will move at a rate of ~0.7 to 12 ft/day. These values are similar to the velocities estimated in the groundwater modeling study performed as part of the remedial investigation of the Omega Chemical Corporation Superfund Site (EPA, 2010). It is important to note that these advective velocities do not account for processes that retard the movement of sorbing compounds.

Contaminant Occurrence

Groundwater trajectories and travel-times to wells were simulated using MODPATH and results from MODFLOW. Results for individual wells are given in table 13, which lists the travel times from

the source zone to each well (for those wells with trajectories that track back to the source zone). The results of the particle-tracking analysis indicate the following:

1. Particles associated with the deepest contaminant-occurrence observation locations (MW24C, MW24D, MW23C, and MW23D) do not track back to the assumed source zone. This is likely due the large vertical anisotropy values identified during calibration. Large vertical anisotropies are needed to reproduce the vertical hydraulic-head gradients that are evident in the hydraulic head data; however, they will likely restrict the vertical movement of the particles that is needed to connect these deeper wells with the shallow-contaminant source zone. As a result, the particle-tracking analysis indicates that water reaching these wells enters the groundwater system at the upstream boundary (see fig. 13).
2. The maximum travel-time for the particles that track backward to the source zone is about 11,300 days, or 31 years. This is within the 33-year travel-time limit that is defined as the time from the beginning of source activity in 1976 (EPA, 2010) and the collection of groundwater quality data in 2009. The travel-time estimates also display a general pattern of increasing travel time with increasing distance from the source and (or) increasing depth at multi-level sampling locations. In addition to the hydraulic conductivity values presented in table 12, the simulated travel times presented in table 13 are a function of porosity and will vary with changes in the value of porosity specified for the uppermost layers of the model. Groundwater advective velocities are defined according to Darcy's law and are inversely proportional to porosity (Freeze and Cherry, 1979). Therefore, travel times will increase if the porosity increases and will decrease if the porosity decreases.
3. The small number of contaminant-occurrence data provides a limited understanding of the lateral and vertical distribution of contaminants along the cross section, with almost no information about the distribution of contaminants south of well MW27. Additional particle-tracking analyses were performed to define the potential distribution of groundwater contamination that originates at the source zone shown in figure 13. A backward-tracking particle-tracking model was used to identify the subarea of the groundwater-flow model that has groundwater flowpaths that intersect the source zone. The results of that analysis, presented in figure 13*A*, indicate that particles with trajectories that originate at the source zone reach a maximum depth of ~230 ft bls at the downstream boundary of the model.
4. The particle-tracking analysis is generally consistent with the analysis of isotopic data. Particles placed at shallow wells MW25B, MW26B, and MW27B track back to the source zone, which suggests that water moving to these wells is locally recharged. This is consistent with the source of groundwater recharge inferred from the stable isotopic data.
5. The groundwater-flow and particle-tracking model described above does not simulate flow paths from the source zone to the deepest monitoring wells at MW24C, MW24D, MW23C, and MW23D. The occurrence of groundwater contamination at these sites, however, indicates the potential for the movement of groundwater contaminants along deeper pathways than simulated in the previous particle-tracking analysis. A second analysis was performed to identify the vertical distribution of these deeper particle trajectories as they track from wells MW23 and MW24 to the downstream boundary. The results, presented in figure 13*A*, indicate the potential for contaminants to be found at depths >360 ft at the downstream boundary, with trajectories that intersect the lower screened zone of production well 18G5 (table 1, pl. 1).

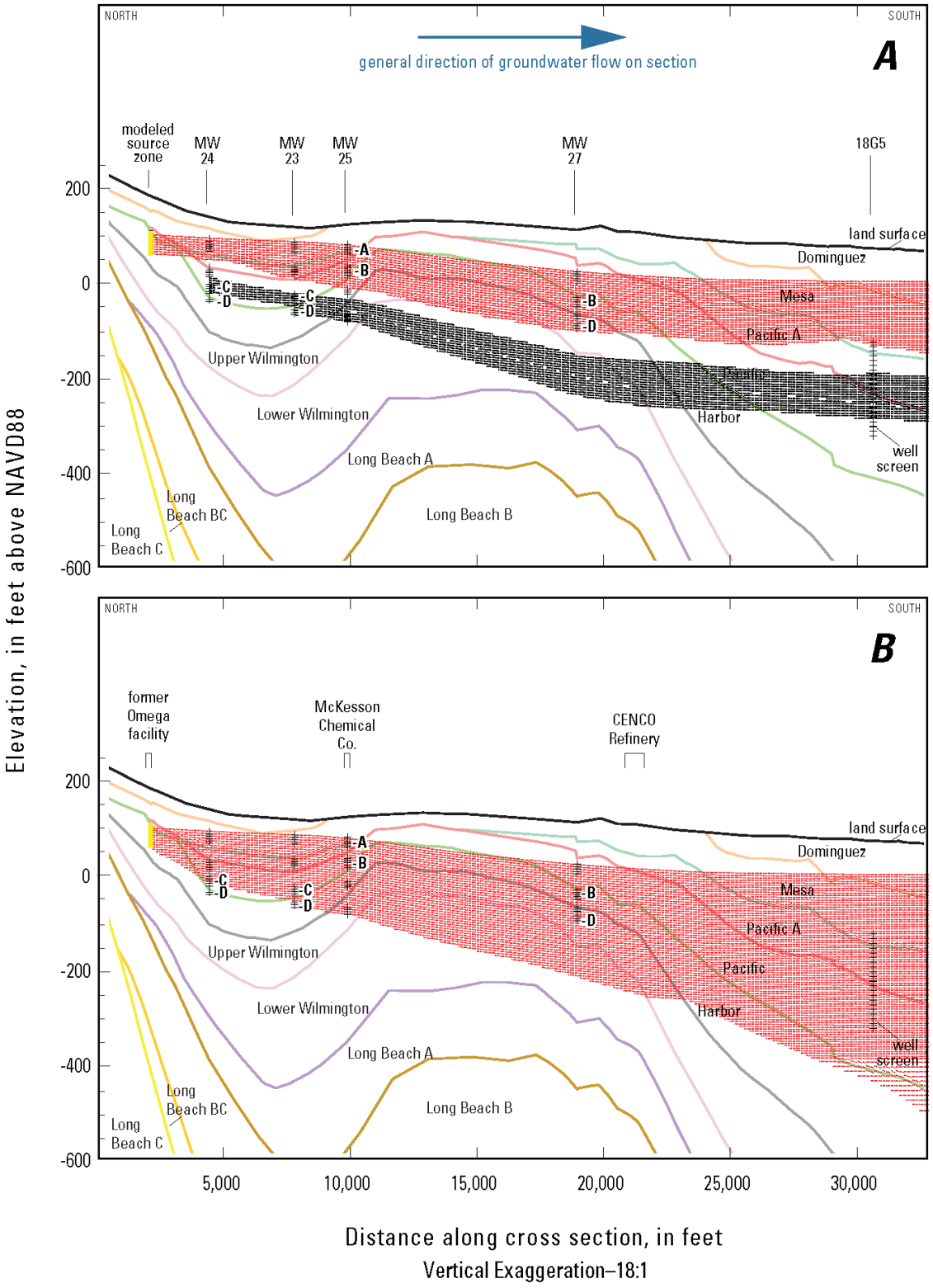

Figure 13. Results of the groundwater-flow and particle-tracking analyses.*A*, parameter values that provide the best fit to groundwater elevation data; *B*, parameter values that reproduce contaminant-occurrence observations at wells MW23 and MW24.

The modeling results described above are based on a simulation model that provides the best fit to hydraulic-head observations. The resulting simulation produces an acceptable fit to the water table (at locations where observations of water table elevations are available) and vertical hydraulic-head gradients that are evident at the multi-level monitoring sites. The model does not, however, simulate particle trajectories to three sites that have occurrences of the OSCs. A second calibration exercise was performed to develop a simulation model with flow paths that connect the source zone to wells MW24C, MW24D, MW23C, and MW23D. The results of that analysis are presented in tables 12 and 13. The calibration resulted in substantial decreases (an order of magnitude or more) in hydraulic conductivity estimates for the Long Beach B and Long Beach C sequences and an increase in the vertical hydraulic conductivity of the Harbor stratigraphic unit. Although the resulting particle-tracking model was able to connect the three deep-monitoring sites to the source zone, the model was not able to retain the close fit to the hydraulic-head observations. The simulated hydraulic head is as much as ~24 ft lower in the updated calibration, and the average hydraulic-head residual is ~19 ft, as compared to ~6 ft in the previous analysis. As a result of the lower simulated water table elevation, observation wells MW16A and MW17A are located in model cells that are simulated as dry.

A particle-tracking analysis was performed to define the potential distribution of groundwater contamination as simulated by the revised parameter values. The results are presented in figure 13*B*. The revised simulation model suggests that contaminant transport pathways could be substantially deeper than predicted by the simulation based on the best fit to hydraulic-head data, with particle trajectories reaching a depth of ~600 ft bls at the downstream boundary. At this depth, migration pathways have moved into the production zone for public supply wells, and the regional groundwater-flow patterns will likely move contaminants toward public supply wells beyond the southern boundary of the model.

Model Limitations

A groundwater-flow model is necessarily a simplified representation of a complex natural system, with many potential sources of error. Therefore, it is important to understand a model's limitations when interpreting model results. Specific sources of uncertainty in the groundwater-flow and particle-tracking model described in this report include the two-dimensional structure of the model, model discretization and parameter zonation, insufficient calibration data, the simplified characterization of the contaminant source, and the effects of contaminant transport processes not simulated by the model.

The representation of the groundwater system with a steady-state, two-dimensional simulation model, is in itself, a limitation and potential source of uncertainty. The model considers groundwater flow along an approximate flow path that traces the general pattern of groundwater movement in this area. Simulated hydraulic heads, particle trajectories, and particle travel-times are controlled in the model by boundary conditions and the structure and values of model parameters, in particular hydraulic conductivity. Groundwater levels and fluxes at the upstream and downstream boundaries are based on groundwater levels simulated by the regional groundwater-flow model currently being developed by the USGS. These general-head boundaries incorporate the effects of the regional geometry of the groundwater system and the stresses that create the vertical variations of hydraulic head at the boundaries. This model, however, does not account for the true three-dimensional nature of groundwater flow in the study area and cannot describe the trajectory of groundwater-flow paths that might move in a direction that is not parallel with the section. Although the model includes a detailed description of the stratigraphic layering, the hydraulic-conductivity field is simulated as uniform over large discrete zones

and does not include the smaller-scale hydraulic-conductivity variability that could influence the pathway and travel-time of contaminant migration.

The groundwater-flow and particle-tracking model presented in this report is a deterministic model that does not consider uncertainties associated with the model parameters. Uncertainty is a component of every groundwater model and can arise with respect to the processes that control groundwater flow and transport, with respect to the parameters that define those processes, or both. As a result of model uncertainty, the simulated hydraulic heads and groundwater flow paths are also uncertain. The results presented in tables 12 and 13, however, represent only two possible outcomes of the model calibration process. While it is possible to quantify model-prediction uncertainty, that analysis is not included within the scope of this report.

The groundwater-flow and particle-tracking model developed in this report is limited by the small number of calibration data and the limited spatial distribution of those data. The hydraulic-head and contaminant-occurrence data are found in a shallow zone that extends to a maximum of ~200 ft bls. Calibration to groundwater-elevation data is dominated by the need to match vertical gradients. The persistence of these gradients with depth, however, is unknown due to the general scarcity of data. In a similar manner, the limited number and spatial extent of contaminant-occurrence data leads to uncertainty about the simulated travel-time and trajectory of groundwater originating at shallow depths in the upgradient region of the model.

The origin of particles simulated by the groundwater-flow and particle-tracking model was defined as a source zone in the shallow groundwater system near the north boundary of the cross section. The actual contaminant source is likely to be more complex and to have evolved over time. Contaminant movement from the land surface downward is affected by vapor phase, aqueous phase, and nonaqueous-phase transport mechanisms. Therefore, the contaminants that originated at or near the ground surface have likely evolved into a spatially– and temporally– varying subsurface reservoir that serves as a long-term source of groundwater contamination (National Research Council, 1997). The simple source description used in this report does not account for the complex and evolving nature of this subsurface reservoir, other contaminant sources (within and outside of the cross section simulated in this report) that might affect groundwater quality at the observation locations, or anomalous conditions (such as movement through a wellbore) that could provide preferential pathways for contaminant migration.

The groundwater-flow and particle-tracking model was intended to provide an enhanced understanding of the relation between shallow groundwater contamination in the northern reach of the cross section and deeper groundwater resources downgradient. The model simulates groundwater advective transport, but does not account for other physical, chemical, and biological processes that might affect the migration and fate of contaminants. Physical processes of diffusion and hydrodynamic dispersion can delay and disperse contaminants in a manner not predicted by advective transport alone, and chemical and biological processes can degrade contaminants or transform them into other compounds (Nationsl Research Council, 1997). Goode (1996) evaluated the effect of hydrodynamic dispersion on groundwater age estimates, and describes the potential for underestimating groundwater travel-time when samples are collected from the leading edge of a dispersed plume. The particle-tracking model presented in this report is unable to account for the potential effects of hydrodynamic dispersion on the estimation of groundwater travel-times based on an advective-transport model.

Discussion and Conclusions

The Central Basin of southern Los Angeles County serves as the primary source of water for more than two million residents in the region. Managing the groundwater resources in the Central Basin requires an understanding of the extent of groundwater contamination and the potential for contaminated groundwater to reach public supply wells. In the Santa Fe Springs–Whittier–Norwalk area, located in the northeast part of the basin, a number of sources of VOCs have been identified, including the Omega Chemical Corporation Superfund Site, that are thought to have contributed to a large, commingled contaminant plume (OU2). Using available data, this multifaceted study was conducted as a conceptual and numerical evaluation of the potential for shallow groundwater contamination in the study area to move into producing aquifer zones.

This study used three interconnected approaches (stratigraphic, geochemical, and numerical) to gain insight into the geologic and hydrologic controls on contaminant migration in the study area and along a cross section that traces the general pattern of groundwater-contaminant movement in the area of the Omega Chemical Corporation Superfund Site. First, we developed a model of the Quaternary and late Pliocene-age strata in the study area, using the principles of sequence stratigraphy, to define bounding unconformities that separate genetically related packages of sediment deposited in response to changes in base level, sediment supply, and accommodation space – changes that are driven largely by glaciation and tectonic deformation.

This chronostratigraphic analysis shows the influence of growth of the Santa Fe Springs Anticline on the stratigraphic units in the study area. Syndepositional folding appears to have caused relative thinning of the units over the crest of the anticline, and possibly preferential erosion of capping aquitards near the anticline crest, that may provide pathways for migration of shallow contaminants into older stratigraphic units. This structural and stratigraphic model may explain why observations of high levels of OSCs appear to migrate from the near-surface Mesa sequence near the former Omega facility, downgradient into the Upper Wilmington sequence north of and adjacent to the anticline crest along the study cross section.

South and southwest of the Santa Fe Springs Anticline axis, the chronostratigraphic units are observed to thicken into the Central Basin. It appears that the Pacific and Harbor sequences may transition downgradient from fluvial facies (in the northern part of the study area) to likely paralic and shallow marine sediment (farther southwest into the Central Basin). As the marine facies of these sequences tend to contain more productive aquifers, they are more likely to be exploited for public supply, and indeed, a majority of the wells in the study area appear to be screened in aquifers within the Upper Wilmington through Pacific A sequences. Therefore, we conclude that contaminated portions of the Upper Wilmington through Pacific A sequences, where they occur near the anticline crest, are likely genetically connected to the aquifers that are being pumped in the Central Basin. Once contaminated, if the hydraulic conditions are appropriate, flow within the sequences could cause the contaminants to migrate into producing zones without the need for further flow between stratigraphic sequences.

Although we cannot precisely define the flow paths, observations of low-level contamination in well 18G5, located at the downgradient end of our study cross section, and VOC detections at depths >200 ft bls in other production wells in the study area, suggest that groundwater migration carrying contaminants within the sequences from the anticline crest to these producing zones may in fact be occurring.

Along the study cross section, characteristic Omega source contaminants are observed at concentrations greater than 10 times the MCL in the Mesa sequence as far as 4.5 mi from the former Omega facility. Observed detections of characteristic Omega source contaminants within older sequences suggest that these contaminants may not have migrated as far as within the Mesa sequence,

but there are very little contaminant data from older units south of the anticline. More data are needed to determine whether characteristic Omega source contaminants have migrated within the Pacific sequence, or in deeper units, farther south than site MW27.

Water chemistry provides a second line of evidence to evaluate the connections between shallow groundwater and production zones in the deeper parts of the groundwater system. New groundwater $\delta^{18}O$, $\delta^{2}H$, chloride, VOC, tritium, carbon-14, and other inorganic chemistry data were collected for this study and integrated with previously collected information to further constrain understanding of groundwater-flow patterns in the study area.

Most groundwater in the study area, particularly along the study cross section, has chloride and isotopic values consistent with being mixtures of San Gabriel native water and local groundwater of various ages. San Gabriel native water originates from precipitation in the San Gabriel Mountains that recharged or passed through the Whittier Narrows, and generally is the predominant source of recharge for groundwater with increasing depth along the study cross section. Local water is derived from precipitation that falls directly onto the study area or the Puente Hills to the northeast, and is the predominant source of recharge for groundwater at shallower depths along the study cross section. Some groundwater, particularly in the western part of the study area, may be mixed with engineered recharge from spreading grounds located to the north along the San Gabriel River. However, engineered recharge is unlikely to be a predominant source of water along the study cross section. Mixing calculations based on $\delta^{18}O$ values indicate that varying fractions of local water (~30 to 60 percent) are present in groundwater from the Mesa, Pacific, and Harbor sequences along the study cross section. In contrast, local water is generally not present or abundant (<10 percent) in the Upper or Lower Wilmington units upgradient of the anticline. However, downgradient of the anticline at monitoring well MW27D, the local fraction in the Upper Wilmington sequence was ~40 percent. This observation is consistent with the distribution of contaminants along the study cross section that suggests that shallow groundwater is migrating into older units near the crest of the Santa Fe Springs Anticline. Unfortunately, isotopic data are not available further downgradient on the study cross section, and the possible occurrence of local recharge to greater depths with distance southwest of the anticline is unknown.

Along the study cross section, characteristic Omega source contaminants occur in higher concentrations in shallow groundwater and are associated with isotopic values indicating groundwater derived from local precipitation that has mixed with San Gabriel native water. Detections and concentrations of VOCs were generally greater, and the fraction of local water greater, in shallower wells (well B at each of four multiple-well monitoring sites) than in deeper wells (well D at each location). The extent of mixing of local recharge containing VOCs at depth varies by site.

Increasing detections and concentrations of characteristic Omega source contaminants in production well 30R3, located near the west edge of the OU2 plume upgradient of the anticline (with a well-screen top located 200 ft bls), indicates that production wells with shallow well screens are vulnerable to contamination. Results of sampling in production well 6N1, located on the south side of the anticline and west of the section but within the OU2 plume, are more ambiguous. TCE and PCE were detected in well 6N1, having screen depths of 335–574 ft bls, ~125 ft below that of the upgradient deep monitoring well MW27D. Both wells are screened in the Upper Wilmington sequence, although VOC concentrations are approximately an order of magnitude higher in upgradient well MW27D. While it may be possible that VOCs are migrating within the Upper Wilmington sequence between wells MW27 and 6N1, we note that the detection of PCE and (or) TCE in regional monitoring wells analyzed for VOCs by this study that are located upgradient or some distance to the west of OU2, indicates that there may be other sources of VOCs affecting wells in the study area. Consequently, use of PCE and

TCE data alone to trace movement of shallow groundwater contamination to greater depths in the groundwater system should be done with caution and be supported by other geochemical and hydrologic data.

A groundwater-flow and particle-tracking model provided the third approach for assessing the potential for shallow groundwater contamination to migrate to deeper zones used for public supply. The two-dimensional (cross-sectional) steady-state model was defined to incorporate the detailed geologic layering provided by the sequence stratigraphic geologic model described in this report. Water levels in the study area were simulated using MODFLOW-NWT, and particle trajectories and travel times from source areas to wells were simulated using MODPATH. An inverse method based on Monte Carlo sensitivity analysis was used to estimate horizontal and vertical hydraulic conductivities that best reproduce the hydraulic-head and contaminant occurrence data. Data that were used to calibrate the model include hydraulic head measurements at 32 wells and contaminant occurrence observations at 19 wells.

The hydraulic conductivity values estimated for the model were generally similar to values estimated in previous groundwater modeling studies. The estimates of hydraulic conductivity obtained in this study ranged from ~20 ft/day to ~700 ft/day, with hydraulic conductivity generally decreasing with depth. Estimates of vertical anisotropy for the various sequences ranged from ~0.0001 to ~0.2. These parameter estimates were made over large discrete zones in the model; smaller-scale hydraulic-conductivity variability that might represent the kinds of small-scale lithologic variations observed within the stratigraphic sequences was not incorporated due to model limitations.

The results of the model calibration were dependent on the goal of the calibration exercise. The particle-tracking analysis differed substantially when the goal of calibration shifted from finding the best fit to groundwater-elevation observations to finding the particle-tracking model that reproduces the contaminant occurrence observations at the deepest monitoring sites. For the simulation model that provides the best fit to hydraulic-head data, the deepest particle path had a trajectory that reached a maximum depth of ~230 ft bls at the downstream boundary. For the model that simulates particles migrating to the deepest locations where OSCs are observed, those particle trajectories reached a maximum of ~600 ft bls at the downstream boundary. It is important to note that the latter particle-tracking analysis also showed potential contaminant flow paths that intersect the well 18G5, the only supply well located on the cross section, along its entire producing zone.

The geologic modeling, water chemistry, and groundwater simulation analyses described in this report are limited by the amount of data along the cross section, especially because those data are mostly restricted to shallow monitoring wells (<200 ft bls). Shallow wells do not provide the information needed to characterize the potential for transport pathways to deeper parts of the groundwater system. The analyses were also constrained by the two-dimensional groundwater-flow and particle-tracking model, and the inherent simplifications used to characterize the complex three-dimensional geologic and hydrologic controls that influence contaminant migration. While the particle-tracking simulations predict that groundwater flow paths will move to greater depths downgradient, as is also inferred from the geologic and geochemical observations and analyses, the simulated flow does not appear to closely parallel inferred chronostratigraphic boundaries. Instead, flow appears to move across stratigraphic boundaries into older units upgradient of and across the anticlinal crest, and, while still moving vertically downward, flow appears to migrate back into younger sequences downgradient of the anticline. This result is subject to the simplifications and uncertainties described above. However, even with these uncertainties, simulated flow paths that cross stratigraphic boundaries may be plausible representations of groundwater flow patterns that are occurring in the region today. Certainly, flow paths crossing downward into older chronostratigraphic units in the upgradient areas are conceptually

reasonable given that substantial vertically downward gradients are present within the system as a result of groundwater withdrawals at depth. These withdrawals have probably had the effect of increasing vertical gradients between stratigraphic units compared to a predevelopment condition where there was no pumping. Current model and data limitations prevent us from assessing whether groundwater flow paths may be more strongly controlled by layered hydraulic conductivity distributions associated with the chronostratigraphic sequences than the current simulations suggest. Continued testing of these conceptual models with three-dimensional models better constrained by geologic and hydrogeochemical data, particularly in the downgradient portions of the study area where data are sparse, will be necessary to refine understanding of the relation of groundwater flow to geologic structure. Nonetheless, conceptual flow models based on the inferred stratigraphic architecture, observed geochemistry, and simulated numerical models, predict that target constituents introduced into groundwater at shallow depths along the study cross section will likely migrate downgradient to depths intercepted by public supply wells.

Opportunities exist to improve the modeling framework and the data that drives the modeling analyses. Specifically, these include:

- Additional data compilation and enhanced facies modeling in three-dimensions are needed to better characterize the types and locations of preferential pathways for vertical migration of contaminants. New high-resolution, shallow seismic-reflection data would likely be most effective in mapping possible channel incisions and other possible pathways for inter-unit groundwater flow.
- Three-dimensional groundwater flow and particle-tracking analysis is needed to simulate the complex three-dimensional groundwater flow patterns that determine the pathways and rates of contaminant movement in the study area. The enhanced model would have a three-dimensional representation of the sequence stratigraphic model, refined discretization of hydraulic conductivities and anisotropies informed by the geology, and would include the effects of hydrologic stresses that could not be included in the two-dimensional cross-section model.
- Additional geologic, hydrologic, and water chemistry data, including age and source water indicators in addition to organic and inorganic constituents, are needed in the OU2 plume area south of site MW27. New monitoring wells installed to explore this area should be drilled deep enough to penetrate the Upper Wilmington sequence to determine if significant contaminant migration may be occurring beneath the currently defined OU2 plume. Geophysical logs, including induction resistivity, natural gamma, and shear-wave velocity, should be obtained from newly drilled wells.

References Cited

American Society for Testing and Materials (ASTM), 1985, Classification of soils for engineering purposes: Annual Book of ASTM Standards D 2487-83, v. 04.08, p. 395–408, at *http://www.astm.org/Standards/D2487.htm*

Anders, Robert, and Schroeder, Roy A., 2003, Use of water-quality indicators and environmental tracers to determine the fate and transport of recycled water in Los Angeles County, California: U.S. Geological Survey Water-Resources Investigation Report 03–4279, 106 p.

Anderson, M.P., and Woessner, W.W., 1992, Applied groundwater modeling–simulation of flow and advective transport: San Diego, Calif., Academic Press, 381 p.

Athy, L.F., 1930, Density, porosity, and compaction of sedimentary rocks: American Association of Petroleum Geologists Bulletin, v. 14, p. 1–24.

Bassinot, F.C., Labeyrie, L.D., Vincent, E., Quidelleu, X., Shackleton, N.J., and Lancelot, Y., 1994, The astronomical theory of climate and the age of the Brunhes-Matuyama magnetic reversal: Earth and Planetary Science Letters, v. 126, p. 91–108.

Blake, G.H., 1991, Review of the Neogene biostratigraphy and stratigraphy of the Los Angeles basin and implications for basin evolution, *in* Biddle, K. T., ed., Active margin basins: American Association of Petroleum Geologists Memoir 52, p. 135–184.

Bull, W.B., 1991, Climatic Geomorphology: Oxford, U.K., Oxford University Press, 326 p.

California Department of Water Resources (CDWR), 1961, Ground water geology, Appendix A *of* Planned utilization of the ground water basins of the coastal plain of Los Angeles County: California Department of Water Resources Bulletin 104, 191 p.

Catuneanu, O., 2006, Principles of Sequence Stratigraphy: New York, Elsevier, 386 p.

CH2M HILL, 2012, Groundwater monitoring report for 2010 and 2011, Omega Chemical Corporation Superfund site, Los Angeles County, California: Riverside, Calif., Report prepared for the U.S. Environmental Protection Agency, contract no. EP-S9-08-04, 179 p., at *http://yosemite.epa.gov/r9/sfund/r9sfdocw.nsf/cf0bac722e32d408882574260073faed/ae709367f75e443288257a1b007ae0c0!OpenDocument*.

Clark, I.D., and Fritz, P., 1997, Environmental isotopes in hydrogeology: Boca Raton, Fla., CRC Press, 328 p.

Coplen, T.B., 2011, Guidelines and recommended terms for expression of stable isotope-ratio and gas-ratio measurement results: Rapid Communications in Mass Spectrometry, v. 25, p. 2538–2560, doi: 10.1002/rcm.5129.

Craig, H., 1961, Isotopic variations in meteoric waters: Science, v. 113, p. 1702–1703.

Dawson-Milby, B.J., Belitz, Kenneth, Land, Michael, and Danskin, W.R., 2003, Stable isotope and volatile organic compounds along seven ground-water flow paths in divergent and convergent flow systems, Southern California, 2000: U.S. Geological Survey Water-Resources Investigations Report 03–4059, 79 p.

Doherty, J., 2005, PEST—Model-Independent Parameter Estimation: User Manual: 5th Edition, Watermark Numerical Computing, 336 p.

Durham, D.L., and Yerkes, R.F., 1964, Geology and oil resources of the eastern Puente Hills area, southern California: U.S. Geological Survey Professional Paper 420–B, 62 p.

Dynamic Graphics, Inc., 2009, EarthVision Users Guide 8.0: Alameda, Calif., Dynamic Graphics, 2987 p.

Faires, L.M., 1993, Methods of analysis by the U.S. Geological Survey National Water Quality Laboratory—determination of metals in water by inductively coupled plasma-mass spectrometry: U.S. Geological Survey Open-File Report 92–634, 28 p.

Ferguson, Jr., E., Smith, E.A., and Jones, D.W., 1996, Results of groundwater characterization of the Oil Field Reclamation Project Study Area (OFRP): Irvine, Calif., McLaren/Hart, Inc., Report prepared for Oil Field Reclamation Project (OFRP), Santa Fe Springs, Calif., project no. 03.0601373.006, 75 p.

Fishman, M.J., and Friedman, L.C., 1989, Methods for determination of inorganic substances in water and fluvial sediments: U.S. Geological Survey Techniques of Water-Resources Investigations, book 5, chap. A1, 545 p.

Fishman, M.J., ed., 1993, Methods of analysis by the U.S. Geological Survey National Water Quality Laboratory–Determination of inorganic and organic constituents in water and fluvial sediments: U.S. Geological Survey Open-File Report 93–125, 217 p.

Fontes, J.C., and Garnier, J.M., 1979, Determination of the initial ^{14}C activity of the total dissolved carbon—A review of the existing models and a new approach: Water Resources Research, v. 15, no. 2, p. 399–413.

Fram, M.S., Olsen, L.D., and Belitz, Kenneth, 2012, Evaluation of volatile organic compound (VOC) blank data and application of study reporting levels to groundwater data collected for the California GAMA Priority Basin Project, May 2004 through September 2010: U.S. Geological Survey Scientific Investigations Report 2012–5139, 94 p.

Freeze, R.A. and Cherry, J.A., 1979, Groundwater: Englewood Cliffs, N.J., Prentice-Hall, 604 p.

Gibbard, P.L., Head, M.J., Walker, M.J.C., and the Subcommission on Quaternary Stratigraphy, 2010, Formal ratification of the Quaternary System/Period and the Pleistocene Series/Epoch with a base at 2.58 Ma: Journal of Quaternary Sciences, v. 25, p. 96–102, doi: 10.1002/jqs.1338.

Goldrath, Dara, Fram, M.S., Land, Michael, and Belitz, Kenneth, 2012, Status of groundwater quality in the Coastal Los Angeles Basin, 2006—California GAMA Priority Basin Project: U.S. Geological Survey Scientific Investigations Report 2012–5048, 64 p.

Goode, D.J., 1996, Direct simulation of groundwater age: Water Resources Research, v. 32, no. 2, p. 289–296.

Hill, M.C., Banta, E.R., Harbaugh, A.W., and Anderman, E.R., 2000, MODFLOW-2000, The U.S. Geological Survey modular ground-water model–User guide to the observation, sensitivity, and parameter-estimation processes and three post-processing programs: U.S. Geological Survey Open-File Report 00–184.

Hill, M.C., and Tiedeman, C.R., 2007, Effective groundwater model calibration—With analysis of data, sensitivities, predictions, and uncertainty: New York, Wiley and Sons, 455 p.

Imbrie, J., Hays, J.D., Martinson, D.G., McIntyre, A., Mix, A.C., Morley, J.J., Pisias, N.G., Prell, W.L., and Shackleton, N.J., 1984, The orbital theory of Pleistocene climate—support from a revised chronology of the marine $\delta^{18}O$ record *in* Berger, A., Imbrie, J., Hays, J., Kukla, G., and Saltzman, B., eds., Milankovich and Climate, part 1: Dordrecht, D. Reidel, NATO Advanced Science Institutes Series C, v. 126, p. 269–305.

Jones, S.R., and Garbarino, J.R., 1999, Methods of Analysis by the U.S. Geological Survey National Water Quality Laboratory–Determination of Arsenic and Selenium in Water and Sediment by Graphite Furnace-Atomic Absorption Spectrometry: U.S. Geological Survey Open-File Report 98–639, 39 p.

Kauffman, L.J., Baehr, A.L., Ayers, M.A., and Stackelberg, P.E., 2001, Effects of land use and travel time on the distribution of nitrate in the Kirkwood-Cohansey aquifer system in southern New Jersey: U.S Geological Survey Water-Resources Investigation Report WRIR-4117, 57 p.

Kendall, C., and Coplen, T.B., 2001, Distribution of oxygen-18 and deuterium in river waters across the United States: Hydrological Processes, v. 15, p. 1363–1393, doi: 10.1002/hyp.217.

Kew, W.S.W, 1937, Los Angeles basin excursion–Santa Monica Mountains-Inglewood Field *in* Guidebook-Field Excursions-Southern California, American Association of Petroleum Geologists, 22nd annual meeting, p. 7–8.

Land, M., Everett, R.R., and Crawford, S.M., 2002, Geologic, hydrologic, and water-quality data from multiple-well monitoring sites in the Central and West Coast Basins, Los Angeles County, California, 1995–2000: U.S. Geological Survey Open-File Report 01–277, 178 p.

Land, M., Reichard, E.G., Crawford, S.M., Everett, R.R., Newhouse, M.W., and Williams, C.F., 2004, Ground-Water Quality of Coastal Aquifer Systems in the West Coast Basin, Los Angeles County, California, 1999–2002: U.S. Geological Survey Scientific Investigations Report 2004–5067, 80 p.

Landon, M., Jurgens, B., Katz, B., Eberts, S.M., Burow, K., and Crandall, C., 2010, Depth-dependent sampling to identify short-circuit pathways to public-supply wells in multiple aquifer settings in the United States: Hydrogeology Journal, v. 18, no. 3, p. 577–593, doi 10.1007/s10040-009-0531-2.

Manning, A.H., Solomon, D.K., and Thiros, S.A., 2005, $^{3}H/^{3}He$ age data in assessing the susceptibility of wells to contamination: Groundwater, v. 43, no. 3, p. 353–367.

Mathany, T.M., Land, Michael, and Belitz, Kenneth, 2008, Ground-water quality data in the coastal Los Angeles Basin Study Unit, 2006—Results from the California GAMA Program: U.S. Geological Survey Data Series 387, 98 p.

McDonald, M.G. and Harbaugh, A.W., 1988, A modular three-dimensional finite-difference ground-water flow model: U.S. Geological Survey Techniques of Water-Resources Investigations, book 6, chap. A1, 586 p.

McDougall, K., Hillhouse, J., Powell, C., II, Mahan, S., Wan, E., and Sarna-Wojcicki, A.M., 2012, Paleontology and geochronology of the Long Beach core sites and monitoring wells, Long Beach, California: U.S. Geological Survey Open-File Report 2011–1274, 235 p.

McFadden, L.D., 1982, The impacts of temporal and spatial climatic changes on alluvial soils genesis in southern California: Tucson, University of Arizona, Ph.D. dissertation, 430 p.

McNichol, A.P., Jones, G.A., Hutton, D.L., and Gagnon, A.R., 1994, The rapid preparation of seawater CO_2 for radiocarbon analysis at the National Ocean Sciences AMS facility: Radiocarbon, v. 36, no. 2, p. 237–246.

Michel, R.L., 1989, Tritium deposition in the continental United States, 1953–83: U.S. Geological Survey Water-Resources Investigations Report 89–4072, 46 p.

Michel, R.L., and Schroeder, R., 1994, Use of long-term tritium records from the Colorado River to determine timescales for hydrologic processes associated with irrigation in the Imperial Valley, California: Applied Geochemistry, v. 9, p. 387–401.

Morton, D.M. and Miller, F.K., 2006, Geologic map of the San Bernardino and Santa Ana 30' x 60' quadrangles, California: U.S. Geological Survey Open-File Report 2006-1217, scale 1:100,000.

Murex Environmental, Inc., 2011, Groundwater investigation report and first quarter 2011 groundwater monitoring report, former CENCO Refinery, 12345 Lakeland Road, Santa Fe Springs, CA: Irvine, Calif., Report prepared for Regional Water Quality Control Board, Los Angeles Region (RWQCB), 484 p.

National Research Council, 1997, Innovation in ground water and soil cleanup–from concept to commercialization: Washington, DC, National Academy Press, 292 p.

Natland, M.L., 1953, Pleistocene and Pliocene stratigraphy of southern California: Los Angeles, University of California, Ph.D. dissertation, 165 p.

Natland, M.L., and W.T. Rothwell, Jr., 1954, Fossil foraminifera of the Los Angeles and Ventura regions, California, *in* Jahns, R.H., ed., Geology of southern California: California Division of Mines Bulletin 170, p. 33–42.

Nishikawa, Tracy, Siade, A.J., Reichard, E.G., Ponti, D.J., Canales, A.G., and Johnson, T.A., 2009, Stratigraphic controls on seawater intrusion and implications for groundwater management, Dominguez Gap area of Los Angeles, California, USA: Hydrogeology Journal, v. 17, p. 1699–1725.

Niswonger, R.G., Panday, Sorab, and Ibaraki, Motomu, 2011, MODFLOW-NWT, A Newton formulation for MODFLOW-2005: U.S. Geological Survey Techniques and Methods 6-A37, 44 p.

Piper, A.M., Garrett, A.A, and others, 1953, Native and contaminated ground waters in the Long Beach-Santa Ana area, California: U.S. Geological Survey Water-Supply Paper 1136, 320 p.

Plesch, A., Tape, C., Graves, R., Small, P., Ely, G., and Shaw, J.H., 2011, Updates for the CVM-H including new representations of the offshore Santa Maria and San Bernardino basin and a new Moho surface: SCEC Annual Meeting, Proceedings and abstracts, v. 21, Palm Springs, Calif.

Plesch, A., Shaw, J.H., Benson, C., Bryant, W.A., Carena S., Cooke, M., Dolan, J., Fuis, G., Gath, E., Grant, L., Hauksson, E., Jordan, T., Kamerling, M., Legg, M., Lindvall, S., Magistrale, H., Nicholson, C., Niemi, N., Oskin, M., Perry, S., Planansky, G., Rockwell, T., Shearer, P., Sorlien, C., Süss, M.P., Suppe, J., Treiman, J., and Yeats, R., 2007, Community fault model (CFM) for Southern California: Seismological Society of America Bulletin, v. 97, no. 6, p. 1793–1802.

Plummer, L.N., Michel, R.L., Thurman, E.M., and Glynn, P.D., 1993, Environmental tracers for age-dating young ground water, *in* Alley, W.M., ed., Regional ground-water quality: New York, Van Nostrand Reinhold, p. 255–294.

Poland, J.F., Garrett, A.A., and Sinnott, A., 1959, Geology, hydrology, and chemical character of ground waters in the Torrance-Santa Monica area, California: USGS Water-Supply Paper 1461, 425 p.

Poland, J.F., Piper, A.M., and others, 1956, Ground water geology of the coastal zone, Long Beach-Santa Ana area, California: USGS Water-Supply Paper 1109, 162 p.

Pollock, D.W., 1994, User's guide for MODPATH/MODPATH-PLOT, Version 3; a particle tracking post-processing package for MODFLOW, the U.S. Geological Survey finite-difference ground-water flow model: U.S. Geological Survey Open-File Report 94–464, 248 p.

Ponti, D.J., 1989, Aminostratigraphy and chronostratigraphy of Pleistocene marine sediments, southwestern Los Angeles basin, California: University of Colorado, unpublished Ph.D. thesis, 409 p.

Ponti, D.J., Ehman, K.D., Edwards, B.D, Tinsley, J.C., III, Hildenbrand, T., Hillhouse, J.W., Hanson, R.T., McDougall, K., Powell, C.W., II, Wan, E., Land, M., Mahan, S., and Sarna-Wojcicki, A.M., 2007, A 3-Dimensional Model of Water-Bearing Sequences in the Dominguez Gap Region, Long Beach, California: U.S. Geological Survey Open-File Report 2007–1013, 38 p.

Powell, C.L., II, and Stevens, D., 2000, Age and paleoenvironmental significance of mega-invertebrates from the "San Pedro" Formation in the Coyote Hills, Fullerton and Buena Park, Orange County, southern California: U.S. Geological Survey Open-File Report 00–319, 83 p., at *http://geopubs.wr.usgs.gov/open-file/of00-319*.

Pratt, T.L.; Shaw, J.H.; Dolan, J.F.; Christofferson, S.A.; Williams, R.A.; Odum, J.K.; Plesch, A., 2002, Shallow seismic imaging of folds above the Puente Hills blind-thrust fault, Los Angeles, California: Geophysical Research Letters, v. 29, no. 9, p. 1304–1307, doi:10.1029/2001GL014313

Quinn, J.P., Ponti, D.J., Hillhouse, J.W., Powell, C.L., II, McDougall, K., Sarna- Wojcicki, A.M., Barron, J.A., and Fleck, R.J., 2000, Quaternary chronostratigraphic constraints on deformation and blind fault activity, northern Los Angeles basin, *in* Quinn, J. P., Collaborative research (Gorian and Associates, Inc. and United States Geological Survey): Geological investigations to evaluate the Wilshire fault blind thrust model. Final Technical Report, 1434-95-G-2523 (Program Element II, Component II.5): 31 p

Reed, R.D., 1933, Geology of California: Tulsa, Okla., American Association of Petroleum Geologists, 355 p.
Regional Water Quality Control Board, Los Angeles Region (RWQCB) , 2011, Groundwater investigation report and first quarter 2011 groundwater monitoring report, former CENCO Refinery, 12345 Lakeland Road, Santa Fe Springs, CA, SLIC No. 0318, ID No. 2040071, CAO 97-118: prepared by Murex Environmental, Inc., 484 p.
Reichard, E.G., Land, Michael, Crawford, S.M., Johnson, Tyler, Everett, R.R., Kulshan, T.V., Ponti, D.J., Johnson, T.A., Paybins, K.S., and Nishikawa, Tracy, 2003, Geohydrology, geochemistry, and ground-water simulation-optimization of the Central and West Coast Basins, Los Angeles, County, California: U.S. Geological Survey Water-Resources Investigations Report 03–4065, 184 p.
Révész, Kinga, and Coplen, T.B., 2008a, Determination of the $\delta(^{2}H/^{1}H)$ of water—RSIL lab code 1574 *of* Révész, Kinga, and Coplen, T.B., eds., Methods of the Reston Stable Isotope Laboratory: U.S. Geological Survey Techniques and Methods 10–C1, chap. C1, 27 p.
Révész, Kinga, and Coplen, Tyler B., 2008b, Determination of the $\delta(^{18}O/^{16}O)$ of water: RSIL lab code 489, *chap. C2 of* Révész, Kinga, and Coplen, Tyler B., eds., Methods of the Reston Stable Isotope Laboratory: U.S. Geological Survey Techniques and Methods, 10–C2, chap. C2, 28 p.
Sanford, W.E., Plummer, L.N., McAda, D.P., Bexfield, L.M., and Anderholm, S.K., 2004, Hydrochemical tracers in the Middle Rio Grande Basin, USA—2. Calibration of a groundwater model: Hydrogeology Journal, v. 12, p. 389–407.
Santi, P.M., McCray, J.E., and Martens, J.L., 2006, Investigating cross-contamination of aquifers: Hydrogeology Journal, v. 14, p. 51–68.
Saucedo, G.J., Greene, H.G., Kennedy, M.P., and Bezore, S.P., 2003, Geologic map of the Long Beach 30' x 60' quadrangle, California—a digital database: California Geological Survey Preliminary Geologic Maps, scale 1:100,000.
Schroeder, R.A., Anders, R., Böhlke, J.K., Michel, R.L., and Metge, D.W., 1997, Water quality at production wells near artificial-recharge basins in Montebello Forebay, Los Angeles County, *in* Kendall, D.R., ed., Conjunctive Use of Water Resources: Aquifer Storage and Recovery: American Water Resources Association Symposium, Herndon, 1997, [Proceedings], p. 273–284.
Shaw, J.H., and Shearer, P.M., 1999, An elusive blind-thrust fault beneath metropolitan Los Angeles: Science, v. 283, no. 5407, p. 1516–1518, doi: 10.1126/science.283.5407.1516.
Shaw, J.H., Plesch, A., Dolan, J.F., Pratt, T.L., and Fiore, P., 2002, Puente Hills blind-thrust system, Los Angeles, California: Seismological Society of America Bulletin, v. 92, no. 8, p. 2946–2960.
Shelton, J.L., Burrow, K.R., Belitz, Kenneth, Dubrovsky, N.M., Land, Michael, and Gronberg, J.M., 2001, Low-level volatile organic compounds in active public supply wells as ground-water tracers in the Los Angeles physiographic basin, California, 2000: U.S. Geological Survey Water-Resources Investigations Report 01–4188, 29 p.
Stuiver, M., and Polach, H.A., 1977, Reporting of ^{14}C data: Radiocarbon, v. 19, p. 355–363.
Suess, M.P., and Shaw, J.H., 2003, P-wave seismic velocity structure derived from sonic logs and industry reflection data in the Los Angeles basin, California: Journal of Geophysical Research, v. 108, no. B3, p. 2170.
Thatcher, L.L., Janzer, V.J., and Edwards, K.W., 1977, Methods for the determination of radioactive substances in water: U.S. Geological Survey Techniques of Water-Resources Investigations, book 5, chap. A5, 95 p.

U.S. Environmental Protection Agency (EPA), 2000, Public input requested, Omega Chemical Corporation Superfund site, Los Angeles County, California: U. S. Environmental Protection Agency Fact Sheet, 8 p., at *http://yosemite.epa.gov/R9/SFUND/R9SFDOCW.NSF/95831d90484434d7882574260072fadf/e2d09607d48e3b828825775900612 69b!OpenDocument*.

U.S. Environmental Protection Agency (EPA), 2010, Omega Chemical Corporation Superfund Site, Operable Unit 2, Los Angeles County, California (Volume 1): U.S. Evironmental Protection Agency Remedial Investigation/Feasibility Study Reports, 458 p., at *http://yosemite.epa.gov/R9/SFUND/R9SFDOCW.NSF/BySite/Omega Chemical Corporation?OpenDocument*.

U.S. Environmental Protection Agency (EPA), 2012, Drinking water standards and health advisories tables: U.S. Environmental Protection Agency, Office of Water, EPA 822-S-12-001, accessed April 2012 at *http://water.epa.gov/drink/standards/hascience.cfm*.

U.S. Geological Survey, variously dated, National field manual for the collection of water-quality data: U.S. Geological Survey Techniques of Water-Resources Investigations, book 9, chaps. A1-A9, at *http://pubs.water.usgs.gov/twri9A*.

Van Wagoner, J.C., Mitchum, R.M., Campion, K.M., and Rahmanian, V.D., 1990, Siliciclastic sequence stratigraphy in well logs, cores, and outcrops: American Association of Petroleum Geologists Methods in Exploration Series, no. 7, 55 p.

Water Replenishment District of Southern California (WRD), 2011, Engineering Survey and Report, 2011(updated May 6, 2011): Lakewood, Calif., Water Replenishment District of Southern California Report, 65 p.

Water Replenishment District of Southern California (WRD), 2012, Regional Groundwater Monitoring Report, Water Year 2010-2011–Central and West Coast Basins, Los Angeles County, California: Lakewood, Calif., Water Replenishment District of Southern California Report, 163 p.

Water Replenishment District of Southern California (WRD), 2013, Regional Groundwater Monitoring Report, Water Year 2011-2012–Central and West Coast Basins, Los Angeles County, California: Lakewood, Calif., Water Replenishment District of Southern California Report, 186 p.

Western Regional Climate Center, 2014, Cooperative climatological data summaries: Western Regional Climate Center at *http://www.wrcc.dri.edu/climatedata/climsum/*.

Winter, H.E., 1943, Santa Fe Springs oil field: California Division of Mines and Geology Bulletin 118, p. 343–346.

Woodring, W.P., Bramlette, M.N., and Kew, W.S.W., 1946, Geology and paleontology of Palos Verdes Hills, California: U.S. Geological Survey Professional Paper 207, 145 p.

Wright, T.L., 1991, Structural geology and tectonic evolution of the Los Angeles basin, California, *in* Biddle, K.T., ed., Active margin basins: American Association of Petroleum Geologists Memoir 52, p. 35–134.

Yerkes, R.F., 1972, Geology and oil resources of the western Puente Hills area, southern California: USGS Professional Paper 420–C, 68 p.

Yerkes, R.F., McCulloh, T.H., Schoellhamer, J.E., and Vedder, J.G., 1965, Geology of the Los Angeles Basin California–an introduction: USGS Professional Paper 420–A, 57 p.